Serial N° :

الجمهورية الجزائرية الديمقراطية الشعبية

PEOPLE'S DEMOCRATIC REPUBLIC OF ALGERIA

وزارة التعليم العالي والبحث العلمي

MINISTRY OF HIGHER EDUCATION AND SCIENTIFIC RESEARCH

جامعة الشهيد حمه لخضر الوادي

ECHAHID HAMMA LAKHDAR UNIVERSITY OF EL-OUED

كلية العلوم الطبيعية والحياة

FACULTY OF NATURAL SCIENCES AND LIFE

قسم البيولوجيا الخلوية والجزيئية

DEPARTMENT OF CELLULAR AND MOLECULAR BIOLOGY

Doctorate Thesis

To Obtain a Diploma of an Academic PhD Degree

In Biological Sciences

Specialty: Fundamental and Applied Toxicology

Theme

Preparation and Characterization of Phyto-Copper Nanoparticles Using *Phragmites australis* and Evaluation of Their Biological and Veterinary Applications

Presented by: Frahtia Ahlem

Examining Committee

President	Pr. Chouikh Atef	Prof	El-Oued University
Supervisor	Pr. Derouiche Samir	Prof	El-Oued University
Co-supervisor	Pr. Niemann Janetta	Prof	Poznań University of Life Sciences
Examiner	Pr. Bouabida Hayette	Prof	Larbi Tebessi University
Examiner	Dr. Fetni Samira	MCA	University of Batna 2
Examiner	Dr. Guemmouda Messaouda	MCA	El-Oued University

Academic year: 2024/ 2025

Dedication

To my dear husband, my constant companion and pillar of strength, your unwavering belief in me has made this journey possible and successful.

To my toddler, who began this journey as a fetus, and has now witnessed every step along the way.

To my beloved family, whose love, sacrifices, and encouragement have shaped me into who I am.

To my supervisor, whose words once echoed in my mind: "It may be due to your good or bad luck that I am your supervisor". While I do not believe in luck, I firmly believe in Allah's plan. For this I am truly thankful for the patience, unconditional support, and unwavering dedication you have shown throughout this journey. I am deeply grateful for the opportunity to learn and grow under your mentorship.

To the exceptional Islam and Sara, who guided me with patience, wisdom, and generosity. Your support in the lab, your invaluable advice, and your readiness to answer my questions were a beacon of light throughout this journey. Though younger in years, you are teachers at heart.

To my babysitter, Khawla, who made it easier for me to balance my responsibilities and study. You gave me the peace of mind I needed to focus on my work.

To my dear friend Abir, who insisted on gifting me the graduation suit, your generosity, positive energy, and belief in me, especially when I struggled to believe in myself, are priceless.

To my dear friends—Louiz, Adila, Ninich and her wonderful family, Douaa, Ouijdane, Basmala, and many others whose names I haven't written—you all mean so much to me and are truly cherished in my heart.

In loving memory of my uncle Achour Hamouda, professor of Anatomical Pathology. Your presence would have surely added even more meaning to my work.

Lastly, as I reflect on my work, I am reminded of the thousands of individuals (who are not just numbers), martyrs, wounded, and the ones still under the rubble, as of writing these words, for more than 456 days. This thesis was written amidst relentless Zionist fire over Gaza. Even as I complete this work, the suffering, bombing, and detonation in Gaza continue...

وإنه لجهاد.. نصر أو استشهاد..

Acknowledgment

"And my success is not my own, but only through Allah, upon Him I have relied, and to Him I return." Quran, Hud 88.

And because he who does not thank people does not thank Allah, I extend my gratitude to my esteemed supervisor ***Pr. Derouiche Samir****, whose unwavering guidance, profound knowledge, and continuous support have been the cornerstone of this research. Your exceptional mentorship not only shaped this thesis but also inspired my intellectual growth throughout my doctoral journey. Your patience, encouragement, and insightful feedback have been invaluable, and I am truly privileged to have had the opportunity to work under your guidance.*

I am truly grateful to my co-supervisor ***Dr. Niemann Janetta*** *for her continuous support and expert guidance throughout my internship. Her generosity and hospitality made a significant impact on my experience. Her help was invaluable to the completion of this thesis.*

I extend my sincere gratitude to ***Pr. Chouikh Attef*** *for the honor of presiding over this thesis. I also thank* ***Pr. Bouabida Hayette, Dr. Fetni Samira,*** *and* ***Dr. Gammouda Messaouda*** *for their agreement to examine my work and for the honor of their presence. I express my deepest respect to each of them.*

A special and wholehearted acknowledgment goes to my husband, ***Abu El Alaa****, whose support has been indispensable in the fulfillment of this thesis. Not only did he provide constant emotional encouragement, but he was actively involved in my research.*

I would like to extend sincere appreciation to ***Dr. Bagui Salah****, a dedicated veterinary doctor, for opening the doors of his chicken coop to facilitate my experiment. His generosity in allowing me to conduct my research on his premises, as well as his invaluable advice and expertise, greatly enriched the quality of this study. I am deeply grateful for his professional support and guidance throughout the research process.*

I would like to express my heartfelt thanks to ***Dr. Zellouma Ahmed****, my English teacher, who graciously accepted the responsibility of proofreading my first scientific journal articles. I am deeply grateful for your unwavering support and for the time and effort you dedicated to helping me refine my writing. Your constant encouragement and the way you affectionately referred to me as "soon to be a doctor" have been invaluable throughout my academic journey.*

I would like to express my sincere gratitude to the owner of the poultry slaughterhouse, who generously agreed to sacrifice my animals free of charge, purely in the service of science. Your selfless support and willingness to contribute to the advancement of this research are deeply appreciated. This act of kindness has been crucial to the success of

my project, and I am truly grateful for your dedication to helping further scientific knowledge.

I am deeply grateful to **Dr. Okka Kamilia** *and* **Dr Benziane Radia** *for their steadfast help and patience in answering all my questions. Their constant support has been invaluable throughout my academic journey, and I am truly grateful for their dedication.*

I would like to express my deepest gratitude to **Dr. Allag Noussaiba**, *whose expertise and dedication were instrumental in interpreting the results of the XRD analysis. Without her invaluable assistance, the findings would have remained ambiguous and lacked significance. Her precision, insight, and willingness to support my research were essential to the success of this study, and I am truly grateful for her contributions.*

It is with great appreciation that I thank **Dr. Belkhir Sami**, *a specialist in anatomopathology, for his expert assistance in preparing and interpreting my tissue slides. I deeply appreciate his time, effort, and invaluable contributions to this study.*

I am deeply grateful to Miss **Goubi Sana**, *the head of the pedagogical laboratories of the Faculty of Natural Sciences and Life at Eloued University, for her invaluable support throughout my research journey. I would also like to extend my thanks to the entire team, especially* **Afaf**, **Bouchra**, *and* **Omar**, *for their assistance, encouragement, and collaboration.*

I am profoundly grateful to **Dr. Chetehouna Sara**, **Boulaares Islam**, **Chouia Maroua** *and* **Hamadi Maroua**, *the esteemed research team at the Laboratory of Biodiversity and Application of Biotechnology in the Agricultural Field, Faculty of Natural Sciences and Life. Their invaluable guidance, support, and expertise have been instrumental in the completion of this work, and I deeply appreciate their priceless contributions to my research journey.*

My heartfelt thanks to Madam **Nis Nedjla** *for her unconditional support and dedication. Her help, always offered with an open heart, has made a significant difference in the lives of many students. Working within the university's academic services, she has been a constant source of guidance and kindness throughout my academic journey.*

I also extend my gratitude to various institutions, national and international, for providing the necessary research facilities to accomplish this work: Scientific and Technical Research Centers in Physico-chemical Analysis (CRAPC) in Biskra and Ouergla, Faculty of Food Science and Nutrition, Faculty of Plant Breeding at the university of life sciences in Poznan, Poland, Tissue culture laboratory, Faculty of Pharmacy, Universiti Teknologi Mara, Selangor, Malaysia, and Nanotechnology research center, Sultan Qaboos University, Oman.

This thesis would not have been possible without the guidance and support of many remarkable individuals, whose help I will forever cherish.

Abstract

This study aims to evaluate the synthesis, characterization, and biological activities—including antioxidant, anti-inflammatory, antibacterial, and antitumor properties—of copper nanoparticles (CuNPs) biosynthesized using aqueous extracts from the leaves and rhizomes of *Phragmites australis*. Furthermore, the study assesses the in vivo safety, toxicity, and potential biovaccination effect of these CuNPs in a broiler chicken model, with a focus on growth performance, survival rate, and physiological biomarkers. The plant extracts have previously undergone both quantitative and qualitative phytochemical analysis. To confirm their size, shape, and stability CuNPs were characterized using various analytical techniques, such as UV-Vis spectroscopy, FTIR, SEM, TEM, XRD, and Zeta potential. *In vitro* assessments were conducted to evaluate the antioxidant and anti-inflammatory properties of both plant extracts and plant-based NPs using standard protocols. The investigation of antibacterial efficacy was performed on both Gram-positive and Gram-negative bacterial strains utilizing the disk diffusion method, wherein the copper nanoparticles synthesized from *P. australis* exhibited intermediate effectiveness. The anti-tumor activity of the plant-based CuNPs was assessed using the MTT assay. Following the *in vitro* studies, *in vivo* experiments were performed in two phases: the first aimed to determine the acute toxicity of the NPs on 15 broiler chickens (Arbor Acres) divided into 5 groups 3 in each: control, 25 mg/Kg BW (Leaf-based CuNPs), 25 mg/Kg BW (Rhizome-based CuNPs), 50 mg/Kg BW (Leaf-based CuNPs), and 50 mg/Kg BW (Rhizome-based CuNPs), while the second phase evaluated the biovaccination effect of the NPs on 100 one-day-old broiler chicks that were randomly divided into five groups (n=20). The first group was injected into the breast muscle, on day 4, with 5mg/Kg BW of leaf-based CuNPs, the second group with 5mg/Kg BW of rhizome-based CuNPs, the third group with a mixture of both synthesized CuNPs (Leaf and rhizome-based CuNPs), the fourth group was left without any injection and the fifth group received the standard vaccination and medication. The three first groups were re-injected after 10 days with the same dose of the plant-based CuNPs, and after 10 days with a double dose. Four birds from each group were sacrificed 4 days after the last injection. Various hematological, biochemical, and oxidative stress parameters were assessed in both study phases. Liver histology was studied as well. Results of the phytochemical analysis of the plant extracts demonstrate their richness of different active compounds: phenols, flavonoids, and terpenoids which may explain the important anti-inflammatory activity revealed according to hemolysis assay results. Regarding the characterization of *P. australis*-based Cu NPs, the UV-Vis absorption spectra indicated prominent peaks at 312 nm and 300 nm for copper nanoparticles derived from leaf and rhizome sources, respectively. The crystalline structure of the phyto-synthesized Cu NPs was substantiated through X-ray diffraction (XRD) analysis, revealing an estimated grain size of 18.06 nm for leaf-based Cu

NPs and 18.24 nm for rhizome-based counterparts. Furthermore, the average diameter of Cu NPs was calculated to be 13.22 nm for those derived from leaf sources and 19.76 nm for those originating from rhizome sources. Additionally, the synthesized nanoparticles demonstrated significant antioxidant properties, as evidenced by IC_{50} values of 4.62 µg/ml and 78.99 µg/ml in DPPH and FRAP assays, respectively, for leaf-derived Cu NPs. The IC_{50} values associated with anti-inflammatory activity in both assessments were notably pronounced, underscoring the considerable potential of green-synthesized Cu NPs. The cytotoxic effects of *Phragmites australis*-mediated Cu NPs against MCF-7 cell lines exhibited a dose-dependent response at minimal concentrations: 3.53 µg/ml for leaf-derived Cu NPs and 2.28 µg/ml for those derived from rhizomes. Moreover, the acute toxicity findings show some changes in biochemical, hematological, and oxidative stress markers without signaling death. On the other hand, the outcomes of the second phase of the *in vivo* study indicate that the injections of *Phragmites australis*-based Cu NPs had no detrimental impact on the growth and survival of broiler chicks. Their weight gain and overall performance remained comparable to those of chickens that received vaccination, medication, and supplemental nutrition. Notably, the mortality rate in the biovaccinated groups was approximately 8%, whereas it exceeded 50% in the untreated group. This suggests that these nanoparticles may not only support healthy development but also significantly enhance survival rates in broiler chickens. Regarding the final weight at the end of the rearing period, the chickens in the group that received the green nanoparticles treatment exhibited a weight comparable to those in the conventional treatment group. More notably, the group that received a mixture of *P. australis*-based copper nanoparticles surpassed the weight of the conventional group, reaching an average of 3,2 kg, compared to 3,09 kg in the conventionally treated group. These findings highlight the potential of *P. australis*-based copper nanoparticles treatments, especially when combined, to positively influence growth and weight gain in broiler chickens. This study points out the valuable advantages of copper nanoparticles (Cu NPs) as a harmless, cost-effective, and efficient product in broiler chicken farming. Additional research is imperative to examine the fundamental mechanisms and long-term consequences of integrating Cu NPs into broiler farming, to optimize production outcomes and enhance the performance of the birds.

Keywords: *Phragmites australis,* Cu NPs, broiler chicken, oxidative stress, cytotoxicity.

Résumé

Cette étude vise à évaluer la synthèse, la caractérisation et les activités biologiques — y compris les propriétés antioxydantes, anti-inflammatoires, antibactériennes et antitumorales — des nanoparticules de cuivre (CuNPs) biosynthétisées à partir d'extraits aqueux des feuilles et des rhizomes de *Phragmites australis*. De plus, l'étude examine la sécurité, la toxicité et l'effet potentiel de biovaccination de ces CuNPs in vivo dans un modèle de poulets de chair, en se concentrant sur la performance de croissance, le taux de survie et les biomarqueurs physiologiques. Les extraits de plantes ont préalablement fait l'objet d'analyses phytochimiques qualitatives et quantitatives. Pour confirmer leur taille, leur forme et leur stabilité, les CuNPs ont été caractérisées à l'aide de diverses techniques analytiques telles que la spectroscopie UV-Vis, la spectroscopie FTIR, la microscopie électronique à balayage (SEM), la microscopie électronique en transmission (TEM), la diffraction des rayons X (XRD) et le potentiel Zêta.

Des évaluations in vitro ont été menées pour étudier les propriétés antioxydantes et anti-inflammatoires des extraits végétaux ainsi que des nanoparticules d'origine végétale, selon des protocoles standard. L'efficacité antibactérienne a été testée sur des souches bactériennes Gram-positives et Gram-négatives, en utilisant la méthode de diffusion sur disque, où les nanoparticules de cuivre synthétisées à partir de *P. australis* ont montré une efficacité intermédiaire. L'activité antitumorale des CuNPs d'origine végétale a été évaluée à l'aide du test MTT.

À la suite des études in vitro, des expériences in vivo ont été réalisées en deux phases : la première visait à déterminer la toxicité aiguë des nanoparticules sur 15 poulets de chair (Arbor Acres) répartis en 5 groupes de 3 sujets chacun : groupe témoin, 25 mg/Kg de poids corporel (CuNPs à base de feuilles), 25 mg/Kg (CuNPs à base de rhizomes), 50 mg/Kg (CuNPs à base de feuilles) et 50 mg/Kg (CuNPs à base de rhizomes). La seconde phase a évalué l'effet de biovaccination des nanoparticules sur 100 poussins d'un jour, répartis aléatoirement en cinq groupes (n=20). Le premier groupe a reçu, par injection dans le muscle pectoral au 4^{e} jour, 5 mg/Kg de CuNPs à base de feuilles, le deuxième groupe a reçu la même dose de CuNPs à base de rhizomes, le troisième groupe a reçu un mélange des deux types de CuNPs (feuilles et rhizomes), le quatrième groupe n'a reçu aucune injection et le cinquième groupe a reçu la vaccination et le traitement standard.

Les trois premiers groupes ont été réinjectés après 10 jours avec la même dose de CuNPs d'origine végétale, puis après 10 jours supplémentaires avec une double dose. Quatre oiseaux de chaque groupe ont été sacrifiés 4 jours après la dernière injection. Divers paramètres hématologiques, biochimiques et de stress oxydatif ont été évalués dans les deux phases de l'étude. L'histologie hépatique a également été étudiée.

Les résultats de l'analyse phytochimique des extraits végétaux ont révélé une richesse en composés actifs variés : phénols, flavonoïdes et terpénoïdes, ce qui pourrait expliquer l'activité anti-inflammatoire significative mise en évidence par les résultats du test d'hémolyse. En ce qui concerne la caractérisation des CuNPs à base de *P. australis*, les spectres d'absorption UV-Vis ont montré des pics marqués à 312 nm pour les nanoparticules dérivées des feuilles et à 300 nm pour celles issues des rhizomes. La structure cristalline des CuNPs phyto-synthétisées a été confirmée par l'analyse de diffraction des rayons X (XRD), révélant une taille de grain estimée à 18,06 nm pour les CuNPs à base de feuilles et 18,24 nm pour celles à base de rhizomes. Par ailleurs, le diamètre moyen des CuNPs a été calculé à 13,22 nm pour celles dérivées des feuilles et à 19,76 nm pour celles issues des rhizomes. De plus, les nanoparticules synthétisées ont démontré des propriétés antioxydantes importantes, comme en témoignent les valeurs IC50 de 4,62 µg/ml et 78,99 µg/ml dans les tests DPPH et FRAP respectivement, pour les CuNPs à base de feuilles. Les valeurs IC50 associées à l'activité anti-inflammatoire dans les deux évaluations étaient particulièrement marquées, soulignant le potentiel considérable des nanoparticules de cuivre (Cu NPs) synthétisées par voie verte. Les effets cytotoxiques des Cu NPs médiées par *Phragmites australis* sur les lignées cellulaires MCF-7 ont montré une réponse dose-dépendante à de faibles concentrations : 3,53 µg/ml pour les Cu NPs dérivées des feuilles et 2,28 µg/ml pour celles issues des rhizomes.

Par ailleurs, les résultats relatifs à la toxicité aiguë ont révélé certaines modifications des marqueurs biochimiques, hématologiques et de stress oxydatif sans provoquer de mortalité. D'un autre côté, les résultats de la deuxième phase de l'étude in vivo indiquent que les injections de Cu NPs à base de *Phragmites australis* n'ont eu aucun effet néfaste sur la croissance ni la survie des poussins de chair. Leur prise de poids et leur performance globale sont restées comparables à celles des poulets ayant reçu la vaccination, la médication et une supplémentation nutritionnelle.

Fait notable, le taux de mortalité dans les groupes biovaccinés était d'environ 8 %, contre plus de 50 % dans le groupe non traité. Cela suggère que ces nanoparticules pourraient non seulement favoriser un développement sain, mais aussi améliorer significativement les taux de survie chez les poulets de chair.

Concernant le poids final à la fin de la période d'élevage, les poulets du groupe ayant reçu le traitement par nanoparticules vertes présentaient un poids comparable à celui du groupe traité de manière conventionnelle. Plus encore, le groupe ayant reçu un mélange de nanoparticules de cuivre à base de *P. australis* a dépassé le poids du groupe conventionnel, atteignant une moyenne de 3,2 kg contre 3,09 kg dans le groupe traité classiquement. Ces résultats mettent en évidence le potentiel des traitements à base de nanoparticules de cuivre issues de *P. australis*, en particulier

lorsqu'ils sont combinés, pour influencer positivement la croissance et la prise de poids des poulets de chair.

Cette étude souligne les avantages prometteurs des nanoparticules de cuivre (Cu NPs) en tant que solution inoffensive, économique et efficace dans l'élevage de poulets de chair. Des recherches supplémentaires sont essentielles pour explorer les mécanismes fondamentaux et les effets à long terme de l'intégration des Cu NPs dans l'aviculture, afin d'optimiser les rendements de production et d'améliorer la performance des volailles.

Mots-clés : *Phragmites australis*, Cu NPs, poulet de chair, stress oxydatif, cytotoxicité.

الملخص

تهدف هذه الدراسة إلى تقييم عملية تخليق وتوصيف الأنشطة البيولوجية — بما في ذلك الخصائص المضادة للأكسدة، والمضادة للالتهابات، والمضادة للبكتيريا، والمضادة للأورام — لجسيمات النحاس النانوية (CuNPs)التي تم تخليقها بيولوجيًا باستخدام مستخلصات مائية من أوراق وجذامير نبات القصب .بالإضافة إلى ذلك، تقيّم الدراسة السلامة والتسمم والتأثير المحتمل للتلقيح البيولوجي لهذه الجسيمات النانوية في نموذج دجاج التسمين، مع التركيز على أداء النمو، ومعدل البقاء على قيد الحياة، والعلامات الحيوية الفسيولوجية . خضعت المستخلصات النباتية لتحليل كيميائي نباتي كمي ونوعي قبل استعمالها في تصنيع الجسيمات النانوية. هذه الأخيرة تم توصيفها باستخدام تقنيات تحليلية مختلفة للتأكد من حجمها وشكلها واستقرارها، مثل مطيافية الاشعة المرئية وفوق البنفسجية والمجهر الالكتروني الماسح والنافذ والاشعة السينية الخاصة بالبلورات ومطيافية الاشعة تحت الحمراء وقياس جهد زيتا. كما تم اجراء تقييمات مختبرية لمعرفة الخصائص المضادة للأكسدة والمضادة للالتهابات لكل من المستخلصات النباتية والجسيمات النانوية باستخدام البروتوكولات المتعارف عليها. هذا واظهرت جزيئات النحاس النانوية نشاطا مضادا للبكتريا ملحوظا وذلك باستخدام طريقة انتشار القرص على كل من البكتيريا موجبة وسالبة الغرام . كما تم تقييم النشاط المضاد للأورام للجسيمات النانوية باستخدام اختبار MTT . بعد الدراسات المختبرية، أُجريت التجارب في الجسم الحي على مرحلتين: الأولى تهدف إلى تقييم السمية لجسيمات النانو على 15 دجاجة من دجاج التسمين مقسمة إلى 5 مجموعات 3 في كل منها: مجموعة ضابطة ومجموعة حقنت في العضلة بـ25 مغ\ كغ وزن الجسم بجسيمات نانوية صنعت باوراق القصب واخرى بنفس الجرعة من جسيمات نانوية صنعت بجذامير القصب. في حين قيّمت المرحلة الثانية التأثير الدوائي للجسيمات النانوية على 100 كتكوت دجاج التسمين بعمر يوم واحد تم تقسيمها عشوائيًا إلى خمس مجموعات (ن=20). المجموعة الأولى تم حقنها في عضلة الصدر، في اليوم الرابع، ب 5 مغ/كغ من الجسيمات النانوية النحاسية الورقية ، والمجموعة الثانية ب 5 مغ/كغ من الجسيمات النانوية النحاسية الجذمورية ، والمجموعة الثالثة بمزيج من كلتا الجسيمات النانوية النحاسية ا (الجسيمات النانوية النحاسية الورقية والجذمورية)، والمجموعة الرابعة تُركت بدون أي حقن، أما المجموعة الخامسة فقد تلقت التطعيم والدواء المعتمد عليه في مزارع التسمين. وأُعيد حقن المجموعات الثلاث الأولى بعد 10 أيام بنفس الجرعة من الجسيمات النانوية النحاسية النباتية الأصل، وبعد 10 أيام بجرعة مضاعفة. تمت التضحية بأربعة دجاجات من كل مجموعة بعد 4 أيام من الحقن الأخير وتم تقييم مختلف معايير تحليل الدم والكيمياء الحيوية والإجهاد التأكسدي في كلتا مرحلتي الدراسة. كما تمت الدراسة التشريحية للكبد أيضًا. أظهرت نتائج التحليل الكيميائي النباتي للمستخلصات النباتية ثراءها بالمركبات النشطة المختلفة: الفينولات والفلافونويدات والتربينويدات التي قد تفسر النشاط المهم المضاد للالتهابات الذي تم الكشف عنه وفقًا لنتائج فحص انحلال الدم. وفيما يتعلق بتوصيف جسيمات النحاس النانوية المصنوعة من مستخلصات نبات القصب, أشارت أطياف الامتصاص بالأشعة فوق البنفسجية والمرئية إلى قمم بارزة عند 312 نانومتر و300 نانومتر للجسيمات النانوية النحاسية

المصنوعة من الأوراق والجذامير على التوالي. تم إثبات التركيب البلوري لجسيمات النحاس النانوية المصنعة نباتيًا من خلال تحليل حيود الأشعة السينية (XRD)، وكشف عن حجم حبيبات يقدر ب 18.06 نانومتر للجسيمات المستمدة من الأوراق و18.24 نانومتر لنظيراتها المستمدة من الجذامير. وعلاوة على ذلك، تم حساب متوسط قطر جسيمات النحاس النانوية ليكون 13.22 نانومترًا لتلك المشتقة من الأوراق و19.76 نانومترًا لتلك المشتقة من الجذامير. وبالإضافة إلى ذلك، أظهرت الجسيمات النانوية المُصنَّعة خصائص كبيرة مضادة للأكسدة، كما يتضح من قيم IC_{50} التي بلغت 4.62 ميكروغرام/مل و78.99 ميكروغرام/مل في اختبارات DPPH وFRAP على التوالي لجسيمات النحاس النانوي المشتق من الأوراق. أما قيم IC_{50} المرتبطة بالنشاط المضاد للالتهابات فكانت مهمة مما يؤكد الإمكانات الكبيرة لجسيمات النحاس النانوي على مكافحة الالتهاب. أظهرت التأثيرات السامة للجسيمات النانوية النحاسية على الخلايا السرطانية MCF-7 فعالية تعتمد على الجرعة عند تركيزات ضئيلة: 3.53 ميكروغرام/مليلتر بالنسبة للجسيمات النحاسية المشتقة من الأوراق و2.28 ميكروغرام/مليلتر بالنسبة لتلك المشتقة من الجذامير. وعلاوة على ذلك، أظهرت نتائج السمية الحادة بعض التغيرات في علامات الكيمياء الحيوية والدموية والإجهاد التأكسدي دون حدوث موت الحيوانات. من ناحية أخرى، تشير نتائج المرحلة الثانية من الدراسة في الجسم الحي إلى أن حقن الجسيمات النحاسية النانوية المصنوعة بمستخلصات نبات القصب كتلقيح بيولوجي لم تحدث أي آثار سلبية على نمو كتاكيت التسمين فقد كان معدل الوفيات في المجموعة المعالجة حوالي 8%، مقارنة بأكثر من 50% في المجموعة غير المعالجة، مما يشير إلى دور هذه الجسيمات النانوية في تحسين معدلات البقاء على قيد الحياة . أما بالنسبة للوزن النهائي عند نهاية فترة التربية، فقد كان وزن الدجاج في المجموعة التي تلقت العلاج النانوي مماثلًا للمجموعة التي خضعت للعلاج التقليدي. والأهم من ذلك، أن المجموعة التي تلقت مزيجًا من الجسيمات النانوية تجاوزت وزن المجموعة التقليدية، حيث بلغ متوسط وزنها 3.2كجم، مقارنة بـ 3.09كجم في المجموعة التي تلقت العلاج التقليدي. هذه النتائج تؤكد أن استخدام الجسيمات النانوية، خاصة عند دمجها كمزيج، قد يكون له تأثيرإيجابي على النمو وزيادة وزن الدجاج اللاحم. تشير هذه الدراسة إلى المزايا القيّمة لجسيمات النحاس النانوية (CuNPs) كمنتج غير ضار وفعال وغيرمكلف في تربية دجاج التسمين، غيرأنه من الضروري إجراء المزيد من البحوث الإضافية لدراسة الآليات الأساسية لعملها والنتائج طويلة الأمد لدمج جسيمات النحاس النانوية في تربية دجاج التسمين، لتحسين نتائج الإنتاج وتعزيز أداء الطيور.

الكلمات المفتاحية: نبات القصب، جسيمات النحاس النانوية ، دجاج التسمين، الإجهاد التأكسدي، السمية الخلوية.

Figures list

Figure 1: Sources of oxidative stress and its impact on poultry (M Estévez, 2015). 9
Figure 2: *Phragmites australis* (Original photo, 2024). 14
Figure 3: The different approaches for synthesizing nanoparticles (Altammar, 2023). 20
Figure 4: Schematic representation of green synthesis of nanoparticles (Altammar, 2023) 21
Figure 5: Preparation method of P. australis aqueous extract. 27
Figure 6: Schematic representation of plant-based CuNPs acute toxicity study. 33
Figure 7: Biovaccination experimental design. 35
Figure 8: Spectrum of GC-MS analysis and their volatile compounds representation of *P. australis* leaf extract. 43
Figure 9: Spectrum of GC-MS analysis and their volatile compounds representation of *P. australis* rhizomes extract. 45
Figure 10: Color change during the formation of copper nanoparticles. 46
Figure 11: Schematic representation of the formation of Cu NPs via *P. australis* extract. 46
Figure 12: FT-IR Spectra of *P.australis* leaf extract (A) and phytosynthsized CuNPs (B). 47
Figure 13: FT-IR Spectra of *P.australis* rhizome extract (A) and phytosynthsized CuNPs (B). 47
Figure 14: UV-Vis spectrum of CuNPs synthesized using *P.australis* leaf extract (A), and rhizome extract (B). 48
Figure 15: Characterization of Cu NPs synthesized using *P.australis* leaf extract using SEM (A), TEM (B) and size distribution analysis (C). 49
Figure 16: Characterization of Cu NPs synthesized using *P.australis* rhizome extract using SEM (A), TEM (B) and size distribution analysis (C). 50
Figure 17: XRD patterns of CuNPs synthesized using *P.australis* leaves(A) and rhizomes (B). 51
Figure 18: Zeta potential measurement of both leaf and rhizome-based Cu NPs. 52
Figure 19: IC_{50} values of the antioxidant activity, using DPPH assay, of the plant extract (A) and the plant-based Cu NPs (B). 52
Figure 20: IC_{50} values of the antioxidant activity, using FRAP assay, of the plant extract (A) and the plant-based CuNPs (B). 53
Figure 21: IC_{50} values of the anti-inflammatory activity, using BSA assay. 54
Figure 22: IC_{50} values of the anti-inflammatory activity, using hemolysis assay. 54
Figure 23: Anti-bacterial activity of both leaf and rhizome-based Cu NPs against gram (+) and gram (-) bacterial strains. 56

Figure 24: Absorbance variation (A), cytotoxicity percentage (B) and microscopic section of anti-proliferative activity of leaf extract-based CuNP (D) against MCF-7cells line compared to untreated cells (C). 56

Figure 25: Absorbance variation (A), cytotoxicity percentage (B) and microscopic section of anti-proliferative activity of rhizome extract-based CuNP (D) against MCF-7cells line compared to untreated cells (C). 57

Figure 26: MDA levels in different organs. 60

Figure 27: GSH levels in different organs.....61

Figure 28: SOD levels in different organs.....61

Figure 29: Histological examination of the liver of control and treated groups stained with hematoxylin (X10 and X40).....63

Figure 30: Hematological parameters of different groups analyzed using ANOVA. 65

Figure 31: MDA levels in muscle and liver. 66

Figure 32: Glycogen values in muscle and liver. 67

Figure 33: Photomicrographs of the liver of different groups stained with hematoxylin (X10, X40). 69

Figure 34: Final weight of all experimental groups during the rearing period. 70

Figure 35: Mortality rate of all experimental groups. 70

Tables list

Table 01: Broilers' vaccination program. 7
Table 02: Main characteristics of CuNPs. 20
Table 03: Procedure of SOD activity assay 36
Table 04: Phytochemical screening of the aqueous extract of *Phragmites australis*. 39
Table 05: Phenolic and flavonoid content of *P.australis* aqueous extract. 39
Table 06: Quantification of volatile compounds by GC-MS of *P. australis* leaf extract. 40
Table 07: Quantification of volatile compounds by GC-MS of *P. australis* rhizome extract. 44
Table 08: Inhibition zone values (mm) of the tested bacterial strains and their corresponding antibiotics. 54
Table 09: Birds' behavior within 24 hours post green CuNPs injection. 57
Table 10: Body weight and relative weight of broilers. 58
Table 11: Hematological parameters of control and experimental groups. 58
Table 12: Biochemical parameters of treated and control groups. groups. 59

Abbreviation list

1XPBS	Phosphate-Buffered Saline
ALT	Alanine aminotransferase
AST	Aspartate aminotransferase
BSA	Bovine Serum Albumin
Conv	Conventional treatment of broilers
DMSO	Dimethyl sulfoxide
DPPH	1,1-diphenyl-2-picryhydrazyl
DTNB	-5'-dithiobis2-nitrobenzoic acid
FCR	Folin-Ciocalteu Reagent
FRAP	Ferric reducing ability of plasma
FTIR	Fourier Transform Infrared spectroscopy
GAE	Gallic acid equivalents
GC-MS	Gas chromatography- mass spectrometry
GD	Gumboro disease
GSH	Reduced Glutathion
HGB	Haemoglobin
HTC	Haematocrit
IP	Inhibition percentage
IR	Infrared spectroscopy
LP-Cu NPs	*Phragmites australis* leaf-based Cu NPs
MDA	Malondialdehyde
MP-Cu NPs	Mixture of both extracts of *Phragmites australis*
MTT	3-[4,5-dimethylthiazole-2-yl]-2, 5-diphenyl tetrazolium bromide
ND/IB	New Castle disease/ Infectious Bronchitis
NBT	Nitro blue Tetrazolium Chloride
RBC	Red blood cell
ROS	Reactive oxygen species
RP-Cu NPs	*Phragmites australis* rhizome-based Cu NPs
SDS	sodium dodecyl sulfate
SEM	Scanning electron microscopy
SOD	Superoxide dismutase
SPR	Surface plasmon resonance
TBA	Thiobarbituric Acid

TBS	Tert-Butyldimethyl Silyl Ethers
TCA	Trichloroacetic acid
TEM	Transmission electron microscopy
TFC /TPC	Total flavonoid content/ Total phenolic content
UV-Vis	Ultraviolet–visible
WBC	White blood cell
XRD	X-ray diffraction

Content

Dedication.....

Acknowledgment.....

Abstract.....

Figures list.....

Tables list.....

Abbreviation list.....

Content.....

INTRODUCTION.....**1**

Literature Review

Chapter I: **Broiler Chicken Farming**

I. Nutritional Value of Broiler.....6

II. Antibiotic Use and Public Health Risks.....6

III. Vaccination Program.....7

IV. Oxidative Stress in Poultry.....8

IV.1. Sources of Oxidative Stress in Poultry.....8

IV.2. Oxidative Stress and Meat Quality.....10

IV.3. Mitigating Oxidative Stress in Poultry.....11

Chapter II: **Phragmites australis.**

I. Taxonomic and botanical description.....13

II. Genetic and Morphological Diversity.....13

III. Potential Applications of Phragmites australis.....14

IV. Traditional Medicine Applications.....15

Chapter III: Nanotechnology

I. Definition of Nanotechnology.....17

II. Nanoparticles.....17

II.1. Definition and Classification.....17

II.2. Properties of Nanoparticles.....18

III. Metal Nanoparticles.....19

III.1. Copper Nanoparticles (CuNPs).....19

IV. Metal NPs Synthesis Approaches.....20

IV.1. Green Synthesis of NPs.....20

V. Advantages and Challenges.....22

VI. Application of Nanotechnology.....22

Experimental Part

Chapter I: Materials & Methods

I. Materials....26
I.1. Plant Collection....26
I.2. Animal Material....26
II. Methods....26
II.1. In vitro study....26
II.1.1. P.australis Aqueous Extract Preparation....26
II.1.2. P. australis Phytochemical Analysis....27
II.1.3. Total Phenolic and Flavonoid Compounds....28
II.1.4. GC-MS Analysis....29
II.1.5. P.australis-based CuNPs Synthesis....29
II.1.6. P.australis-based CuNPs Characterization....30
II.1.7 Biological Activities....30
II.2. In Vivo Study....33
II.2.1. P.australis-based CuNPs Acute Toxicity....33
II.2.2. Biovaccination Effect of P. australis-based CuNPs....33
II.2.3. Homogenates Preparation and Tissue Biochemical Parameters....35
II.2.4. Oxidative Stress Parameters....35
II.2.5. Liver Histological Study....37
II.3. Statistical analysis....37

Chapter II: Results

I. Part one: In vitro study....39
I.1. In vitro essays of Phragmites australis....39
I.1.1. Phytochemical study....39
I.1.2. GC-MS analysis....39
I.2. P. australis-based CuNPS Synthesis and Characterization....45
I.2.1. Infrared analysis results....46
I.2.2. UV-Vis Spectroscopy results....48
I.2.3. SEM and TEM analysis....48
I.2.4. X- ray Diffraction analysis....50
I.2.5. Stability Analysis....51
I.3. Biological Activities....52
I.3.1. Antioxidant Activity....52

I.3.2. Anti-inflammatory Activity 53
I.3.3. Antibacterial Activity 54
I.3.4. Cytotoxic Activity 56
II. Part Two: In Vivo Study 57
II.1. Acute Toxicity Test of P.australis-based CuNPs 57
II.1.1 Hematological parameters 58
II.1.2. Biochemical parameters 58
II.1.3. Oxidative Stress Evaluation 59
II.1.4. Liver Histopathological Examination 62
II.2. Biovaccination Effect 64

Chapter III: Discussion

Part One: In Vitro Study 72
Qualitative, Quantitative, and Biological Activity Study of Phragmites australis 72
Copper Nanoparticles Study 74
Characterization 74
Biological Activity 76
Part Two: In Vivo Study 78
Acute Toxicity Test of P.australis-based CuNPs 78
Behaviour and Body Weight 78
Study of Hematological Analysis 78
Study of Biochemical Analysis 80
Study of Oxidative Stress Markers 82
Biovaccination Effect of P.australis-based CuNPs 84
Hematological Parameters 84
Lipid Peroxidation Marker 84
Final Body Weight 86
Conclusion & Perspectives 87
References 90
Annex 112

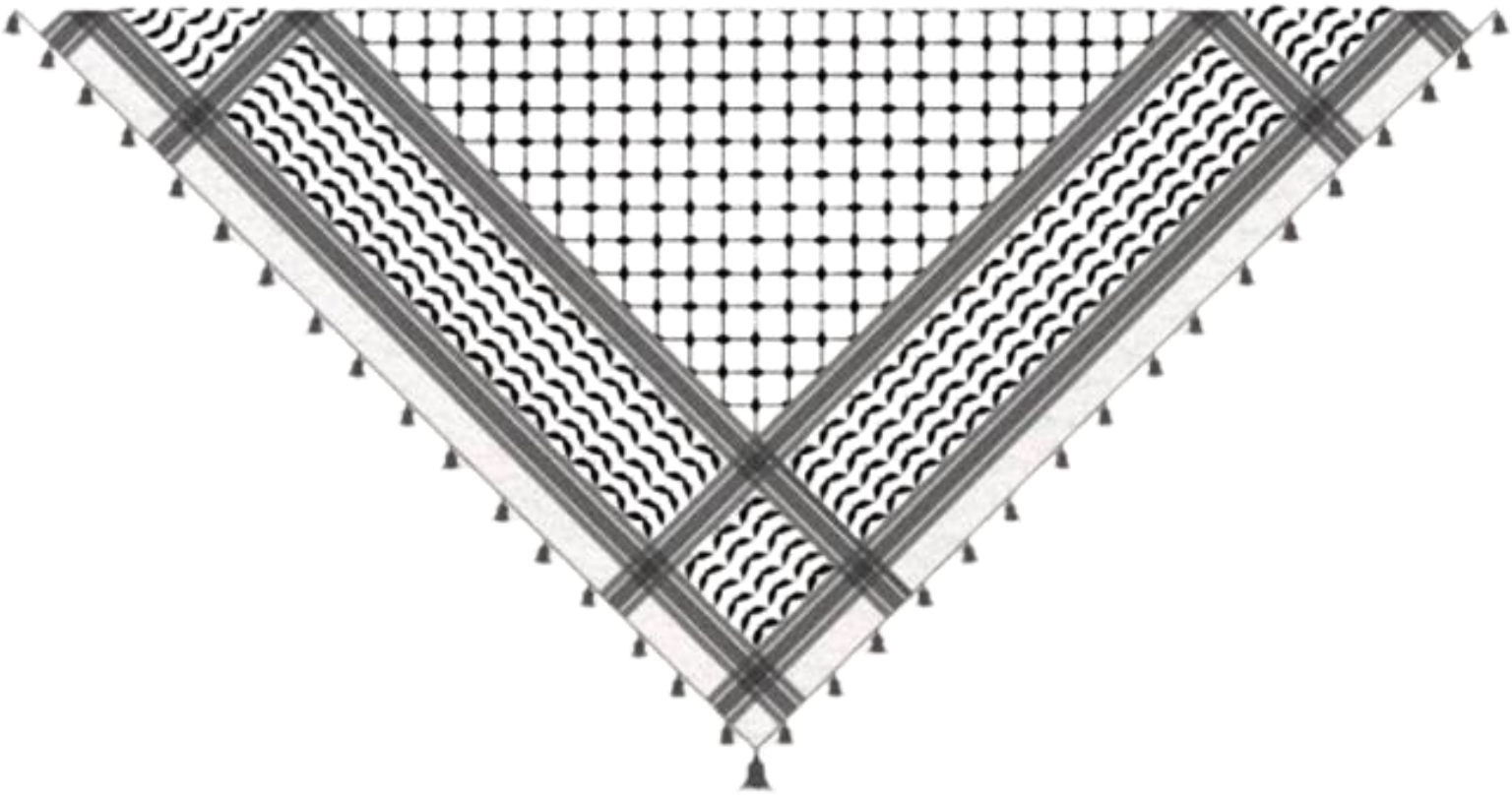

INTRODUCTION

Introduction

Poultry production is experiencing significant growth on a global scale. Among various poultry products, chicken meat is the most widely consumed and its demand continues to escalate. Given that poultry meat is recognized as a fundamental source of animal protein in developing nations and serves as the principal reservoir of high-quality protein, it occupies a pivotal role within their economic structures (Al-Saeedi & Al-Khafaji, 2024). Nonetheless, poultry poses considerable risks to human health, particularly as a vehicle for infectious diseases associated with prominent foodborne pathogens such as Campylobacter, Salmonella, and Listeria (Abu Hafsa, Ibrahim, Eid, & Hassan, 2020; Chowdhury et al., 2023).

The use of plant-based additives in broiler chicken production has attracted considerable interest as a substitute for antibiotics. This method helps to mitigate concerns regarding antibiotic resistance and residues in meat, while also supporting growth and health in poultry (Valli & Kavitha, 2023).

Phragmites australis, commonly referred to as common reed, represents a wetland species characterized by a significant presence of bioactive constituents in aqueous plant extracts, including tannins, phenolic compounds, flavonoids, terpenoids, and glycosides (Oladipo et al., 2020). This plant has been employed in traditional medicine for the treatment of various ailments affecting both humans and livestock (Sohaib, Al-Barakah, Migdadi, & Husain, 2022). Extracts derived from *Phragmites australis* have exhibited notable anti-inflammatory and antiviral properties *in vitro*. These extracts impede the synthesis of inflammatory mediators and pro-inflammatory cytokines, indicating prospective therapeutic applications in the management of inflammation-associated disorders in livestock (Zhu et al., 2017).

Nanotechnology, defined as the precise manipulation of matter at the atomic and molecular dimensions, has significantly revolutionized various fields including healthcare, electronics, and environmental sciences. Central to this innovation is the fabrication of nanoparticles, which are minuscule entities exhibiting distinct properties attributable to their diminutive scale. Recent empirical investigations have revealed that the attributes and potential applications of nanoparticles are contingent upon their phases, dimensions, and morphological characteristics. A burgeoning trend in the synthesis of nanoparticles is the adoption of green technologies, which seek to mitigate ecological ramifications and enhance sustainability (Ahmad et al., 2019; Balasooriya et al., 2017; Iravani, 2011).

Phytonanotechnology refers to the biogenic production of nanomaterials through the utilization of bioactive compounds derived from living organisms, including but not limited to plants, bacteria, fungi, and algae. The phytochemicals, such as phenolic compounds, flavonoids,

and alkaloids, function as bioreducing, stabilizing, and capping agents (Hameed et al., 2023). The eco-friendly synthesis of nanoparticles (NPs) is characterized by its environmental sustainability, economic efficiency, simplicity, and scalability (Abdel-Azeem, Nada, O'Donovan, Thakur, & Elkelish, 2020). Moreover, methodologies for green synthesis frequently yield nanoparticles exhibiting improved biocompatibility and applicability within biomedical and environmental domains (Murugan, Senthilkumar, Senbagam, & Al-Sohaibani, 2014). A variety of metal and metal oxide nanoparticles, including Au, ZnO, Se, Cu, CuO, Fe3O4, Ag, among others, have been fabricated using green technologies for a multitude of biological applications (Hameed et al., 2023; A. A. Mohamed, Abu-Elghait, Ahmed, & Salem, 2021). Nanoparticles have exhibited significant potential in the realm of poultry nutrition, particularly through the utilization of essential mineral nanoparticles, including calcium, zinc, copper, selenium, and chromium. These nanoparticles have been investigated for their prospective advantages in enhancing growth efficiency, feed consumption, and the overall health status of avian species (Patra & Lalhriatpuii, 2020). Furthermore, nanoparticles are being explored as substitutes for antibiotics in broiler chicken farming, drawing notable scholarly interest for their capacity to strengthen immunity, while confronting the challenges related to antibiotic resistance (Naumenko et al., 2023). Empirical evidence suggests that the administration of trace minerals in nanoparticle form not only exerts substantial antibacterial effects against prevalent avian diseases but also fosters gastrointestinal health by encouraging the proliferation of beneficial microorganisms (Dukare et al., 2021).

Copper nanoparticles have demonstrated considerable promise as a viable substitute for conventional antibacterial agents and growth promoters, illustrating resilience against oxidative and thermal adversities (Al-Saeedi & Al-Khafaji, 2024; Patra & Lalhriatpuii, 2020).

Despite the increasing demand for poultry products, the industry continues to face persistent challenges due to infectious diseases and the growing threat of antibiotic resistance. Moreover, not only antibiotics but also vaccines and other chemical molecules are becoming progressively less effective, underscoring the urgent need for alternative, sustainable solutions that protect both animal and human health. In this context, plant-derived bioactive compounds and green-synthesized metal nanoparticles have emerged as promising candidates. Nevertheless, comprehensive studies evaluating their biological efficacy, toxicity, and physiological impacts, particularly in broiler chickens, remain limited.

Therefore, this study aims to assess the following aspects:

1- To provide an extensive examination of the environmentally friendly synthesis of copper nanoparticles utilizing the aqueous extracts derived from *P. australis* (leaves and

rhizomes), emphasizing their antioxidant properties, anti-inflammatory effects, and cytotoxic capabilities, while also accentuating their physicochemical attributes.

2- To investigate the acute toxicity of *P. australis*-based CuNPs, and their biovaccination effect on broiler health, growth, and meat quality.

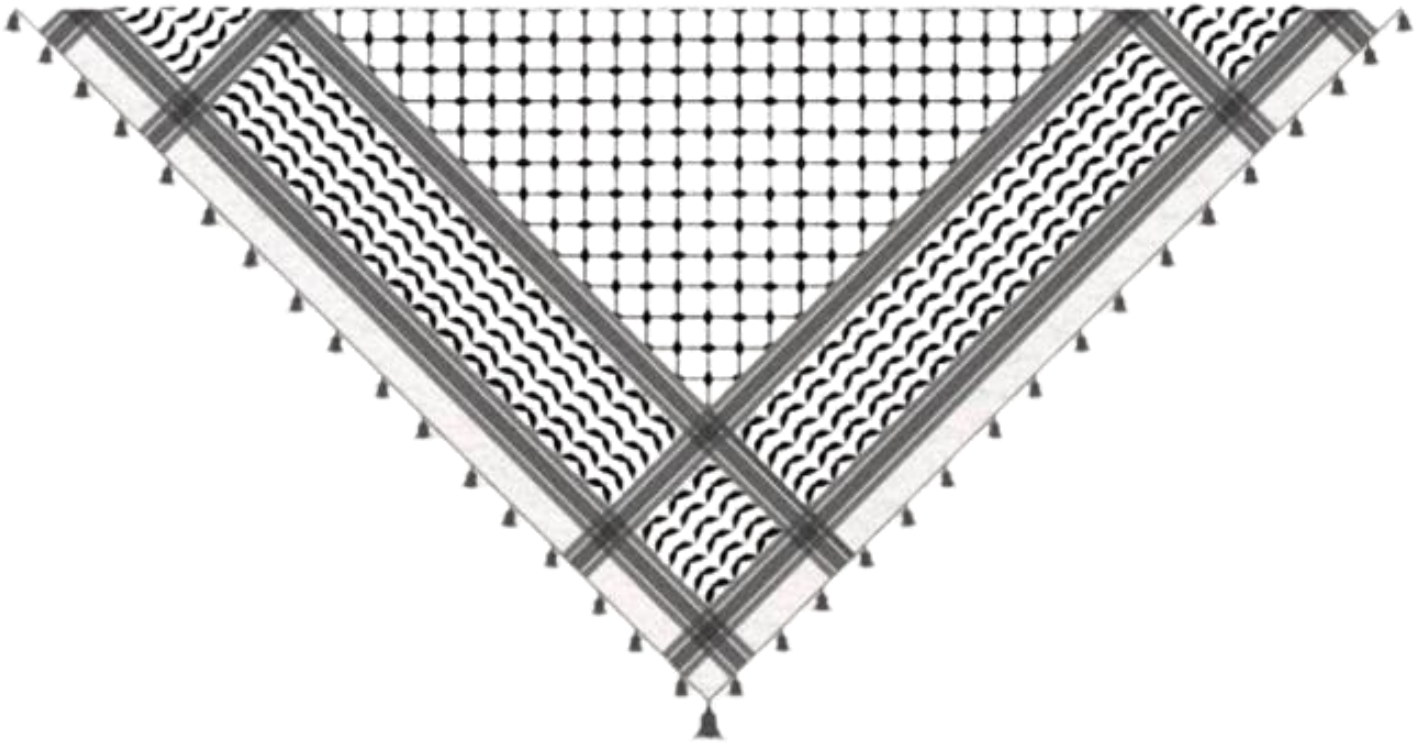

Literature Review

Chapter I
Broiler Chicken Farming

I. Nutritional Value of Broiler

The broiler chicken industry is rapidly expanding, drawing significant research and development efforts aimed at enhancing productivity, health, and resistance to diseases (Hidayat et al., 2024). The broiler sector is instrumental in ensuring food security and generating income, especially within developing nations. Nonetheless, it encounters economic obstacles, including competition from imported goods and the necessity for cohesive policies that promote sustainable methodologies (Lekhisa & Muroyiwa, 2024; Queenan et al., 2021).

Broiler chickens are primarily raised for meat production due to their soft, tender meat, low-fat content, and short production cycle. Globally, broilers play a significant role in enhancing food security, providing a reliable protein source, and contributing to employment opportunities in the agricultural sector. Their rapid growth and efficient feed conversion make them a valuable food animal, supporting both local economies and global food demands (Kryger, Thomsen, Whyte, & Dissing, 2010).

Broiler breast musculature comprises roughly 21-23% protein and 1.90-1.97% lipid content, whereas the thigh musculature contains 19.03-19.93% protein and 4.70-6.05% lipid content (Kralik & Kralik, 2017). Moreover, broiler meat serves as a substantial source of vital minerals including phosphorus, magnesium, iron, copper, and manganese, with the pectoral muscles contributing significantly to the nutrient reference values associated with these minerals (Goluch et al., 2023). It is also a significant source of essential amino acids, such as lysine, methionine, and threonine, which play a vital role in promoting human health (Radu-Rusu, Vacaru-Opris, & Usturoi, 2010). In terms of fatty acid composition, the muscular tissue of the thigh exhibits a greater concentration of omega-3 fatty acids in comparison to the breast muscular tissue, which is characterized by a more dietary profile. Furthermore, the cholesterol concentration in thigh muscles is elevated, attaining levels of 82-83 mg per 100 g (Radu-Rusu et al., 2010).

While broiler meat serves as a valuable nutritional resource, its inherent nutritional attributes may be affected by a multitude of variables, encompassing the formulation of feed and the methodologies employed in rearing practices. The incorporation of targeted feed additives and alterations in dietary composition can augment the nutritional characteristics of broiler meat, thereby rendering it significantly more advantageous for human ingestion (Choi, Kong, Bowker, Zhuang, & Kim, 2023).

II. Antibiotic Use and Public Health Risks

The rearing of chickens is facilitated through the consistent application of antibiotics, which serve not only to prevent and treat diseases but also to enhance bodily growth. The excessive and

improper utilization of antibiotics in livestock is exacerbating the escalating concern of antibiotic resistance (Haque et al., 2020).

Antibiotics represent a critical category of compounds in veterinary pharmacology that are crucial to both animal dietary requirements and the management of livestock production. The administration of antibiotics for addressing bacterial infections is, to a considerable extent, indispensable (Arsène et al., 2022).

Antibiotics are employed in broiler production for curative applications, prophylactic measures, and as agents for growth promotion. Their efficacy in augmenting growth is attributable to the enhancement of feed conversion efficiency and the mitigation of disease prevalence, which consequently elevates economic returns (Alabi, Makinde, Egena, Mbajiorgu, & Adewara, 2024).

The occurrence of antibiotic residues in broiler meat presents significant health hazards to consumers, encompassing allergic responses, toxicity, and the emergence of antibiotic-resistant bacterial strains. Furthermore, these residues have the potential to interfere with the soil microbial community upon their excretion into the environment (Arsène et al., 2022; Nirala, Anjana, Mandal, & Jayachandran, 2018).

The application of antibiotics in the context of broiler production is currently subject to critical examination owing to the potential emergence of drug-resistant bacterial strains. A paradigm shift towards antibiotic-free production is occurring, propelled by consumer preferences and public health considerations. Nonetheless, this transition poses significant challenges in ensuring both food safety and the welfare of chickens in the absence of antibiotic usage (Haque et al., 2020).

III. Vaccination Program

Vaccination constitutes a fundamental element in the prophylaxis of diseases within broiler production. In Algeria, a multitude of vaccination protocols are utilized to address prevalent avian diseases.

Table 01 provides a simplified vaccination program offered by LAPROVET, which is a French veterinary laboratory involved in the development of livestock sectors in Africa (Akue, Lare, & Talaki, 2023).

Table 01: Broilers' vaccination program.

Age	Treatment/ Vaccination	Mode of Administration
Day 1	Primo vaccine Newcastle Disease (ND) Infectious bronchitis (IB)	Beak dipping or nebulization
Day 1-3	Anti-stress	Drinking water
Day 4-6	Hepatoprotective	Drinking water
Day 7	Primo vaccine Gumboro	Drinking water
Day 7-10	Vitamin complex	Drinking water

Day 14	Gumboro vaccine booster	Drinking water
Day 14-16	Hepatoprotective	Drinking water
Day 17	Newcastle vaccine booster	Nebulization or drinking water
Day 17-18	Vitamin complex	Drinking water
Day 19	Infectious bronchitis vaccine	Nebulization or drinking water
Day 19-20	Vitamin complex	Drinking water
Day 21	Gumboro vaccine booster	Drinking water
Day 21-23	Minerals and trace elements	Drinking water
Day 24-26	Anticoccidial	Drinking water
Day 30	Newcastle booster vaccine	Nebulization or drinking water

IV. Oxidative Stress in Poultry

Oxidative stress (OS) is defined as a pathological state that is distinguished by an imbalanced ratio between pro-oxidants and antioxidants, favoring the accumulation of pro-oxidants (Derouiche, Djermoun, & Abbas, 2017). OS occurs when the concentration of reactive species (RS) exceeds the capacity of animal cells to utilize antioxidants effectively (Derouiche, Degachi, & Gharbi, 2020). The body perpetually produces reactive oxygen species (ROS) as a consequence of standard metabolic processes (Derouiche, Chetehouna, & Atoussi, 2022). ROS are predominantly generated within the mitochondrial respiratory chain, and their overproduction subsequently exerts detrimental effects on the mitochondrial respiratory chain, culminating in mitochondrial dysfunction (Z. Chen et al., 2022). These compounds possess intense reactivity and are capable of modifying a diverse array of crucial macromolecules within biological systems. Such phenomena lead to oxidative stress and resultant oxidative damage, which subsequently contribute to the development of various metabolic dysfunctions (Derouiche & Kechrid, 2013). Oxidative stress induces the oxidation of proteins and lipids within muscle tissues, which subsequently compromises the nutritional quality of chicken meat. This phenomenon culminates in suboptimal appearance, texture, juiciness, tenderness, and olfactory attributes, all of which are essential for consumer approval (Nawaz & Zhang, 2021). Moreover, deterioration of mitochondrial functionality and disturbances in calcium homeostasis may precipitate pathological states such as ferroptosis, subsequently exacerbating the quality of meat by augmenting moisture exudation, also known as drip loss, and shear strength, while concurrently diminishing the pH level (Z. Chen et al., 2022).

IV.1. Sources of Oxidative Stress in Poultry

Oxidative stress in poultry is a multifaceted issue arising from various endogenous and exogenous sources (Figure 1). One of the most challenging environmental stressors associated with poultry production is elevated temperature. The phenomenon of heat stress engenders a redox imbalance that preferentially promotes prooxidants in comparison to antioxidants, rendering it a substantial contributor to systemic oxidative stress (Wasti, Sah, & Mishra, 2020). Elevated

ambient temperatures significantly intensify oxidative stress through the augmentation of mitochondrial activity, resulting in heightened superoxide generation and subsequent mitochondrial impairment (Akbarian et al., 2016; Nawaz & Zhang, 2021). Alterations in feed consumption, suboptimal growth performance, immunological suppression, hypoxic conditions, and elevated mortality rates have all been associated with thermal stress. Furthermore, thermal stress adversely impacts the quality of poultry meat (Mishra & Jha, 2019). Another source is the environmental pollution by heavy metals such as lead (Pb) and cadmium (Cd) which can provoke oxidative stress by increasing the production of reactive oxygen species (ROS) and reactive nitrogen species (RNS) while inhibiting the antioxidant defense system (Ebrahimi, Ebrahimi, & Shakeri, 2023). Moreover, oxidized fats, oils, and mycotoxins in feed can disrupt redox homeostasis, leading to oxidative stress (Bacou, Walk, Rider, Litta, & Perez-Calvo, 2021) for the reason that the gastrointestinal tract (GIT) is a critical site for nutrient absorption and is susceptible to oxidative stress from nutritional and environmental factors, affecting overall poultry performance (Y. Li, Wang, & Li, 2024; Mishra & Jha, 2019). Viral infections can also trigger ROS production, disrupting the redox balance (Rehman et al., 2018), since viruses increase the synthesis of reactive oxygen species, including superoxide and nitric oxide, while inhibiting the biosynthesis of catalase, superoxide dismutase, and glutathione peroxidase (Akyildiz & Denli, 2016). The diminished production and functionality of these enzymatic antioxidants culminate in a compromised immune response, as these enzymes are essential in elevated concentrations for the optimal functioning of immune cells relative to other cellular types (Akyildiz & Denli, 2016).

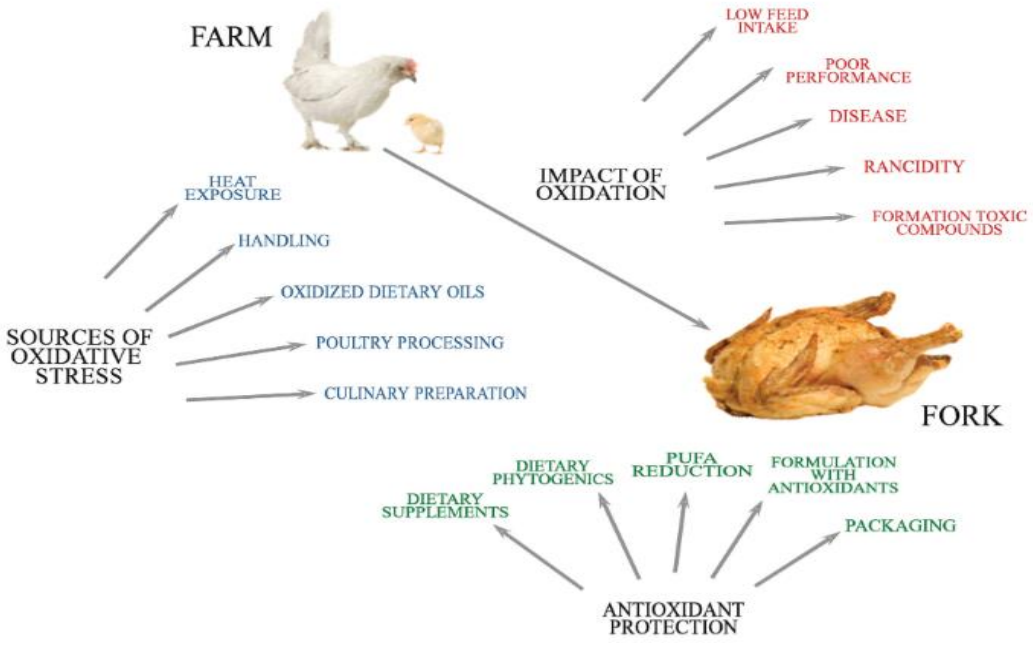

Figure 1: Sources of oxidative stress and its impact on poultry (M Estévez, 2015).

IV.2. Oxidative Stress and Meat Quality

Intensive farming practices, genetically selected broilers, and global warming contribute to oxidative stress, posing a significant challenge to the poultry meat industry. This stress negatively impacts broiler production performance and meat quality, resulting in substantial economic losses for producers and potential health risks for consumers (Z. Chen et al., 2022), in other words, oxidative reactions are not only detrimental to animal production and food quality but also pose potential health risks to consumers through the consumption of oxidized foods (M Estévez, 2015). Lipid oxidation is a key factor affecting meat quality, with significant implications for carcass quality and shelf life. It influences texture, color, odor, taste, and nutritional value, directly impacting consumer acceptance and the overall success of meat production (Desbruslais & Wealleans, 2022). Chicken meat is highly susceptible to oxidative processes post-mortem due to its high content of unsaturated lipids. Oxidation of lipids and proteins significantly impacts the shelf life and overall quality of the meat product (Desbruslais & Wealleans, 2022). Peri-mortem oxidative stress is believed to contribute to emerging poultry breast muscle myopathies, including woody breast, spaghetti meat, and white striping. These conditions result in significant economic losses for producers due to the downgrading or rejection of affected meat during processing (Cai et al., 2018; Hubert & Athrey, 2020).

After slaughter, the interruption of blood flow halts metabolic processes, allowing unsaturated fatty acids to interact with molecular oxygen and initiate free-radical chain reactions that form peroxides (Amaral, Silva, & Lannes, 2018). The cell membrane contains phospholipids, rich in polyunsaturated fatty acids, and it is there where the oxidation process begins, catalyzed by heme proteins such as hemoglobin, myoglobin, and iron, along with other molecules (Desbruslais & Wealleans, 2022). Concurrently, the body's antioxidant mechanisms partially collapse, and biochemical changes during the conversion of muscle to meat further promote oxidation (Amaral et al., 2018). A decline in pH enhances the redox cycling of myoglobin, increasing its pro-oxidant activity (Mario Estévez, 2011). Additionally, post-mortem changes, such as disrupted cellular compartmentalization and the release of free catalytic iron and oxidizing enzymes, contribute to lipid and protein oxidation in post-rigor meat.(Amaral et al., 2018; M Estévez, 2015). The oxidative stress increases the concentration of $O2^{\cdot -}$ within the mitochondria of chicken skeletal muscle (Mujahid, Yoshiki, Akiba, & Toyomizu, 2005). The dysfunction of mitochondrial operations would precipitate disturbances in calcium homeostasis and the initiation of intrinsic apoptosis, which serves as a significant contributor to the deterioration of meat quality (Z. Chen et al., 2022). The oxidative processes affecting lipids and proteins are regarded as the principal factors contributing to the degradation of meat, leading to alterations in coloration, diminished

water retention capacity, and a reduction in nutritional value within the meat (Falowo, Fayemi, & Muchenje, 2014).

It is worth mentioning that the Islamic method of animal slaughter significantly reduces the effects of lipid peroxidation by facilitating optimal exsanguination, as blood promotes the proliferation of spoilage microorganisms and serves as a vector for foodborne pathogens. Furthermore, the presence of residual blood within the meat corresponds to an increase in hemoglobin levels which act as a potent catalyst for lipid oxidation (Nakyinsige et al., 2014); therefore, enhanced exsanguination can elevate the quality of the meat during preservation (Ali, Lawson, Tauson, Fris Jensen, & Chwalibog, 2007).

IV.3. Mitigating Oxidative Stress in Poultry

A plethora of research indicates that oxidative stress exposes avian species to various diseases and welfare concerns. Consequently, the formulation of a cost-effective strategy to mitigate oxidative stress is of paramount importance (Afzal et al., 2023). The consumption of a dietary that is rich in antioxidants has been demonstrated to diminish free radical levels in the intestine and promote the health of the intestinal mucosa thereby supporting the overall performance (Riaz Rajoka et al., 2021). Supplementation with Vitamin C and E has been shown to enhance growth performance and carcass yield in broilers, particularly under heat-stress conditions. A study demonstrated that a combination of these vitamins improved growth performance, nutrient digestibility, and antioxidant capacity in broilers exposed to high temperatures (Chetehouna, Boulaares, Atoussi, Guemari, & Derouiche, 2024; A. S. Mohamed, Milošević, Mohany, Al-Rejaie, & Elwan, 2024). The incorporation of methionine supplementation is instrumental in augmenting the antioxidant capacity of poultry. It facilitates the functioning of enzymes such as catalase (CAT), superoxide dismutase (SOD), and glutathione peroxidase (GPx), which are essential for the neutralization of free radicals and the mitigation of oxidative stress (Kachungwa Lugata, Ortega, & Szabó, 2022). Plant flavonoids, specifically, have been recognized as promising feed additives owing to their capacity to stabilize reactive oxygen species (ROS) and to enhance the expression of antioxidant enzymes. Nevertheless, their limited solubility within the gastrointestinal tract underscores the imperative need for the advancement of efficacious delivery technologies (Seomoon & Jang, 2022). On top of that, the implementation of management practices, encompassing appropriate architectural design, effective ventilation, and meticulous temperature regulation, is paramount in alleviating stressors that exacerbate oxidative stress (Mangan & Siwek, 2024).

Chapter II
Phragmites australis.

I. Taxonomic and botanical description

Phragmites australis, is recognized by an array of designations, encompassing common reed, common cane, wild cane, reed grass, and additional appellation (Beaudette, 2020). It is a globally distributed plant species and it is recognized as one of the most invasive wetland plants (Hurley, Lynn, DeVries, Reid, & Elsey-Quirk, 2024).

The botanical classification of Phragmites australis is a subject of interest due to its widespread distribution and ecological significance. It belongs to the family *Poaceae*, also known as *Gramineae* (Watson & Clifford, 1976), and it is classified within the class *Liliopsida*, which is distinguished by its monocotyledonous flowering plant species. This class is encompassed within the broader taxonomic group of angiosperms, commonly referred to as flowering plants (Singh, 2003). Phragmites is the genus to which *Phragmites australis* belongs, this genus is characterized by its widespread distribution and comprises numerous species that have evolved to thrive in wetland ecosystems (Lambertini, Sorrell, Riis, Olesen, & Brix, 2012).

P. australis is characterized by annual cane-like stems that arise from a robust and extensive rhizomatous system. The stems are capable of attaining heights of up to 6 meters, exhibit a diameter ranging from 4 to 10 millimeters, and possess hollow internodes measuring 10 to 25 centimeters in length (Mal & Narine, 2004). Rhizomes are characterized as perennial structures that exhibit both horizontal and vertical growth orientations. The horizontal components of rhizomes facilitate the expansion of the clonal population, whereas the vertical segments are responsible for the emergence of annual erect stems. Furthermore, rhizomes are composed of extensive aerenchymatous tissue, which aids in gas exchange. Roots originate from rhizomes and various submerged portions of the shoots. The leaves exhibit a smooth texture, are alternately arranged, and possess narrow-lanceolate laminae measuring 20–70 cm in length and 1–5 cm in width, characterized by closely spaced nerves and tapering to elongated slender tips (Haslam, 1972). The inflorescence manifests as a terminal panicle, frequently measuring approximately 30 cm in length, characterized by a lax structure and exhibiting a color range from dull purple to yellow, with the principal branches supporting numerous spikelets. The branches are characterized by a smooth texture, typically adorned with sporadic clusters of elongated silky trichomes (Haslam, 1972).

II. Genetic and Morphological Diversity

Phragmites australis displays considerable genetic variability, encompassing various subspecies and genotypes that have evolved to thrive in diverse climatic and geographical contexts. For example, within Europe, there exist pronounced genetic distinctions between Mediterranean

and temperate forms of *Phragmites australis*, which are also associated with other species such as *Phragmites mauritianus* in Africa and *Phragmites karka* in Asia (Lambertini et al., 2012).

The genetic diversity is further underscored by the existence of various ploidy levels within the species, which span from triploid to octoploid, with tetraploid and octoploid constituting the predominant forms (Gorenflot, 1976).

Figure 2: *Phragmites australis* (Original photo, 2024).

III. Potential Applications of *Phragmites australis*

The plant exhibits an extraordinary capacity for the uptake and sequestration of heavy metals, thereby rendering it an instrumental agent in the field of phytoremediation. It possesses the efficacy to eliminate metallic contaminants such as zinc, copper, and lead from polluted ecosystems, as substantiated by its application in engineered wetlands dedicated to the treatment of wastewater (Sellal & Belattar, 2024).

Beyond its ecological functions, *Phragmites australis* presents promising opportunities for implementation in sustainable construction practices. The ash derived from this species, when employed as a partial substitute for cement, demonstrates pozzolanic characteristics, albeit it may lead to a diminution in the compressive strength of mortar. This application advances sustainable

development by harnessing plant waste and mitigating cement consumption (Khatib, ElKhatib, Assaad, & El Kordi, 2023).

Additionally, a recent study has explored the plant's capacity to boost immune responses and support liver health in fish indicating it could offer similar advantages in livestock, potentially promoting overall health and increasing resistance to disease (R. Wang et al., 2022).

IV. Traditional Medicine Applications

The taxonomic group Phragmites has historically been employed for the management of diverse health ailments. Its derived extracts demonstrate a spectrum of pharmacological properties, encompassing analgesic, antidiabetic, antihyperlipidemic, anti-inflammatory, antimicrobial, antioxidant, and hepatoprotective actions (Farouk, Fahim, Attia, & Kamel, 2023).

Chapter III
Nanotechnology

I. Definition of Nanotechnology

Nanotechnology refers to the science and engineering involved in developing functional materials, devices, and systems by controlling matter at the atomic and molecular levels. This process entails manipulating materials on a nanoscale to take advantage of unique phenomena and properties that emerge at this scale, such as quantum effects and enhanced surface area(Dahman, Nasr, Prekh, Alhamami, & Kaur, 2018; Echiegu, 2017). The field is distinguished by two primary approaches: the top-down approach, which involves scaling down bulk materials, and the bottom-up approach, which focuses on constructing materials from atomic or molecular constituents (Dahman, 2017; Oluwasanu et al., 2019). Nanotechnology is fundamentally interdisciplinary, incorporating knowledge and techniques from fields such as physics, chemistry, biology, medicine, and engineering, among others (Ghernaout, Alghamdi, Touahmia, Aichouni, & Ait Messaoudene, 2018; Rafique, Tahir, Rafique, & Hamza, 2020). The field of nanotechnology began to take shape in the 1980s due to the amalgamation of substantial experimental innovations, notably including the creation of the scanning tunneling microscope in 1981 and the identification of fullerenes in 1985 (Altammar, 2023). The identity of the originator of nanoscience and technology remains ambiguous; nevertheless, Richard Feynman is widely acknowledged for his seminal contributions to the foundational principles of contemporary nanotechnology(Rafique et al., 2020). The conceptual framework for nanotechnology goals gained popularity following the 1986 publication of the book *Engines of Creation* by Kim Eric Drexler (Bayda, Adeel, Tuccinardi, Cordani, & Rizzolio, 2019). Nanotechnology's applications encompass a broad spectrum and extend into multiple domains, such as healthcare, agricultural practices, energy production, and the food sector. In the field of medicine, nanotechnology has revolutionized it, leading to significant advancements in diagnostics, treatment, and drug delivery. Nanoscale materials are used in imaging with contrast agents and in targeted drug delivery systems for cancer treatment. Additionally, nanomedicine encompasses the development of biocompatible materials and noninvasive vaccination methods, including DNA-based vaccines (Dahman et al., 2018).

II. Nanoparticles

II.1. Definition and Classification

Nanoparticles (NPs) are defined as entities that are situated within the nanoscale dimension, generally measuring between 1 to 100 nanometers. These particles demonstrate distinct characteristics that markedly diverge from their macroscopic equivalents due to their diminutive dimensions and elevated surface area (Horikoshi & Serpone, 2013).

Nanoparticles are complex structures composed of three layers: (a) the surface layer, which can be functionalized with small molecules, metal ions, surfactants, or polymers; (b) the shell

layer, made of a material chemically distinct from the core; and (c) the core, which forms the central part of the nanoparticle and typically refers to the nanoparticle itself (I. Khan, Saeed, & Khan, 2019).

Nanoparticles are classified into different types based on their size, shape, and composition, which significantly influence their properties and applications:

Size-Based Classification: The nanoparticles' size significantly influences their physicochemical characteristics, including melting point and reactivity (S. K. Gupta, Talati, & Jha, 2008).

Shape-Based Classification: Nanoparticles exhibit a diverse array of geometrical configurations, encompassing spherical, cubic, and rod-like structures, in addition to more intricate morphologies such as pentagonal or hexagonal platelets (Petroski, Green, & El-Sayed, 2001). Advanced techniques such as complex Fourier descriptor analysis and Bayesian object classification are used to categorize nanoparticle shapes, offering quantitative and high-throughput methods for monitoring and classifying shapes during synthesis and application (Konomi et al., 2013; Rice, Saunders, & Stoykovich, 2012).

Composition-Based Classification: The composition of nanoparticles constitutes a fundamental element in their systematic classification. Various metals, including silver, copper, and zinc, can be categorized according to their physicochemical characteristics, which significantly affect their toxicological reactions (Sayes, Smith, & Ivanov, 2013). The introduction of dopants modifies their dimensions, morphology, and magnetic characteristics, rendering them appropriate for a wide array of applications such as imaging and catalysis (Holmberg, Aharen, & Murugesu, 2012).

Structural and Functional Classification: Nanoparticles are further categorized according to their structural nanoelements, which significantly influence their deformation characteristics and mechanical attributes (Glezer, 2011). Nanoparticle classification also depends on their intended applications, such as in pharmaceuticals, where specific shapes and sizes are designed for drug delivery systems (DeSimone et al., 2013).

II.2. Properties of Nanoparticles

- **High Surface Area to Volume Ratio**: This characteristic increases their reactivity, allowing more surface atoms to engage in chemical reactions (Goesmann & Feldmann, 2010). The large surface area is essential for applications like catalysis, drug delivery, and sensors, where surface interactions play a critical role (Edebali, Oztekin, & Arslan, 2018).
- **Enhanced Mechanical Properties**: Nanoparticles display improved mechanical properties, including greater strength and hardness, attributed to their small size and high surface energy

(Nanjwade, Sarkar, & Srichana, 2019). These qualities are advantageous in applications that require durable materials, such as coatings and composites (Dan Guo, Xie, & Luo, 2013).

- **Electrical properties:** Nanoparticles often exhibit improved electrical conductivity compared to their bulk counterparts. This is due to the quantum effects that become prominent at such small scales, affecting electron movement and energy levels (Rafique et al., 2020).
- **Magnetic properties**: Nanoparticles can exhibit superparamagnetism, where they show magnetic behavior only in the presence of an external magnetic field. This property is particularly useful in applications like magnetic resonance imaging (MRI) and data storage (Rafique et al., 2020)

III. Metal Nanoparticles

Metal nanoparticles (NPs) are exclusively composed of metallic elements. These NPs possess unique electrical characteristics attributed to the well-documented phenomenon of localized surface plasmon resonance (LSPR). Copper (Cu), silver (Ag), and gold (Au) nanoparticles demonstrate a wide absorption spectrum within the visible range of the solar electromagnetic spectrum. The utilization of metal NPs spans various scientific disciplines, owing to their enhanced attributes such as the controlled synthesis of facets, dimensions, and morphologies of metal NPs (I. Khan et al., 2019).

III.1. Copper Nanoparticles (CuNPs)

Copper nanoparticles can be fabricated utilizing a multitude of methodologies, such as chemical reduction, hydrothermal synthesis, and green synthesis employing botanical extracts. The selection of the synthesis technique significantly impacts the dimensions, morphology, and characteristics of the nanoparticles, which subsequently affect their potential applications (Naz, Gul, Zia, & Javed, 2023; Sadhvi, Rajeshkumar, Roy, & Lakshmi, 2014). They demonstrate significant antimicrobial, anticancer, and antioxidant characteristics, rendering them highly valuable in the field of nanomedicine. The biocompatibility and effectiveness of these nanoparticles in biomedical applications are contingent upon their method of synthesis and their physicochemical attributes (Naz et al., 2023). Table 02 recapitulates the main characteristics of CuNPs.

Table 02: Main characteristics of CuNPs.

	Size	Shape/ structure	Optical properties	Toxicity
CuNPs	1-100 nm (I. Khan et al., 2019).	Cubes, rods, tetrahedron, spherically shaped particles (Mott, Galkowski, Wang, Luo, & Zhong, 2007).	Highly conductive, can be made transparent or translucent (Altammar, 2023).	Low toxicity (W. Yang, Wang, Mettenbrink, DeAngelis, & Wilhelm, 2021).

IV. Metal NPs Synthesis Approaches

There are three primary approaches for synthesizing nanoparticles: physical, chemical, and biological. The physical method is referred to as the top-down approach, while the chemical and biological methods are collectively known as the bottom-up approach. The biological method is also called the green synthesis of nanoparticles. Each of these approaches can be further divided into various subtypes based on the specific techniques used (Altammar, 2023).

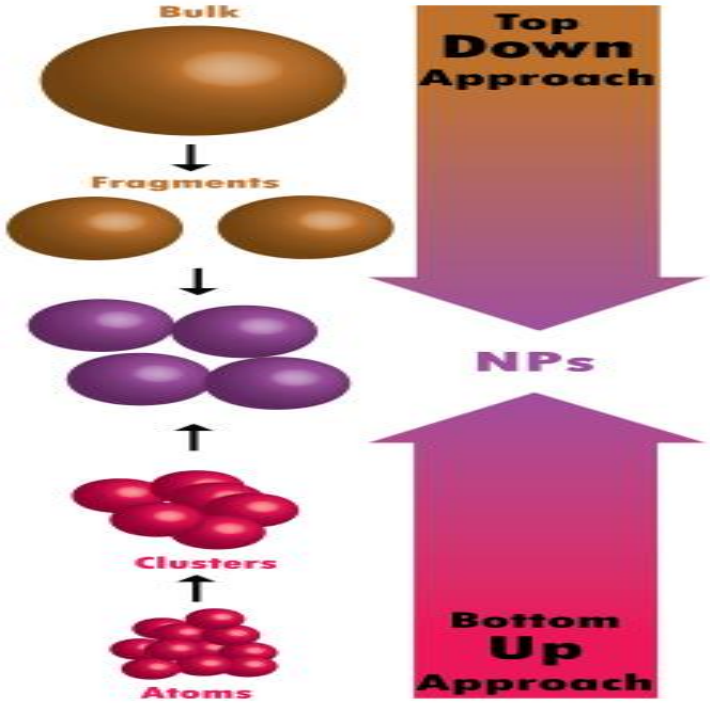

Figure 3: The different approaches for synthesizing nanoparticles (Altammar, 2023).

IV.1. Green Synthesis of NPs

The green synthesis of nanoparticles is an emerging field that emphasizes the use of environmentally friendly methods such as plant extracts, fungi, and bacteria (Figure 03), which act as reducing and stabilizing agents, to produce nanoparticles with minimal toxicity and environmental impact (Nair, Sajini, & Mathew, 2022; Ojha, 2022). Green-synthesized

nanoparticles demonstrate improved biocompatibility and diminished toxicity, rendering them appropriate for incorporation in drug delivery systems and various biomedical applications. Empirical evidence suggests that these nanoparticles exhibit antimicrobial, antioxidant, and anticancer characteristics (Sudheer et al., 2022). Additionally, these nanoscale particles possess significant potential for application in the domains of aqueous remediation and environmental pollution mitigation, given their capacity to efficiently decompose various dyes and other contaminants (Nandeshwar, Kalkar, & Agrawal, 2022).

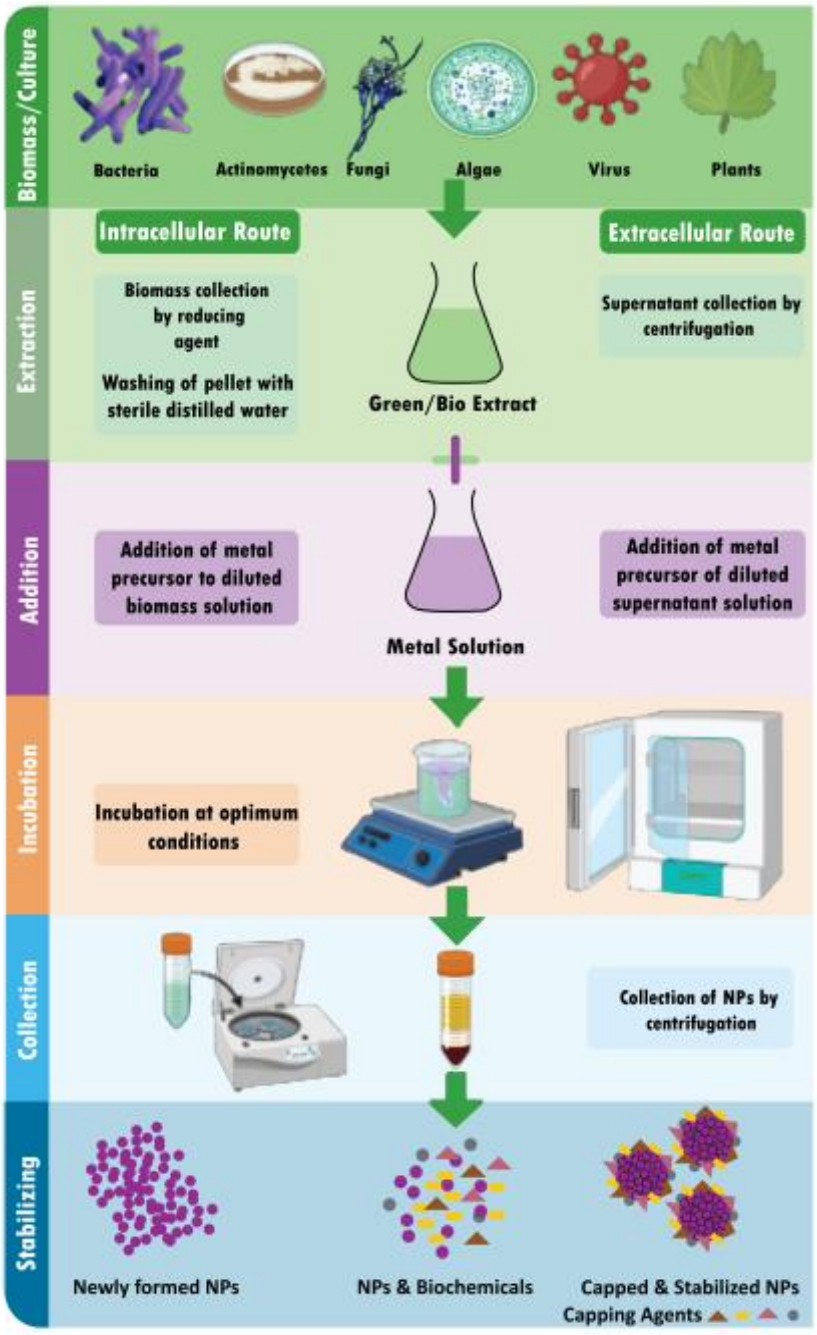

Figure 4: Schematic representation of green synthesis of nanoparticles (Altammar, 2023)

V. Advantages and Challenges

Nanoparticles' green synthesis is cost-effective, eco-friendly, and synthesizes nanoparticles exhibiting distinctive characteristics, including elevated stability and uniformity (Santo-Orihuela, Desimone, & Catalano, 2023). Notwithstanding its advantages, green synthesis encounters obstacles including scalability issues, regulation of nanoparticle size and shape, as well as the necessity for an enhanced comprehension of the mechanisms that underlie the synthesis procedure (D. Gupta, Boora, Thakur, & Gupta, 2023; Santo-Orihuela et al., 2023).

VI. Application of Nanotechnology

Nanotechnology is revolutionizing agriculture by enhancing the efficiency of fertilizers and pesticides through nanoformulations, such as nanoclays and zeolites, that allow for targeted delivery and controlled release (Manjunatha, Naik, & Usharani, 2019).

In the food industry, nanotechnology is utilized to augment both the quality and safety of food products. This encompasses the incorporation of nanomaterials within food packaging to prolong shelf life, as well as in food processing to enhance nutrient delivery and bioavailability (Echiegu, 2017; Fúnez, Duaso, & Gómez, 2016); additionally, it facilitates the monitoring of contaminants and the integration of health supplements into food items (Echiegu, 2017).

In energy-related applications, nanotechnology encompasses the advancement of more efficient solar cells and superior energy storage systems. The distinctive characteristics of nanomaterials, including augmented surface area and improved conductivity, are utilized to enhance energy conversion and storage mechanisms (Ghernaout et al., 2018; Razvarz, Chavez, & Vargas-Jarillo, 2020).

Environmental applications encompass water purification and pollution mitigation, wherein nanomaterials are employed to eliminate contaminants and enhance the quality of water resources (Fúnez et al., 2016).

In biomedicine, nanoparticles have been extensively employed for drug delivery, imaging, and diagnostics, attributable to their capacity to engage with biological systems at the molecular level (Bharathala & Sharma, 2019; Utreja, Verma, Rahman, & Kumar, 2020). Their diminutive dimensions facilitate the advancement of noninvasive drug delivery methodologies and enhance imaging techniques including MRI, CT, and PET/SPECT (Bharathala & Sharma, 2019). Nanoparticles possess the capability to transport anti-inflammatory pharmaceuticals directly to affected tissues, thereby minimizing systemic exposure and associated adverse effects (Oshi et al., 2022). Moreover, one of the most notable implications is recognized within the area of oncology. Nanomaterials facilitate the earlier and more precise identification of malignancies, which is crucial for achieving favorable therapeutic results. Furthermore, they possess the capability to

transport pharmacological agents directly to neoplastic cells, thereby enhancing treatment efficacy and minimizing adverse effects (Xie, 2023).

In veterinary medicine, nanoparticles are undergoing extensive investigation as potential antiviral platforms, presenting a compelling alternative to conventional vaccination strategies (Fawzy et al., 2021). Moreover, nanomaterials exhibiting antifungal characteristics are currently under investigation to address mycosis and mycotoxicosis in various animal species. These nanoantifungal agents hold potential applications in pharmaceutical formulations, immunobiological preparations, and farm disinfectants (Alghuthaymi et al., 2021).

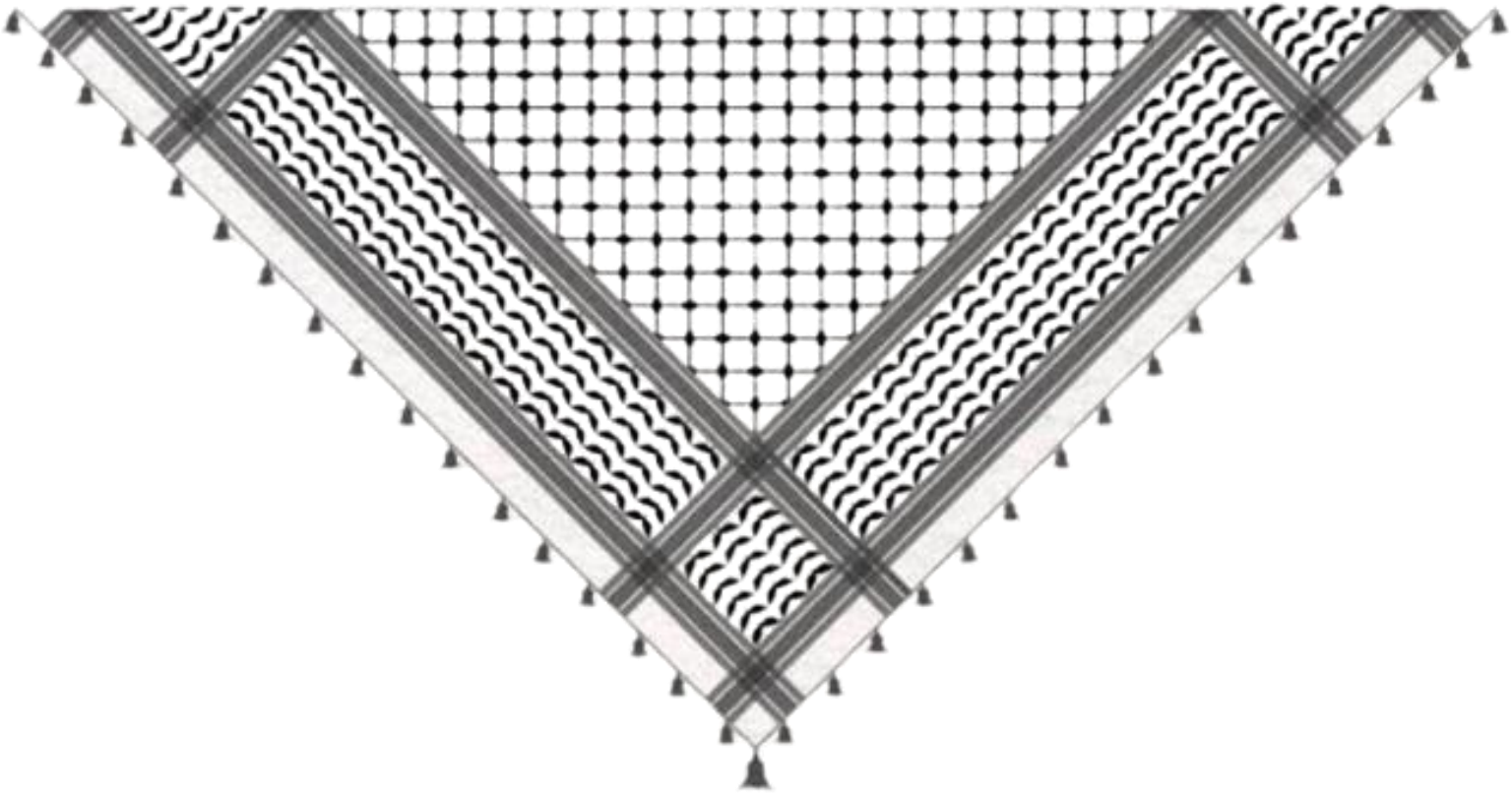

Experimental Part

Chapter I
Materials & Methods

I. Materials

I.1. Plant Collection

The plant was collected from the region of Djamaa in Algeria in October 2022. Leaves and rhizomes were separated from the specimens, washed with water to eliminate particulate matter and contaminants, and subsequently permitted to desiccate in a shaded environment before being ground into a fine powder.

I.2. Animal Material

The experimental study was conducted within a broiler chicken coop that was owned and supervised by a veterinarian accredited by the Algerian government- Dr Bagui Salah, City of Robbah, Oued Souf . For the acute toxicity test, all chickens were vaccinated and provided with conventional nutritional supplementation. The experimental subjects were housed together within the same chicken coop. However, for the biovaccination experiment, the chickens were divided into five distinct groups: a conventional treatment group, an untreated control group, and three experimental groups that received biovaccination with LP-CuNPs, RP-CuNPs, and MP-CuNPs, respectively.

II. Methods

II.1. *In vitro* study

II.1.1. *P.australis* Aqueous Extract Preparation

The aqueous extract of the leaves was prepared using the following methodology: 5 g of the powdered leaves of *Phragmites australis* were combined with 50 ml of distilled water. The resultant solution was maintained at a temperature of 50° C and subjected to stirring for two hours. Following this, the preparation was permitted to undergo maceration for 24 hours at ambient temperature. After being filtered through a muslin cloth and filter paper, the resulting filtrate was subsequently dried in a laboratory oven and stored in a freezer for future applications. An identical procedure was performed with the rhizomes (Derouiche, Azzi, & Hamida, 2019).

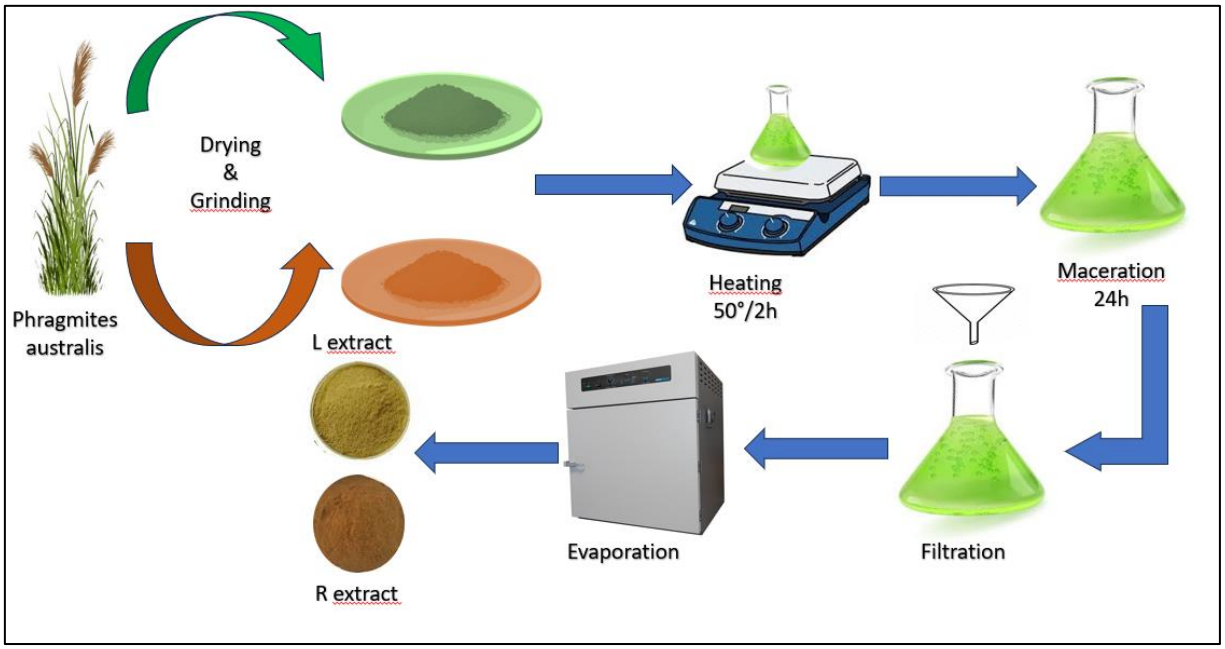

Figure 5: Preparation method of *P. australis* aqueous extract.

II.1.2. *P. australis* Phytochemical Analysis

Both extracts of *P. australis* (leaves and rhizomes) were subjected to an analytical screening to identify the presence of an array of phytochemical constituents, including phenolic compounds, tannins, alkaloids, steroids, saponins, flavonoids, and terpenoids, utilizing standard procedures for phytochemical analysis (A. Harborne, 1998; J. B. Harborne, 1973; Wadood et al., 2013).

- **Phenolic Compounds**

5 mL of the extract was introduced into a test tube, and a few drops of a 5% aqueous solution of ferric chloride were subsequently added. The emergence of a dark green coloration signifies the existence of phenolic compounds.

- **Flavonoids**

5 mL of the extract was introduced into a test tube, followed by the addition of 5 mL of diluted ammonia and 1 mL of sulfuric acid (H2SO4). The manifestation of a yellow hue indicates the presence of flavonoids.

- **Alkaloids**

One milliliter of the aqueous extract was subjected to treatment with several drops of hydrochloric acid, after which 1 to 3 drops of Wagner's reagent were incorporated. The formation of a brown precipitate confirms the presence of alkaloids within the sample.

- **Tannins**

In a test tube, the incorporation of 5 mL of the extract followed by the addition of 1 mL of a 2% aqueous solution of ferric chloride (FeCl3) was conducted. The presence of tannins was signified by the emergence of a greenish or bluish-black coloration.

- **Terpenoids**

The development of a reddish-brown hue signifies the existence of terpenoids, achieved through the incorporation of 2 mL of chloroform and 3 mL of concentrated sulfuric acid into 5 mL of the plant extract.

- **Reducing compounds**

The introduction of Fehling's solution (comprising 1 mL of reagent A and 1 mL of reagent B) to the extract, followed by incubation in a boiling water bath, resulted in the appearance of a brick-red precipitate, indicating the presence of reducing sugars.

- **Saponins**

In a test tube, the addition of 5 mL of the extract, followed by mixing with 5 mL of distilled water and vigorous manual agitation, led to the formation of a persistent foam, which indicates the presence of saponins.

- **Steroids**

To 1 mL of plant extract, the addition of 0.5 mL of acetic acid solution and 0.5 mL of concentrated H_2SO_4 results in a reaction where the absence of a green color serves as evidence for unsaturated steroids. In a separate tube, the addition of the same volume of H_2SO_4 leads to the appearance of a red color, indicating the presence of steroid derivatives.

II.1.3. Total Phenolic and Flavonoid Compounds

The total phenolic content (TPC) of *P.australis* extract (Leaf and rhizome) was quantified utilizing the Folin-Ciocalteu methodology (Boizot & Charpentier, 2006). A volume of 100 µL of the extract was combined with 500 µL of the Folin-Ciocalteu reagent and 400 µL of a 7.5% (w/v) sodium carbonate solution. Following 10 minutes of agitation and incubation in a dark environment at ambient temperature, the absorbance of the resultant solution was assessed at a wavelength of 760 nm employing a UV spectrophotometer. The findings are represented in terms of milligrams of gallic acid equivalent per gram of dry extract, referencing the calibration curve of gallic acid. The calibration curve is established utilizing gallic acid at varying concentrations (50-100-150-200 … g/mL) while maintaining consistent conditions and procedures throughout the assay. Consequently, the results are articulated in terms of milligrams of gallic acid per gram of dry extract (mg of EAG/g).

The total flavonoid content (TFC) of the extract derived from *P. australis* was quantified following the methodology outlined by Dehpour *et al*., 2009 (Dehpour, Ebrahimzadeh, Fazel, & Mohammad, 2009). A total of 500 µL of the extract was combined with 100 µL of AlCl3, 100 µL of 1 M sodium acetate, and 2.8 mL of distilled water. The resultant mixture was subjected to a dark incubation at ambient temperature for 30 minutes following thorough agitation. The blank

control was prepared by substituting the extract with 95% methanol, and the absorbance was subsequently measured at 415 nm utilizing a UV spectrophotometer. The findings are articulated in terms of mg equivalent quercetin per gram of dry extract material, referencing the quercetin calibration curve (0.01 - 0.03 - 0.05 - 0.07 - 0.09 mg/mL).

II.1.4. GC-MS Analysis

Plant extracts from both leaves and rhizomes were prepared using methanol as a universal solvent, with 1µl of the extract used to quantify volatile compounds via GC-MS analysis. The extraction of volatiles was performed using headspace solid-phase micro-extraction (SPME) with a DVB/CAR/PDMS fiber. Initially, the fiber was conditioned in the GC injection port at 270°C for 4 hours. After conditioning, the fiber was placed into a vial containing the sample for 15 minutes at room temperature using an adapter. The fiber was then inserted into the gas chromatograph's injection port for desorption, which lasted 10 minutes at 260°C in splitless mode. The analysis was carried out using an Agilent 7890A GC system coupled with a 5975C VL Triple-Axis mass detector. Separation was performed on a DB-5MS capillary column (25 m × 0.2 mm; 0.33 µm film thickness) with helium as the carrier gas at a flow rate of 0.6 mL/min. The injector and transfer line temperatures were set at 260°C and 280°C, respectively. The oven temperature program started at 40°C (held for 3 minutes), then increased by 4°C/min to 160°C, followed by a 10°C/min increase to 280°C, with the final temperature held for 3 minutes. Masses were scanned from 33 to 333 Da, with an ionization energy of 70 eV. The GC-MS data interpretation was conducted using the National Institute of Standards and Technology (NIST) database, which assisted in identifying unknown chemicals by comparing the sample data to the NIST library. The molecular data, including the name, formula, weight, and structure of volatile components, was determined from this analysis.

II.1.5. *P.australis*-based CuNPs Synthesis

Copper nanoparticles (Cu NPs) were synthesized through the addition of 4 grams of copper sulfate to a total volume of 400 milliliters of distilled water, followed by the incorporation of 20 milliliters of the plant extracts (leaves and rhizomes separately) and 10 milliliters of ascorbic acid. The resultant mixture was subjected to heating and stirring at a controlled temperature of 70°C and a rotational speed of 1500 rpm. A notable color transition from blue to dark green occurred within the initial 15 minutes, serving as an indicative marker for the synthesis of Cu NPs. The pH of the solution was pre-measured and maintained within a basic range (Dinda, Halder, Vazquez-Vazquez, Lopez-Quintela, & Mitra, 2015; Nasrollahzadeh & Sajadi, 2015). After a duration of four hours, the samples underwent centrifugation and were subsequently washed twice with distilled water and once with ethanol, before being dried in an electric furnace set to 70°C.

II.1.6. *P.australis*-based CuNPs Characterization

A variety of techniques were employed to elucidate the characteristics of our green synthesized copper nanoparticles (NPs). Ultraviolet-visible (UV-Vis) spectroscopy was utilized to authenticate the synthesis of NPs, employing the PG Instruments T80 Spectrometer within the wavelength range of 200 to 400 nm. Distilled water served as the reference blank. Fourier-transform infrared (FT-IR) spectroscopy was utilized to illustrate the participation of bioactive phytochemicals from the plant extract in the reduction and stabilization of nanoparticles (Agilent Technologies). The morphology and dimensions of the NPs were assessed utilizing Scanning Electron Microscopy (SEM) (Zeiss) and Transmission Electron Microscopy (TEM) (Tecnai). The crystalline structure and grain size were ascertained through X-ray diffraction analysis via a diffractometer (PROTO® AXRD Benchtop), employing a 2θ angle range of 10-80° with copper K-alpha radiation (λ=1.540593Å). The stability of the nanoparticles was assessed by measuring their zeta potential using a NICOMP 380 ZLS particle sizer.

II.1.7 Biological Activities

- **Antioxidant Activity**

The antioxidant activity of both plant extracts and their biosynthesized CuNPs was evaluated using two assays: the DPPH free-radical scavenging activity, following the method described by Nwidu *et al*. (Nwidu, Elmorsy, Aprioku, Siminialayi, & Carter, 2018), and the ferric reducing antioxidant power (FRAP) assay, as outlined by Oyaizu (Oyaizu, 1986).

For DPPH (1,1-diphenyl-2-picryhydrazyl) assay, stock solutions of the extracts and their biosynthesized CuNPs, with a concentration of 5 mg/ml, were systematically prepared and subsequently diluted to achieve final concentrations of 200, 100, 50, 25, 12.5, and 6.25 µg/mL in ethanol. A volume of 160 µL of 0.1 mM DPPH in ethanol solution was incorporated into 20 µL of the extracts or the standard, followed by the addition of 20 µL of H_2O, and the resultant mixture was thoroughly homogenized. Ascorbic acid, utilized as a control solution, was evaluated across the concentration spectrum of 1.56, 0.78, 0.39, 0.195, and 0.0975 mg/mL under analogous experimental conditions. The resultant mixtures were subjected to an incubation period at 37 °C for 40 minutes, shielded from light exposure. The absorbance of the samples was subsequently measured at a wavelength of 517 nm.

For FRAP assay, the procedure involves taking 500 µl of the sample, adding 1.25 mL of buffer solution (0.2 M, pH 6.6), and incubating for 20 minutes in a water bath at 50°C. After incubation, 1.25 mL of aqueous TCA solution (10%) is added to stop the reaction, followed by centrifugation at 3000 rpm for 5 minutes. Then, 1.25 mL of the supernatant is mixed with 1.25 mL of distilled water and 250 µL of FeCl3 (0.1%). The absorbance is read at 700 nm against a blank.

The results are expressed as IC_{50} values, after calculating the ferric-reducing antioxidant power (FRAP) according to the following equation:

$$IP\ (\%) = 100 - \frac{OD\ controle}{OD\ sample} \times 100$$

- **Anti-inflammatory Activity**

The anti-inflammatory effect of *Phragmites australis* and biosynthesized copper nanoparticles (Cu NPs) was investigated *in vitro* using two methods. The first method involved measuring protein denaturation inhibition, as described by Vennila *et al.* (Vennila, Chitra, Balagurunathan, & Palvannan, 2018), while the second method assessed the protection of red blood cells (RBCs) against hemolysis, following the procedure outlined by Vinjamuri *et al*. (Vinjamuri, Afshan, Shekar, & Saraswathi, 2015).

The procedure of the first assay involves adding different concentrations (10–50 µg/mL) of the sample to a 1% bovine serum albumin (BSA) solution, followed by incubation for 30 minutes at room temperature. The pH of the solution is then adjusted to 2 by dropwise addition of concentrated HCl. After incubation, the mixture is heated at 72°C for 30 minutes, and all tubes are subsequently cooled for 10 minutes. The turbidity of the solution is measured at a wavelength of 660 nm, with diclofenac used as the standard. The results are expressed as IC_{50} values, after calculating the inhibition percentage (IP).

$$IP\ (\%) = A0 - \frac{A1}{A0} \times 100$$

The hemolysis assay, the second assay, is used to determine the protective effect of anti-hemolytic compounds present in the sample against erythrocyte membrane lysis induced by 1X PBS. The extent of membrane lysis is detected by measuring the concentration of hemoglobin in blood plasma at 540 nm using a spectrophotometer. In the procedure, 5 mL of blood is collected from healthy volunteers into tubes containing 5.4 mg of EDTA to prevent coagulation. The blood is then centrifuged at 1000 rpm for 10 minutes at 4°C. After centrifugation, the plasma is carefully removed, and the white buffy coat layer is aspirated with a pipette. The erythrocytes are washed three times with 1X PBS (pH 7.4) for 5 minutes. The washed erythrocytes are stored at 4°C and used within 6 hours for the hemolysis assay. For the assay, 50 µL of a 10-fold dilution of erythrocyte suspension (100 µL erythrocytes and 900 µL 1X PBS) is mixed with 100 µL of test samples (20-80 ng/mL), with 100 µL of 1X PBS serving as the control. The reaction mixture is incubated at 37°C in a water bath for 60 minutes. The volume of the reaction mixture is then

brought to 1 mL by adding 850 µL of 1X PBS. After centrifuging the reaction mixture at 300 rpm for 3 minutes, the concentration of hemoglobin in the supernatant is measured at 540 nm using a spectrophotometer. The percentage of hemolysis is calculated as follows:

$$Hemolysis\ inhibition\ (\%) = 100 - \frac{OD\ sample}{OD\ control} \times 100$$

- **Antibacterial Activity**

The antibacterial efficacy of copper nanoparticles (Cu NPs) was assessed against *Escherichia coli, Klebsiella pneumoniae, Staphylococcus aureus*, and *Bacillus subtilis* utilizing the standard disc diffusion assay. The bacterial strains were cultivated in nutrient broth for a duration of 24 hours at a temperature of 37 ◦C. The active culture was subsequently inoculated onto Mueller Hinton agar medium utilizing sterile swabs and allowed to dry at ambient temperature. A volume of 20 µl of Cu NP solution, dissolved in dimethyl sulfoxide (DMSO) at concentrations of 5, 10, 20, and 40 mg/ml, was absorbed by sterile discs and positioned within the agar plates. Amoxicillin and gentamicin served as positive controls, whereas DMSO was employed as a negative control. The plates were incubated at a consistent temperature of 37 ◦C for 24 hours. The outcomes were evaluated by quantifying the inhibition zone in millimeters.

- **Cytotoxic Activity – MTT Assay**

The MTT (3-[4,5-dimethylthiazole-2-yl]-2, 5-diphenyl tetrazolium bromide) assay facilitates the elucidation of the impact of phytosynthesized copper nanoparticles on MCF7 cells, which represent an epithelial cell line derived from a patient's breast tissue diagnosed with metastatic adenocarcinoma. In summary, the cells underwent treatment with varying concentrations of Cu nanoparticles (0.15, 0.31, 0.62, 1.25, 2.5 mg/mL) for a duration of 72 hours subsequent to their seeding in a 96-well plate and an initial incubation period of 24 hours. Dimethyl sulfoxide was employed to solubilize the resultant formazan, and the absorbance was quantified at 520 nm utilizing a microtiter plate reader. Ultimately, the percentage of cytotoxicity was computed in accordance with the following equation:

$$Cytotoxicity\ percentage\ \% = \left(\frac{(A\,c - A\,bg) - (A\,s - A\,bg}{A\,c - A\,bg}\right) x\ 100$$

A c is the control's absorbance, A bg is the background's absorbance, and A s is the sample's absorbance.

II.2. *In Vivo* Study

II.2.1. *P.australis*-based CuNPs Acute Toxicity

A total of thirty-eight-day-old Arbor Acres broiler chickens (n=15) were allocated into three groups, each comprising three individuals, with weights ranging from 2.13 to 2.41 Kg, and were subjected to an 8-hour fasting period. Subsequently, the animals were administered an intramuscular injection (in the breast muscle) of a singular dose of *P. australis* rhizome extract-based CuNPs (control, 25, and 50 mg/kg BW). The animals were meticulously monitored for behavioral changes post-injection during the initial 4 hours, followed by periodic observations over a 24-hour duration prior to their sacrifice.

- **Sample Collection**

Upon the completion of a 24-hour period subsequent to the administration of phytosynthesized CuNPs, the chickens were subjected to exsanguination via the incision of their jugular vein following their measurement of mass. The resultant blood samples were gathered in 5 mL EDTA tubes and were promptly conveyed to the hematology laboratory for the purpose of conducting hematological analyses. Subsequently, the liver, heart, kidney, and segments of the breast muscle were expeditiously excised, cleansed with a physiological solution, weighed, and preserved at -20 °C for subsequent investigation. A sample from each liver was retained in a formalin solution to facilitate histological evaluation. Additionally, a fraction from each organ collected was utilized to evaluate the antioxidant capacity and the degree of lipid peroxidation. Figure 06 recapitulates all the steps of the cute toxicity test.

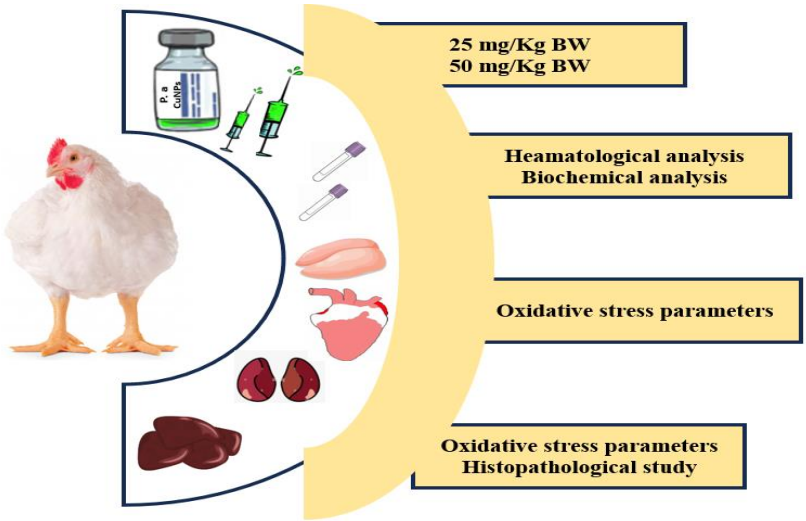

Figure 6: Schematic representation of plant-based CuNPs acute toxicity study.

II.2.2. Biovaccination Effect of *P. australis*-based CuNPs

One hundred Arbor Acres chicks, one day old, were divided into five groups, each comprising 20 birds (Figure 07):

- **Group 1:** comprising avian specimens that will not participate in any vaccination program or dietary supplementation, symbolized by None.
- **Group 2:** comprising avian specimens that will participate in a conventional vaccination program, antibiotic administration, and dietary supplementation as follow:

Day 7: Combined vaccination of ND/IB.

Day 14: GD vaccination.

Day 21: ND/IB Booster.

Day 28: GD Booster.

Day 35: ND/IB booster.

Day 1-4: Trimethoprim/Sulphamethoxazole + Hepatoprotective.

Day 11-16: ADE Vitamins.

Day 20-22: Complex B vitamin.

Day 23-24: Anticoccidial.

Day 29- 32: Vitamin D booster.

Day 33-36: Yeast.

Day 37-40: Vit complex.

This group is symbolized by Conv.

- **Group 3:** comprising avian specimens that will not be subjected to any vaccination protocol or nutritional enrichment. Nevertheless, they will be administered three doses of 5mg/kg body weight of leaf extract-based copper nanoparticles via intramuscular injection on days 4, 14, and 26, respectively, symbolized by LP-CuNP.
- **Group 4:** comprising avian specimens that will not be subjected to any vaccination protocol or nutritional enrichment. Nevertheless, they will be administered three doses of 5mg/kg body weight of rhizome extract-based copper nanoparticles via intramuscular injection on days 4, 14, and 26, respectively, symbolized by RP-CuNP.
- **Group 5:** comprising avian specimens that will not be subjected to any vaccination protocol or nutritional enrichment. Nevertheless, they will be administered three doses of 5mg/kg body weight of a mixture of both plant-based copper nanoparticles via intramuscular injection on days 4, 14, and 26, respectively, symbolized by MP-CuNP.

Four chickens from each group will be slaughtered after four days after the last injection. Blood and some organs will be recuperated immediately for later analysis.

The birds were raised under standard hygienic conditions with straw litter, and temperature and humidity were carefully regulated. They had ad libitum access to water and feed suitable for

each stage of the rearing period. All birds were fed a commercial broiler diet consisting of starter, grower, and finisher phases.

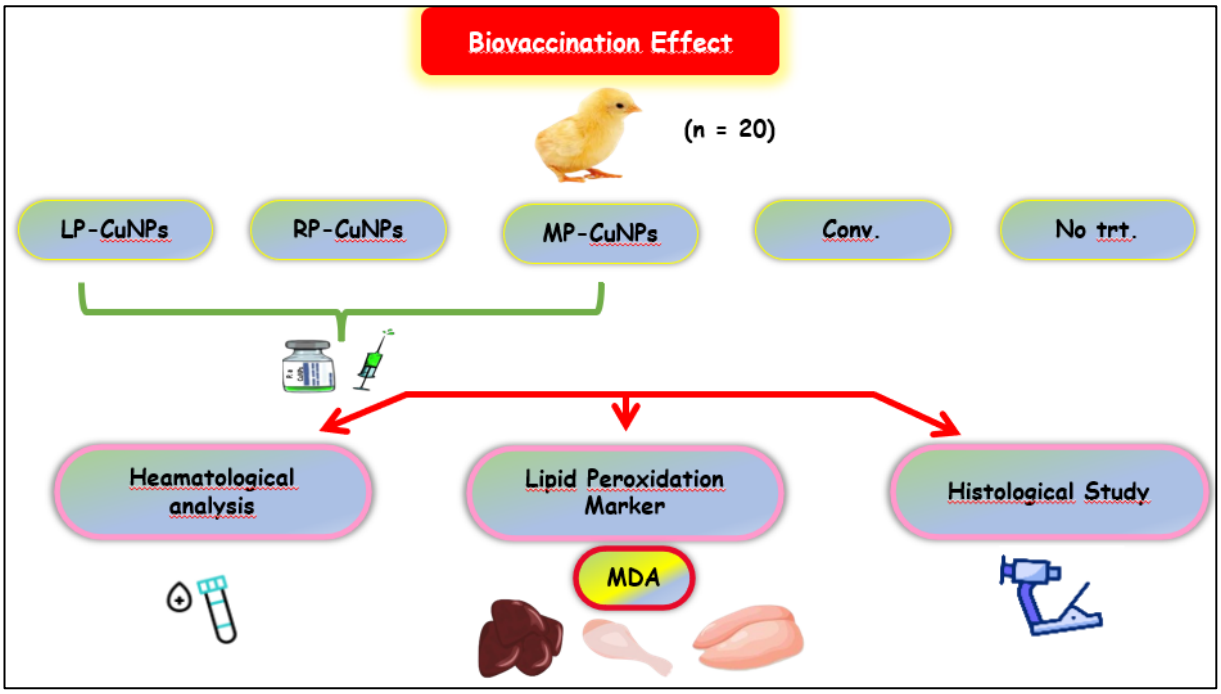

Figure 7: Biovaccination experimental design.

II.2.3. Homogenates Preparation and Tissue Biochemical Parameters

2g of tissue (liver and breast muscle) were milled in 5ml of TBS (Tris 50 Mm; NaCl 150 mM; pH 7,4) and 0,5 ml TCA 20%. The suspension was centrifuged 10 minutes at 3000 rpm. While the supernatant was kept in the freezer for oxidative stress markers and glycogen determination.

- **Glycogen Determination**

Liver and muscle glycogen were evaluated using anthrone reagent method as described by Duvhåteau and Florkin (Duvhåteau & Florkin, 1959): Two milliliters of anthrone-sulfuric acid reagent are added to 50 µl of the sample (homogenate 1), and the mixture is then placed in a water bath at 80°C for 10 minutes. A green coloration develops, with its intensity being proportional to the amount of carbohydrates present in the sample. The optical density is measured at $\lambda = 620$ nm against a reagent blank containing distilled water. The absorbance value is calculated and converted into an equivalent carbohydrate concentration using a calibration curve established with glucose (0.2, 0.4, 0.6, 0.8, 1.0 mg/ml) under the same experimental conditions. Figure 04 recapitulates all the steps of the acute toxicity experiment.

II.2.4. Oxidative Stress Parameters

- **Lipid Peroxidation Evaluation**

The procedure relies on the condensation of MDA within an acidic environment and in the presence of heat alongside thiobarbituric acid (TBA). This chemical process results in the creation

of a pink compound involving two TBA molecules, which can subsequently be quantified through absorption spectrophotometry at a wavelength of 532 nm. The concentration of MDA is reported in units of nanomoles per gram of tissue (Yagi, 1976).

In brief, 100 µl of the sample and 400 µl of TBA reagent were pipetted into glass screw-cap test tubes, which were then sealed. The mixture was heated in a water bath at 100°C for 15 minutes. Following the heating process, the tubes were cooled in a cold-water bath for 30 minutes, left open to allow the evacuation of gases produced during the reaction. The mixture was then centrifuged at 3000 rpm for 5 minutes, and the absorbance of the supernatant was measured at 532 nm using a spectrophotometer. The TBARS concentration was determined using the MDA molecular extinction coefficient (å = 1.53×10^5 $M^{-1} \cdot cm^{-1}$).

- **Determination of superoxide dismutase activity assay**

The methodology employed for the assessment of superoxide dismutase (SOD) activity via the nitroblue tetrazolium (NBT) assay, which utilizes the superoxide anion (O2 .), serves as a foundational approach for the identification of SOD presence through the spectrophotometric measurement of absorbance at 560 nm as described by Beauchamp and Fridovich (Beauchamp & Fridovich, 1971)

Table 03: Procedure of SOD activity assay

Collect in tubes	Blank (In the dark)	Sample (Illuminated tube)	Concentration in the reaction medium
EDTA-Met	1000µl	1000µl	0,1mM EDTA
Phosphate buffer	892.2µl	892.2µl	13mM Met
Sample	0	50µl	/
Phosphate buffer	1000µl	950µl	50Mm
NBT	85.2µl	85.2µl	75µM
Riboflavin	22.6µl	22.6µl	2µM

The results are expressed following the equation:

$$\mathbf{SOD} = \frac{\boldsymbol{OD\ blank} - \mathbf{OD\ sample}}{\boldsymbol{OD\ blank}}$$

- **Determination of Reduced Glutathione Level Assay**

The level of reduced glutathione (GSH) is determined by measuring the optical density resulting from the formation of 2-nitro-5-mercapturic acid, which occurs through the reduction of dithio-bis-2-nitrobenzoic acid, commonly known as the Ellman reagent, with the SH groups present in GSH. In the procedure, 800 µl of homogenate samples are added to 200 µl of salicylic

acid (0.25%), and the mixture is then centrifuged at 1000 rpm for 5 minutes. After centrifugation, 500 µl of the supernatant is mixed with 1000 µl of Tris buffer (Tris 0.4 mol, 0.02 mol NaCl, pH = 8.9) and 25 µl of DTNB (0.01 mol/l). The absorbance is then read at 412 nm after a 5-minute incubation period (Weckbecker & Cory, 1988).

$$GSH\ (nM/mg\ of\ tissue\ ) = \frac{(OD \times 1 \times 1.525)}{13133 \times 0.8 \times 0.5 \times mg\ of\ tissue}$$

II.2.5. Liver Histological Study

This portion of the research was carried out in the laboratories of the Faculty of Natural Sciences and Life, as well as in Dr. Balkhir's private laboratory for anatomopathological studies.

Following the sacrifice of the birds, liver specimens from each group were placed in a fixative solution and then embedded in paraffin blocks. The samples were subsequently sectioned into 5µm thick slices using a rotary microtome, and stained with hematoxylin and eosin to be finally observed with a microscope.

II.3. Statistical analysis

The dataset was depicted through graphical representations and histograms utilizing Microsoft Excel 2016. The results are articulated as means ± standard deviations (Mean ± SD). ANOVA tests were conducted to ascertain statistically significant differences. The outcomes of the *in vivo* experiments were conveyed as Mean ± Standard Error of the Mean (Mean ± SEM) and were compared across the studied groups employing the student's t-test. The MINITAB version 18 software was utilized for all computational analyses.

Chapter II
Results

I. Part one: *In vitro* study

I.1. In vitro essays of Phragmites australis

I.1.1. Phytochemical study

- **Qualitative phytochemical analysis of *Phragmites australis***

The phytochemical screening results showed that *Phragmites australis*'s aqueous extract of both parts (leaves and rhizomes) is rich in different compounds such as flavonoids, phenols, and carbohydrates (Table 04).

Table 04: Phytochemical screening of the aqueous extract of *Phragmites australis*.

Phytochemical compound	*Phragmites australis* aqueous extract	
	Leaves	Rhizomes
Polyphenols	+	+
Flavonoids	+	+
Alkaloids	+	+
Tannins	+	+
Saponins	+	+
Terpenoids	+	-
Carbohydrates	+	-
Unsaturated steroids	+	+
Derived steroids	+	+

(+): Present, (-): Absent

- **Phenolic and flavonoid content**

The total phenolic content is quantified in terms of gallic acid equivalents (mg GA eq/g of dry plant extract), while the total flavonoid content is quantified in terms of quercetin equivalents (mg Q eq/g of dry plant material), utilizing the following equation derived from the calibration curve: $Y = 0.007x + 0.009$ ($R^2 = 0.985$) for phenolic compounds and $Y = 0.006x + 0.031$ for flavonoid compounds ($R^2 = 0.993$). The findings are illustrated in Table 05.

Table 05: Phenolic and flavonoid content of *P.australis* aqueous extract.

Compounds	Total phenols (mg of GAE/g of extract)	Total flavonoids (mg QE/g of extract)
Leaf aqueous extract	70.74± 1.94	3.64± 0.98
Rhizomes aqueous extract	30.0± 0.54	5.92± 1.01

I.1.2. GC-MS analysis

The examination and characterization of volatile constituents from *P. australis* extracts (leaves and rhizomes) were performed utilizing GC-MS analysis. Through the application of GC-MS methodologies, more than 200 components were identified (Table 06, and Table 07). The chemical constituents of *P. australis* leaf extract were dominated by 1-Dodecanol (48.25%),

Pyrazine, tetramethyl (.128%), Heptadecane, 2,6,10,15-tetramethyl (0.91%), Cyclopentasiloxane, decamethyl (0.93%) and Cyclotetrasiloxane, octamethyl (0.56%), while the rhizome extract was dominated by 1-Dodecanol (48.25%), Decyl octyl ether (3.722%), Phthalic acid, 8-bromoctyl isobutyl ester (1.382%), Pyrazine, tetramethyl- (1.287%), Cyclopentasiloxane, decamethyl- (0.939%) and Cyclotetrasiloxane, octamethyl- (0.566%).

Table 06: Quantification of volatile compounds by GC-MS of *P. australis* leaf extract.

Peak #	Name	Formula	R.T. (s)	Area %
1	Pyridine, 2,4,6-trimethyl-	$C_8H_{11}N$	519.375	0.185
2	Cyclotetrasiloxane, octamethyl-	$C_8H_{24}O_4Si_4$	525.98	0.566
3	1-Hexanol, 2-ethyl-	$C_8H_{18}O$	560.425	0.198
4	Cyclohexene, 4-ethenyl-1,4-dimethyl-	$C_{10}H_{16}$	563.796	0.179
5	Pyrazine, tetramethyl-	$C_8H_{12}N_2$	623.786	1.287
6	Linalyl acetate	$C_{12}H_{20}O_2$	637.587	0.071
7	Nonanal	$C_9H_{18}O$	641.938	0.088
8	Cyclopentasiloxane, decamethyl-	$C_{10}H_{30}O_5Si_5$	691.491	0.939
9	Undecane	$C_{11}H_{24}$	738.646	0.049
10	Cyclodecanol	$C_{10}H_{20}O$	744.805	0.054
11	1,5-Dimethyl-1-vinyl-4-hexenyl butyrate	$C_{14}H_{24}O_2$	792.808	0.057
12	m-Ethylacetophenone	$C_{10}H_{12}O$	804.602	0.007
13	Dodecane, 2,6,11-trimethyl-	$C_{15}H_{32}$	816.363	0.029
14	(1R,3R,4S,5S)-1-Isopropyl-4-methylbicyclo[3.1.0]hexan-3-yl acetate-rel	$C_{12}H_{20}O_2$	829.467	0.031
15	Dodecane, 2,6,11-trimethyl-	$C_{15}H_{32}$	833.846	0.081
16	Undecanal	$C_{11}H_{22}O$	841.331	0.019
17	Trimethylsilylcatecholpyruvatetris(trimethylsilyl) ether	$C_{21}H_{40}O_5Si_4$	856.708	0.49
18	Triacetin	$C_9H_{14}O_6$	875.414	0.201
19	Tridecane, 5-methyl-	$C_{14}H_{30}$	882.295	0.02
20	Pentanoic acid, 2,2,4-trimethyl-3-hydroxy-, isobutyl ester	$C_{12}H_{24}O_3$	887.91	0.305
21	Dodecane, 3-methyl-	$C_{13}H_{28}$	890.952	0.092
22	Pentanoic acid, 2,2,4-trimethyl-3-hydroxy-, isobutyl ester	$C_{12}H_{24}O_3$	905.368	0.477
23	Octadecane, 6-methyl-	$C_{19}H_{40}$	922.984	0.015
24	Dodecanal	$C_{12}H_{24}O$	931.787	0.063
25	Bicyclo[5.2.0]nonane, 2-methylene-4,8,8-trimethyl-4-vinyl-	$C_{15}H_{24}$	953.746	0.04
26	1-Dodecanol	$C_{12}H_{26}O$	986.66	48.251
27	2,5-Cyclohexadiene-1,4-dione, 2,6-bis(1,1-dimethylethyl)-	$C_{14}H_{20}O_2$	988.172	0.083

28	Ethanone, 1-(6,6-dimethylbicyclo[3.1.0]hex-2-en-2-yl)-	$C_{10}H_{14}O$	999.155	0.031
29	3-Ethoxy-1,1,1,7,7,7-hexamethyl-3,5,5-tris(trimethylsiloxy)tetrasiloxane	$C_{17}H_{50}O_7Si_7$	1005.56	0.363
30	Tetracontane, 3,5,24-trimethyl-	$C_{43}H_{88}$	1007.09	0.186
31	Oxirane, dodecyl-	$C_{14}H_{28}O$	1017.19	0.026
32	Dodecanoic acid, methyl ester	$C_{13}H_{26}O_2$	1026.9	0.123
33	Ethyl dodecyl ether	$C_{14}H_{30}O$	1032.92	0.086
34	Lilial	$C_{14}H_{20}O$	1036.4	0.039
35	Hexadecane	$C_{16}H_{34}$	1041.66	0.028
36	Decane, 5-propyl-	$C_{13}H_{28}$	1044.73	0.015
37	Benzene, (1-propylheptyl)-	$C_{16}H_{26}$	1048.45	0.016
38	Dodecane, 5-methyl-	$C_{13}H_{28}$	1049.38	0.019
39	Hexane, 3,3-dimethyl-	C_8H_{18}	1060.39	0.011
40	Heptadecane, 2,6,10,14-tetramethyl-	$C_{21}H_{44}$	1064.15	0.03
41	2-Methyl-1-undecanol	$C_{12}H_{26}O$	1080.98	0.19
42	1-Iodo-2-methylundecane	$C_{12}H_{25}I$	1086.69	0.185
43	Diethyl Phthalate	$C_{12}H_{14}O_4$	1087.61	0.164
44	Diphenyl sulfide	$C_{12}H_{10}S$	1088.24	0.025
45	trans-2-Dodecen-1-ol	$C_{12}H_{24}O$	1097.83	0.01
46	Benzene, (1-butylheptyl)-	$C_{17}H_{28}$	1117.73	0.036
47	Cyclopentaneacetic acid, 3-oxo-2-pentyl-, methyl ester	$C_{13}H_{22}O_3$	1132.68	0.243
48	Octane, 1,1'-oxybis-	$C_{16}H_{34}O$	1135.74	0.056
49	3-Isopropoxy-1,1,1,7,7,7-hexamethyl-3,5,5-tris(trimethylsiloxy)tetrasiloxane	$C_{18}H_{52}O_7Si_7$	1138.43	0.355
50	Tetradecane, 2,2-dimethyl-	$C_{16}H_{34}$	1140.89	0.018
51	Benzene, (1-ethylnonyl)-	$C_{17}H_{28}$	1141.76	0.021
52	n-Hexyl salicylate	$C_{13}H_{18}O_3$	1152.93	0.025
53	1-Iodo-2-methylundecane	$C_{12}H_{25}I$	1162.12	0.159
54	Heptadecane, 2,6,10,14-tetramethyl-	$C_{21}H_{44}$	1166.71	0.11
55	Hydrazinecarboxamide	CH_5N_3O	1186.1	0.012
56	Undecane, 4,6-dimethyl-	$C_{13}H_{28}$	1194.08	0.051
57	n-Hexadecanoic acid	$C_{16}H_{32}O_2$	1203.45	0.041
58	Hydrazinecarboxamide	CH_5N_3O	1225.78	0.006
59	1-Iodo-2-methylundecane	$C_{12}H_{25}I$	1233.77	0.109
60	Hexadecane, 2,6,10,14-tetramethyl-	$C_{20}H_{42}$	1240.95	0.079
61	Benzene, (1-methylundecyl)-	$C_{18}H_{30}$	1243.14	0.017
62	Benzoic acid, 2-hydroxy-, 2-methylbutyl ester	$C_{12}H_{16}O_3$	1245.87	0.013
63	13-Methyltetradecanal	$C_{15}H_{30}O$	1246.8	0.026
64	Isoamyllaurate	$C_{17}H_{34}O_2$	1265.1	0.411
65	Dodecanoic acid, 1,1-dimethylpropyl ester	$C_{17}H_{34}O_2$	1267.63	0.081
66	Caffeine	$C_8H_{10}N_4O_2$	1275.72	0.017

67	Hydrazinecarboxamide	CH_5N_3O	1281.58	0.002
68	(1R,2R,4S)-2-(6-Chloropyridin-3-yl)-7-methyl-7-azabicyclo[2.2.1]heptane	$C_{12}H_{15}ClN_2$	1282.25	0.008
69	Pentadecane	$C_{15}H_{32}$	1302.02	0.05
70	Benzenemethanol, α-[1-(ethylmethylamino)ethyl]-, [R-(R*,S*)]-	$C_{12}H_{19}NO$	1312.82	0.105
71	Benzene, (1-methylnonadecyl)-	$C_{26}H_{46}$	1313.44	0.017
72	Hydrazinecarboxamide	CH_5N_3O	1326	0.024
73	n-Hexadecanoic acid	$C_{16}H_{32}O_2$	1340.11	0.075
74	Dibutyl phthalate	$C_{16}H_{22}O_4$	1348.07	0.146
75	Cyclooctasiloxane, hexadecamethyl-	$C_{16}H_{48}O_8Si_8$	1355.79	0.173
76	Dodecane, 4,6-dimethyl-	$C_{14}H_{30}$	1367.08	0.022
77	Semicarbazide	CH_5N_3O	1395.08	0.006
78	Hydrazinecarboxamide	CH_5N_3O	1419.5	0.001
79	Nickel tetracarbonyl	C_4NiO_4	1440.13	0.001
80	Hydrazinecarboxamide	CH_5N_3O	1443.12	0.008
81	3-Ethoxy-1,1,1,7,7,7-hexamethyl-3,5,5-tris(trimethylsiloxy)tetrasiloxane	$C_{17}H_{50}O_7Si_7$	1449.59	0.121
82	dl-Alanyl-l-alanine	$C_6H_{12}N_2O_3$	1451.96	0.003
83	Semicarbazide	CH_5N_3O	1458.17	0.001
84	Hydrazinecarboxamide	CH_5N_3O	1466.48	0.001
85	Benzenemethanol, α-(1-aminoethyl)-	$C_9H_{13}NO$	1468.36	0.002
86	Semicarbazide	CH_5N_3O	1512.72	0.002
87	Hexasiloxane, tetradecamethyl-	$C_{14}H_{42}O_5Si_6$	1534.62	0.108
88	Hydrazinecarboxamide	CH_5N_3O	1548.59	0.007
89	dl-Alanyl-l-alanine	$C_6H_{12}N_2O_3$	1558.04	0.001
90	Hydrazinecarboxamide	CH_5N_3O	1564.48	0.009
91	dl-Alanyl-l-alanine	$C_6H_{12}N_2O_3$	1566.33	0.001
92	Hydrazinecarboxamide	CH_5N_3O	1581.87	0.006
93	Semicarbazide	CH_5N_3O	1602.56	0.002
94	Benzoic acid, octadecyl ester	$C_{25}H_{42}O_2$	1610.92	0.025
95	3-Isopropoxy-1,1,1,7,7,7-hexamethyl-3,5,5-tris(trimethylsiloxy)tetrasiloxane	$C_{18}H_{52}O_7Si_7$	1613	0.111
96	Semicarbazide	CH_5N_3O	1615.36	0.001
97	1,2-Propanediamine	$C_3H_{10}N_2$	1625.08	0.001
98	Carbonic acid, bis(2-ethylhexyl) ester	$C_{17}H_{34}O_3$	1656.5	0.01
99	Benzoic acid, hexyl ester	$C_{13}H_{18}O_2$	1665.64	0.011
100	Semicarbazide	CH_5N_3O	1676.88	0.002
101	Nickel tetracarbonyl	C_4NiO_4	1679.45	0.001
102	2-(2,2-Dimethyl-propionyl)-1-(hydroxy-phenyl-methyl)-1,2,3,4-tetrahydroisoquinoline-3-carboxylic acid	$C_{22}H_{25}NO_4$	1680.59	0.017
103	Heptadecane, 2,6,10,15-tetramethyl-	$C_{21}H_{44}$	1712.86	0.043

104	Hexanoic acid, 2-ethyl-, anhydride	$C_{16}H_{30}O_3$	1717.27	0.028
105	Heptadecane, 2,6,10,15-tetramethyl-	$C_{21}H_{44}$	1732.3	0.912
106	Nickel tetracarbonyl	C_4NiO_4	1754.93	0.002
107	Cyclononasiloxane, octadecamethyl-	$C_{18}H_{54}O_9Si_9$	1757.19	0.114
108	N-(4-Nitrophenyl)-2-pyrrolidinecarboxamide, N'-acetyl	$C_{13}H_{15}N_3O_4$	1758.46	0.008
109	Semicarbazide	CH_5N_3O	1776.52	0.002
110	L-Prolinamide	$C_5H_{10}N_2O$	1786.44	0.004
111	Semicarbazide	CH_5N_3O	1796.76	0.001
112	Nickel tetracarbonyl	C_4NiO_4	1800.03	0
113	3-Methylhexan-2-amine	$C_7H_{17}N$	1800.99	0.001
114	Hydrazinecarboxamide	CH_5N_3O	1809.92	0.001
115	Semicarbazide	CH_5N_3O	1829.39	0.002
116	Squalene	$C_{30}H_{50}$	1835.7	0.13
117	3-Isopropoxy-1,1,1,7,7,7-hexamethyl-3,5,5-tris(trimethylsiloxy)tetrasiloxane	$C_{18}H_{52}O_7Si_7$	1839.53	0.104
118	Hydrazinecarboxamide	CH_5N_3O	1843.67	0.057
119	Hydrazinecarboxamide	CH_5N_3O	1896.43	0.005
120	1,2-Propanediamine	$C_3H_{10}N_2$	1910.64	0.002
121	dl-Alanyl-l-alanine	$C_6H_{12}N_2O_3$	1915.17	0.001
122	Hydrazinecarboxamide	CH_5N_3O	1936.29	0.004
123	Semicarbazide	CH_5N_3O	1958.34	0.002

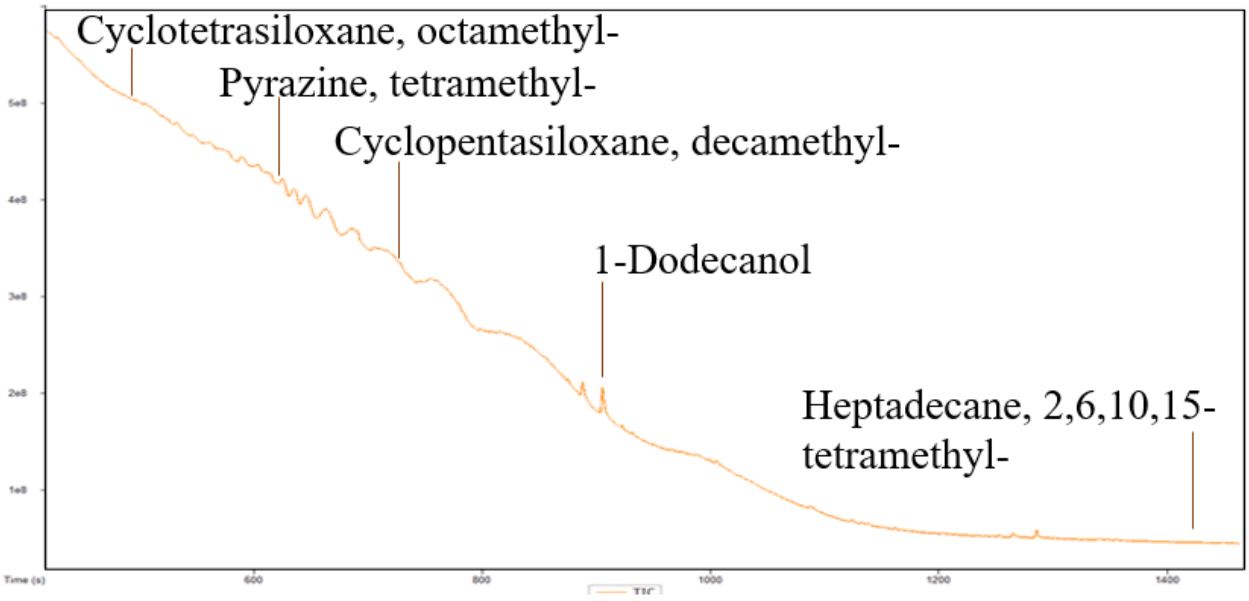

Figure 8: Spectrum of GC-MS analysis and their volatile compounds representation of *P. australis* leaf extract.

Table 07: Quantification of volatile compounds by GC-MS of *P. australis* rhizome extract.

Peak #	Name	Formula	R.T. (s)	Area %
1	Pyridine, 2,4,6-trimethyl-	C8H11N	519,375	0,185
2	Cyclotetrasiloxane, octamethyl-	C8H24O4Si4	525,98	0,566
3	1-Hexanol, 2-ethyl-	C8H18O	560,425	0,198
4	Cyclohexene, 4-ethenyl-1,4-dimethyl-	C10H16	563,796	0,179
5	Pyrazine, tetramethyl-	C8H12N2	623,786	1,287
6	Cyclopentasiloxane, decamethyl-	C10H30O5Si5	691,491	0,939
7	Trimethylsilyl catecholpyruvate tris(trimethylsilyl) ether	C21H40O5Si4	856,708	0,49
8	Triacetin	C9H14O6	875,414	0,201
9	Pentanoic acid, 2,2,4-trimethyl-3-hydroxy-, isobutyl ester	C12H24O3	887,91	0,305
10	Pentanoic acid, 2,2,4-trimethyl-3-hydroxy-, isobutyl ester	C12H24O3	905,368	0,477
11	1-Dodecanol	C12H26O	986,66	48,251
12	3-Ethoxy-1,1,1,7,7,7-hexamethyl-3,5,5-tris(trimethylsiloxy)tetrasiloxane	C17H50O7Si7	1005,56	0,363
13	Tetracontane, 3,5,24-trimethyl-	C43H88	1007,09	0,186
14	Decyl octyl ether	C18H38O	1013,65	3,722
15	Pentanoic acid, 2,2,4-trimethyl-3-carboxyisopropyl, isobutyl ester	C16H30O4	1089,74	0,185
16	trans-2-Dodecen-1-ol	C12H24O	1097,83	0,01
17	Benzene, (1-butylheptyl)-	C17H28	1117,73	0,036
18	Cyclopentaneacetic acid, 3-oxo-2-pentyl-, methyl ester	C13H22O3	1132,68	0,243
19	3-Isopropoxy-1,1,1,7,7,7-hexamethyl-3,5,5-tris (trimethylsiloxy)tetrasiloxane	C18H52O7Si7	1138,43	0,355
20	Bis(tert-butyldimethylsilyl) 2,3-bis((tert-butyldimethylsilyl)oxy)fumarate	C28H60O6Si4	1253,3	0,284
21	Phthalic acid, 8-bromoctyl isobutyl ester	C20H29BrO4	1285,68	1,382
22	3-Ethoxy-1,1,1,7,7,7-hexamethyl-3,5,5-tris(trimethylsiloxy)tetrasiloxane	C17H50O7Si7	1449,59	0,121
23	3-Isopropoxy-1,1,1,7,7,7-hexamethyl-3,5,5-tris(trimethylsiloxy)tetrasiloxane	C18H52O7Si7	1613	0,111

24	Heptadecane, 2,6,10,15-tetramethyl-	C21H44	1732,3	0,912
25	Cyclononasiloxane, octadecamethyl-	C18H54O9Si9	1757,19	0,114
26	Squalene	C30H50	1835,7	0,13
27	3-Isopropoxy-1,1,1,7,7,7-hexamethyl-3,5,5-tris(trimethylsiloxy)tetrasiloxane	C18H52O7Si7	1839,53	0,104
28	1,2-Propanediamine	C3H10N2	1910,64	0,002
29	dl-Alanyl-l-alanine	C6H12N2O3	1915,17	0,001
30	2-Hydroxybenzene-1,3-dicarboxylic acid, trimethylsilyl ether, bis(trimethylsilyl) ester	C17H30O5Si3	1941,64	0,11

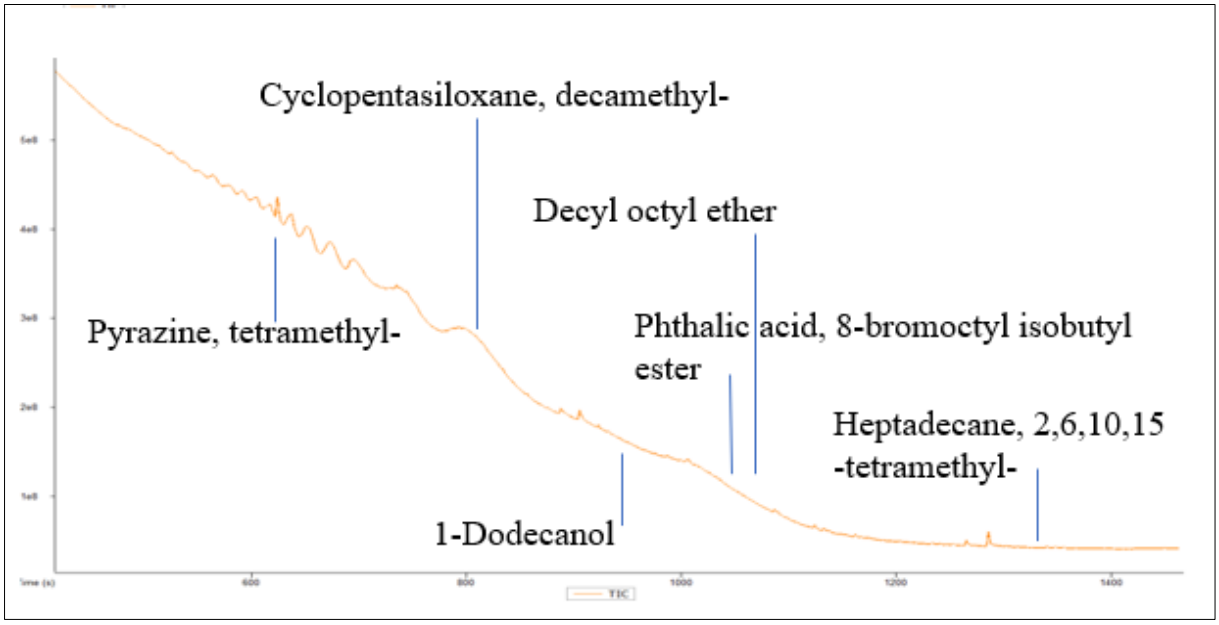

Figure 9: Spectrum of GC-MS analysis and their volatile compounds representation of *P. australis* rhizomes extract.

I.2. *P. australis*-based CuNPS Synthesis and Characterization

The current investigation demonstrates that the incorporation of both aqueous extracts (from leaves and rhizomes) of *P. australis*, individually, into the copper sulfate solution elicits a chromatic transformation from blue to a greenish-dark hue, thereby signifying the synthesis of copper nanoparticles (Figure 10). Figure 11 provides a schematic illustration of the biochemical interactions occurring between the biomolecules inherent in the plant extract and the copper metal ions, facilitating the generation of Cu NPs.

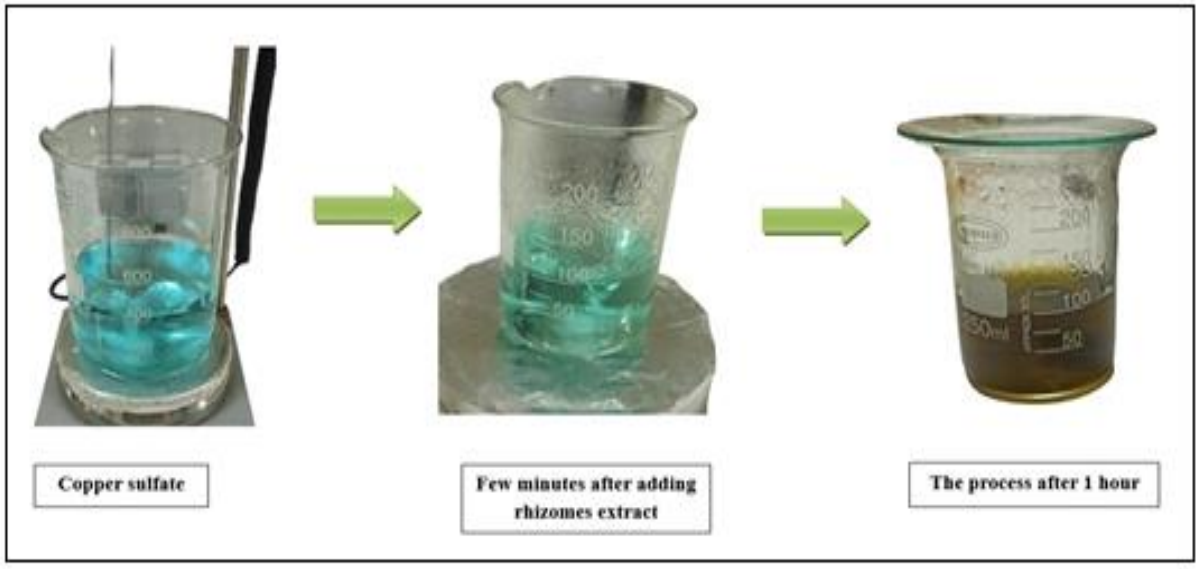

Figure 10: Color change during the formation of copper nanoparticles.

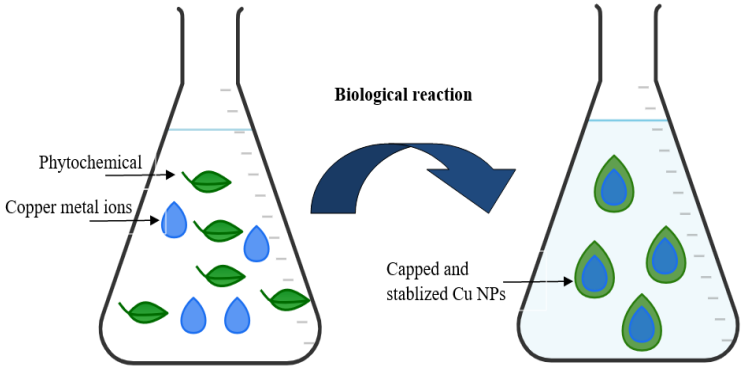

Figure 11: Schematic representation of the formation of Cu NPs via *P. australis* extract.

I.2.1. Infrared analysis results

The FT-IR analysis was conducted on both *P. australis* leaf and rhizome extracts, as well as the green synthesized Cu NPs, to identify potential biomolecules involved in the bioreduction process. The scan range was from 500 to 4000 cm^{-1}. In the leaf extract, the FT-IR spectrum (Figure 12-A) shows a broad peak at 3208 cm^{-1}, corresponding to H–bonded (–OH) groups, which slightly shifted to a higher wavenumber of 3300 cm^{-1} with lower intensity in the Cu NPs solution (Figure 12-B). Peaks at 1596 cm^{-1} and 1407 cm^{-1} indicate stretching vibrations of C–C, C=C, or C–O in aromatic cycles, with much lower intensity in the Cu NPs spectrum. A peak at 1097 cm^{-1} suggests the presence of C–H and C–O stretching from carboxylic acids, alcohols, esters, and ethers. These functional groups, commonly found in polyphenols, display lower intensity in the CuNPs, suggesting their role in reducing copper ions and stabilizing the nanoparticles. A sharp and intense

peak at 608 cm^{-1} in Figure 12-B corresponds to CuO vibrations, confirming the formation of copper nanoparticles. Similarly, in the rhizomes extract, the FT-IR spectrum (Figure 13-A) shows a broad peak at 3300 cm^{-1} for H–bonded (–OH) groups, which also shifted to a higher wavenumber of 3300 cm^{-1} with reduced intensity in the Cu NPs solution (Figure 13-B). Peaks at 1600 cm^{-1} suggest C–C, C=C, or C–O stretching in aromatics, with mild changes and slightly lower intensity in the Cu NPs spectrum. A peak at 1100 cm^{-1} indicates C–H and C–O stretching, with functional groups found in polyphenols playing a similar role in reducing and stabilizing Cu NPs. A sharp peak at 600 cm^{-1} is observed in Figure 13-B.

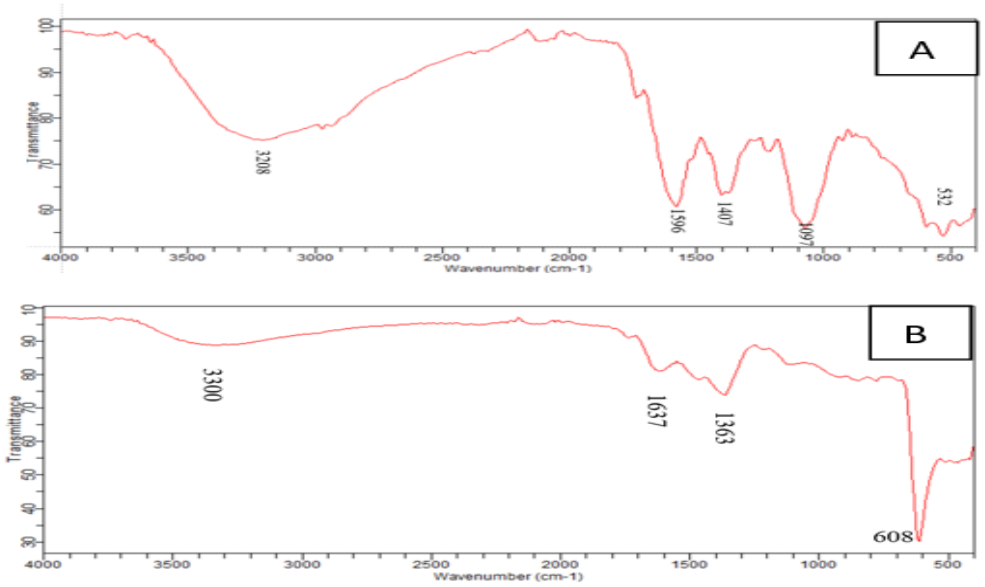

Figure 12: FT-IR Spectra of *P.australis* leaf extract (A) and phytosynthsized CuNPs (B).

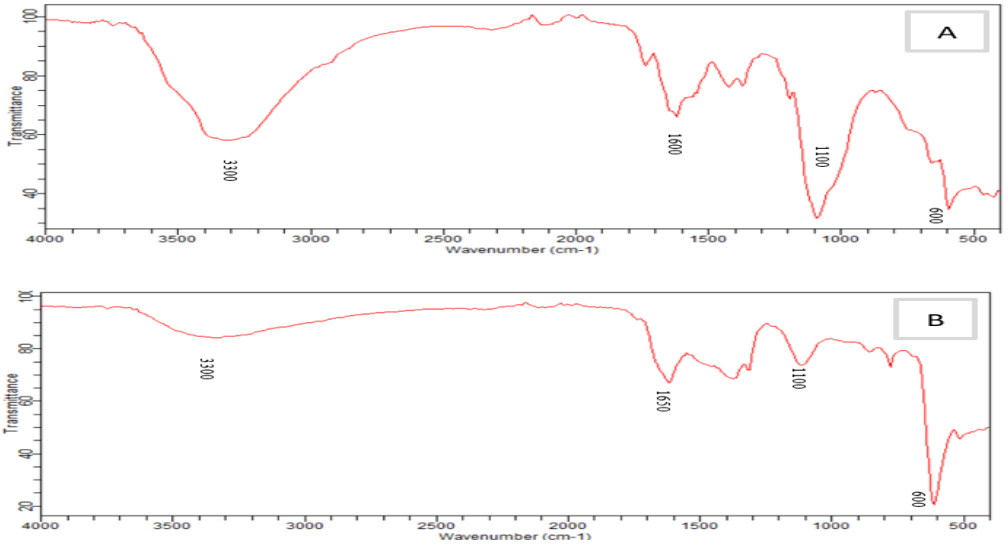

Figure 13: FT-IR Spectra of *P.australis* rhizome extract (A) and phytosynthsized CuNPs (B).

I.2.2. UV-Vis Spectroscopy results

The Surface Plasmon Resonance (SPR) characteristics of CuNPs synthesized from P. australis were assessed utilizing a UV-Vis spectrophotometer. A prominent peak at 312 nm was identified for the leaf extract, while a peak at 300 nm was observed for the rhizome extract (Figure 14).

A B

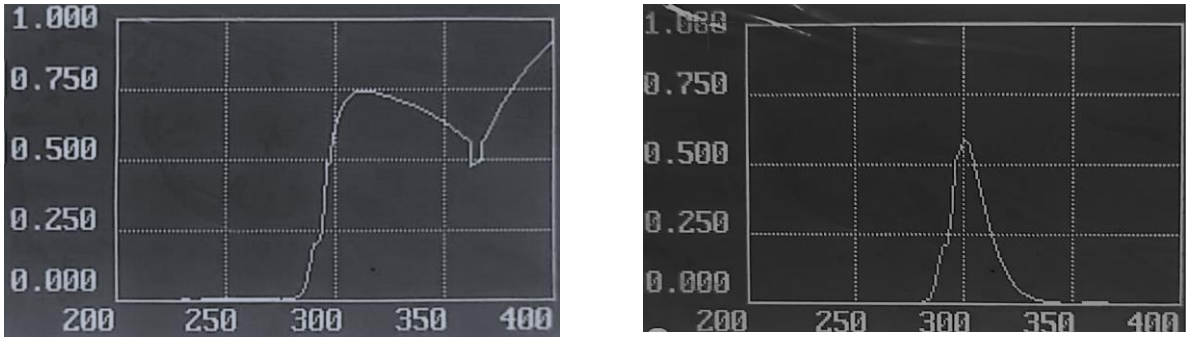

Figure 14: UV-Vis spectrum of CuNPs synthesized using *P.australis* leaf extract (A), and rhizome extract (B).

I.2.3. SEM and TEM analysis

As evidenced by the scanning electron microscopy (SEM) images (Figure 15-A and Figure 16-A), the particles exhibit an irregular morphology, albeit with a general approximation to spherical form. Transmission electron microscopy (TEM) images further corroborated our observation regarding the spherical-like morphology and provided additional insights regarding the dimensional characteristics (Figure 15-B and Figure 16-B). The TEM analysis revealed the presence of exceptionally fine nanoparticles exhibiting sizes ranging from 7,59 nm and 16,61 nm and from 7.22 nm to 30.05 nm (leaf-based CuNPs and rhizome-based CuNPs respectively). The mean diameter was determined to be approximately 13,22 nm for leaf-based CuNPs and 19.76 nm for rhizome-based CuNPs (Figure 15-C and Figure 16-C).

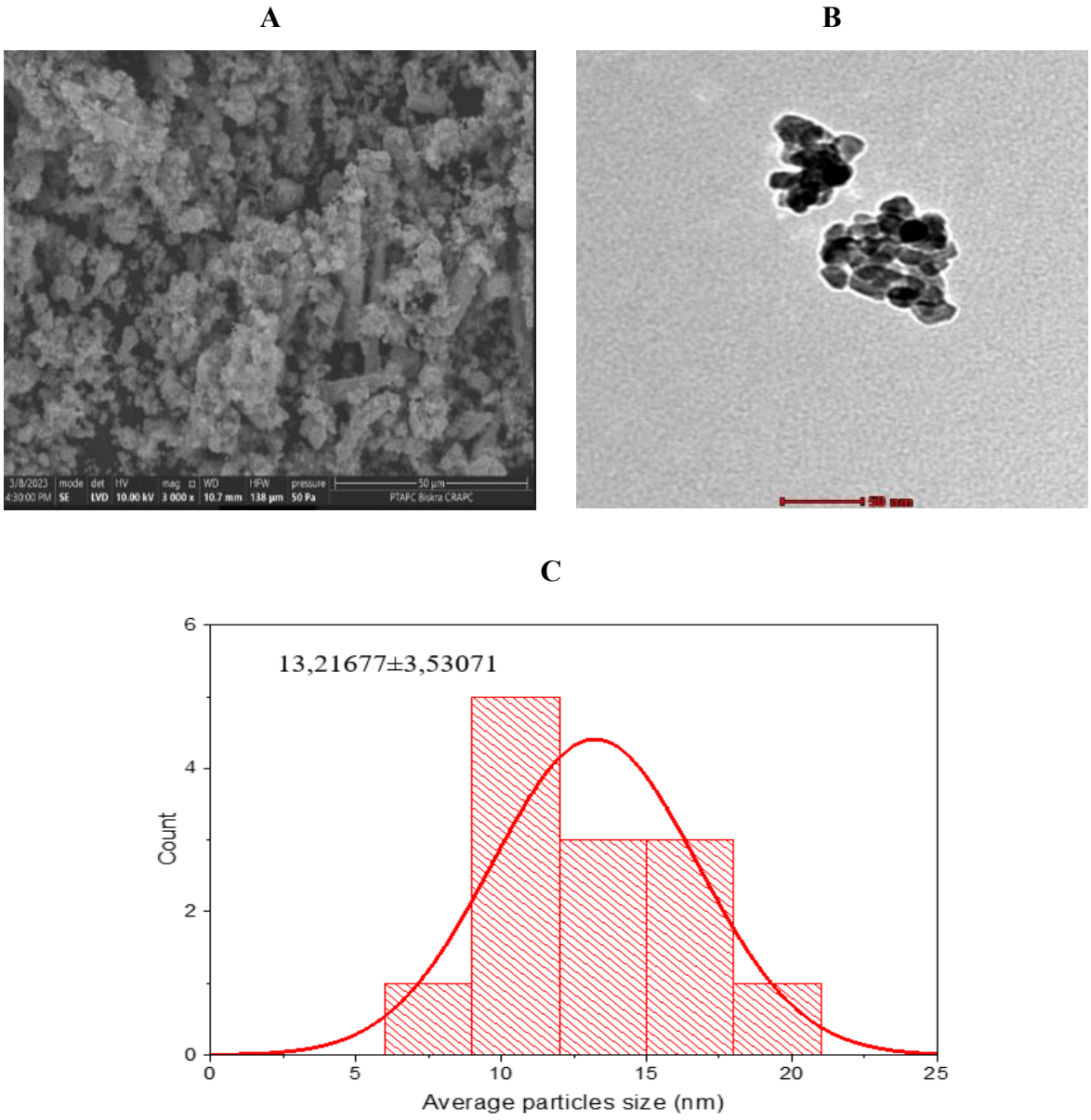

Figure 15: Characterization of Cu NPs synthesized using *P.australis* leaf extract using SEM (A), TEM (B) and size distribution analysis (C).

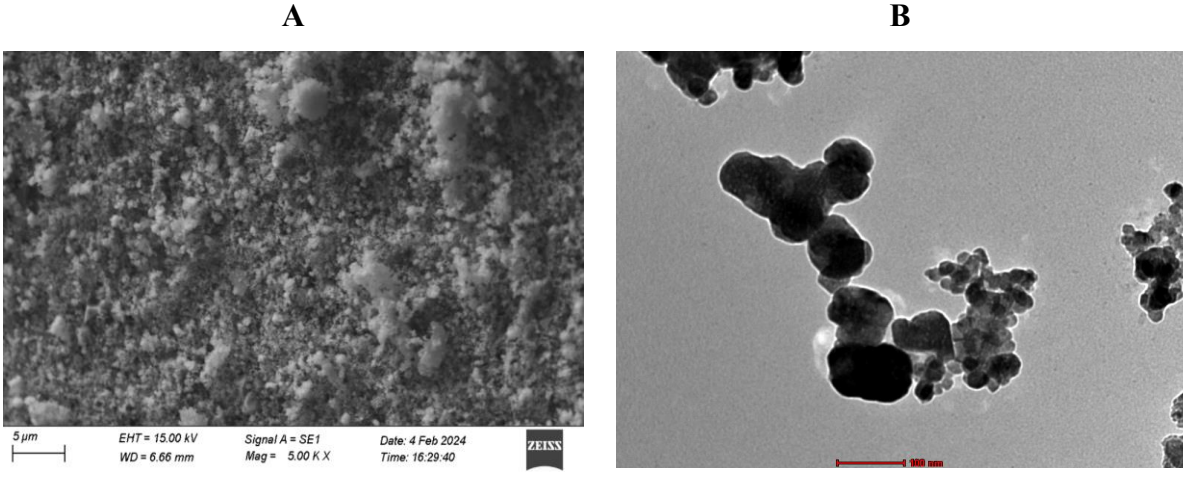

C

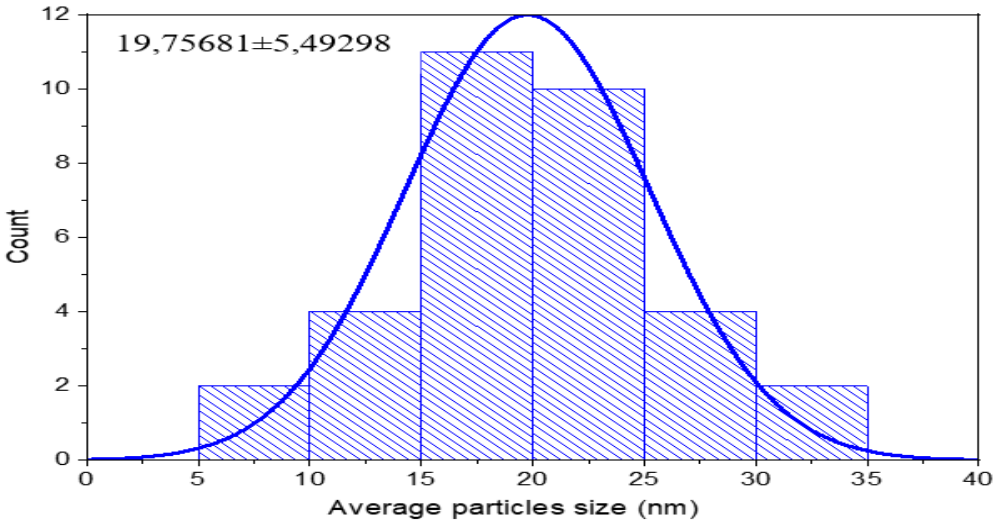

Figure 16: Characterization of Cu NPs synthesized using *P.australis* rhizome extract using SEM (A), TEM (B) and size distribution analysis (C).

I.2.4. X- ray Diffraction analysis

For the leaf-based CuNPs sample, major diffraction peaks were observed at 29.71°, 36.49°, 42.44° ,61.48° and 77.53° corresponding to the following Miller indices 110, 111, 200, 220, 222 (JCPDS 01-077-0199) assigned to Cu_2O. Besides, another diffraction peak at 50.46° assigned to Miller indices 200, corresponding to Cu (JCPDS 01-070-3038). In the rhizome-based CuNPs sample, major diffraction peaks were observed at 29.64°, 36.49°, 42.37°,61.46° and 73.63° corresponding to Miller indices 110, 111, 200, 220, 311 (JCPDS 01-075-1531), assigned to Cu_2O. The grain size of crystallite was calculated using Scherrer equation which can be written as : $D = 0{,}9\lambda/\beta\cos\theta$, where λ is the X-ray wavelength, β is the line broadening at half the maximum intensity (FWHM) and θ is the Bragg angle (Shende, Ingle, Gade, & Rai, 2015). The result demonstrates an average size of 18,06 nm for leaf-based CuNPs and 18,24 nm for rhizome-based CuNPs (Figure 17).

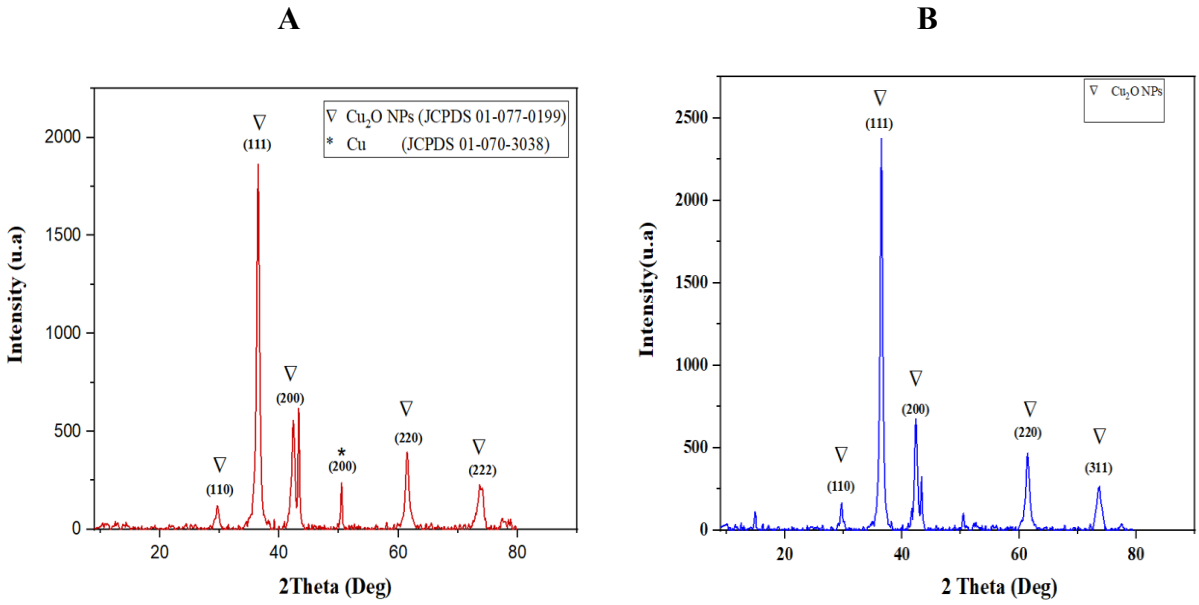

Figure 17: XRD patterns of CuNPs synthesized using *P.australis* leaves(A) and rhizomes (B).

I.2.5. Stability Analysis

Zeta potential measurement as shown in Figure 16 ranges between -37,78 mV and –45,38mV for leaf-based Cu NPs, and between -89,65 mV and -97,56mV for rhizome-based Cu NPs. The values are all negative, and the differences between the samples are relatively small.

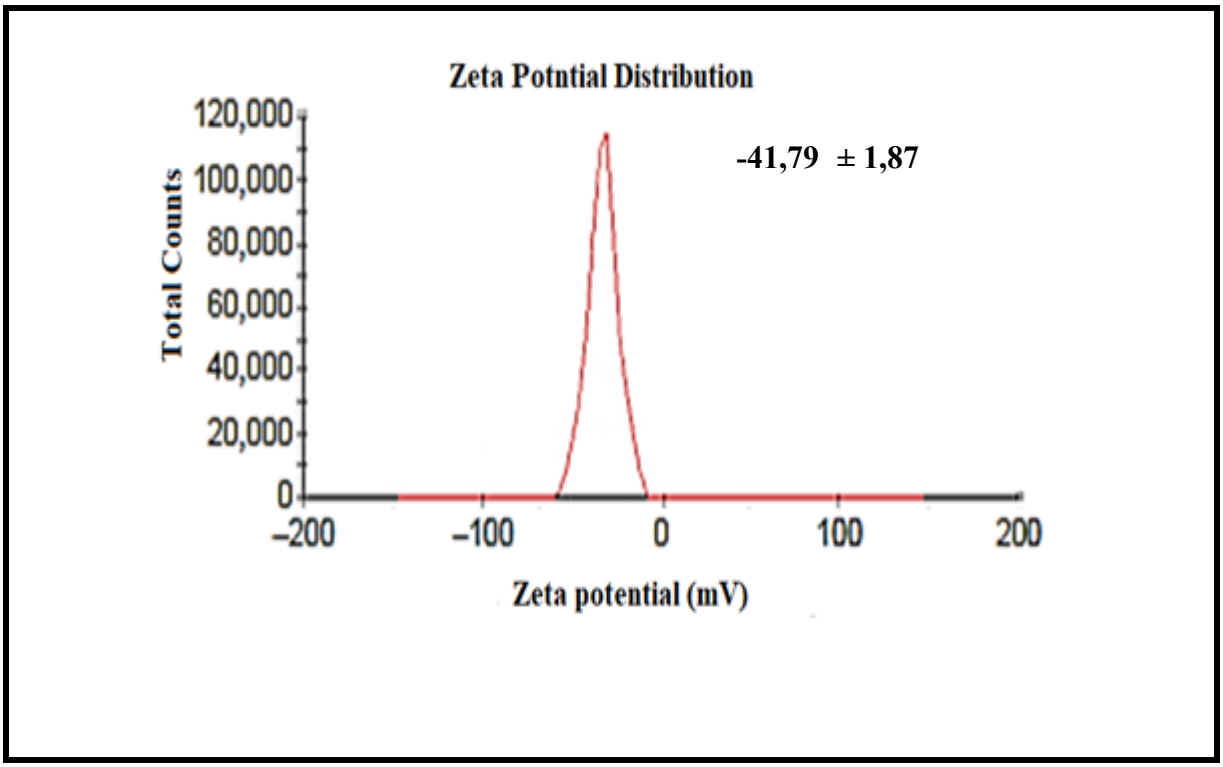

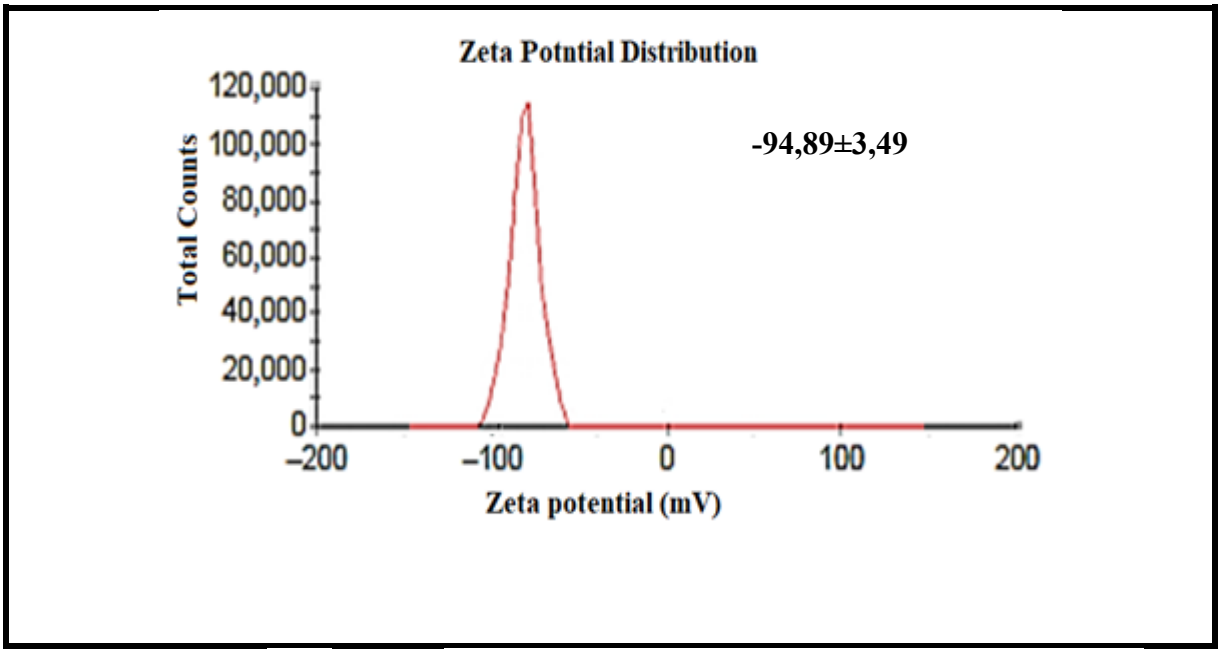

Figure 18: Zeta potential measurement of both leaf and rhizome-based Cu NPs.

I.3. Biological Activities

I.3.1. Antioxidant Activity

Figure 19 for the DPPH assay and Figure 20 for the FRAP assay present results of the antioxidant activity of both parts of *P. australis* and their synthesized Cu NPs.

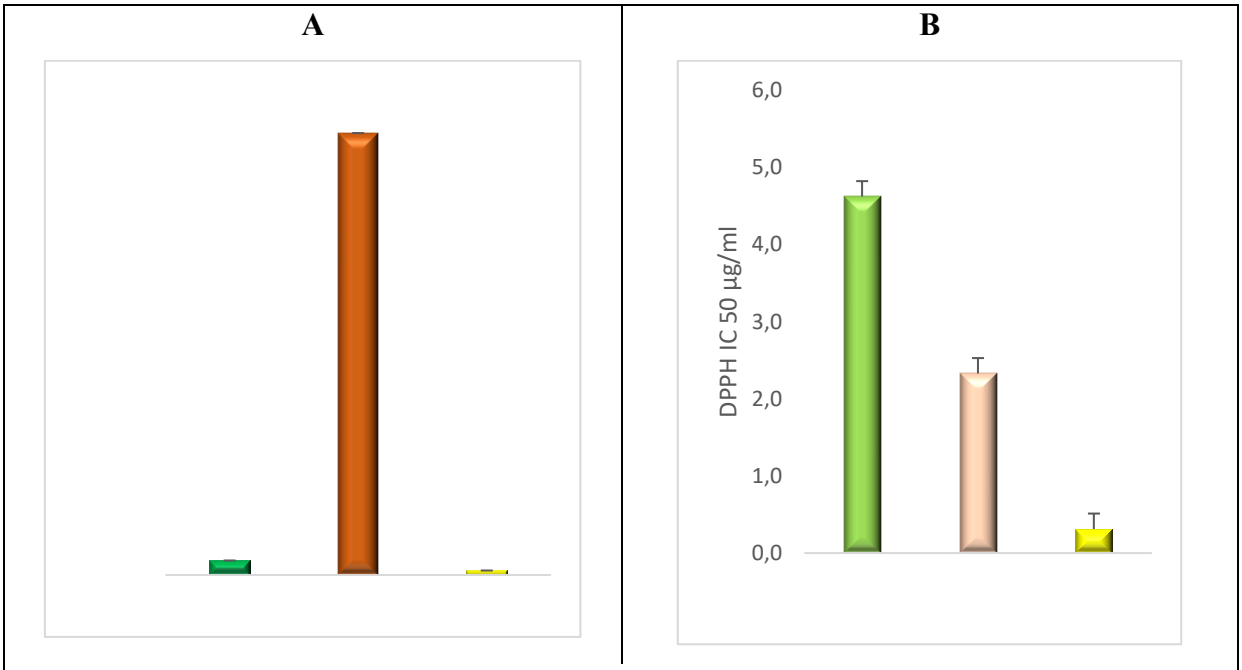

Figure 19: IC_{50} values of the antioxidant activity, using DPPH assay, of the plant extract (A) and the plant-based Cu NPs (B).

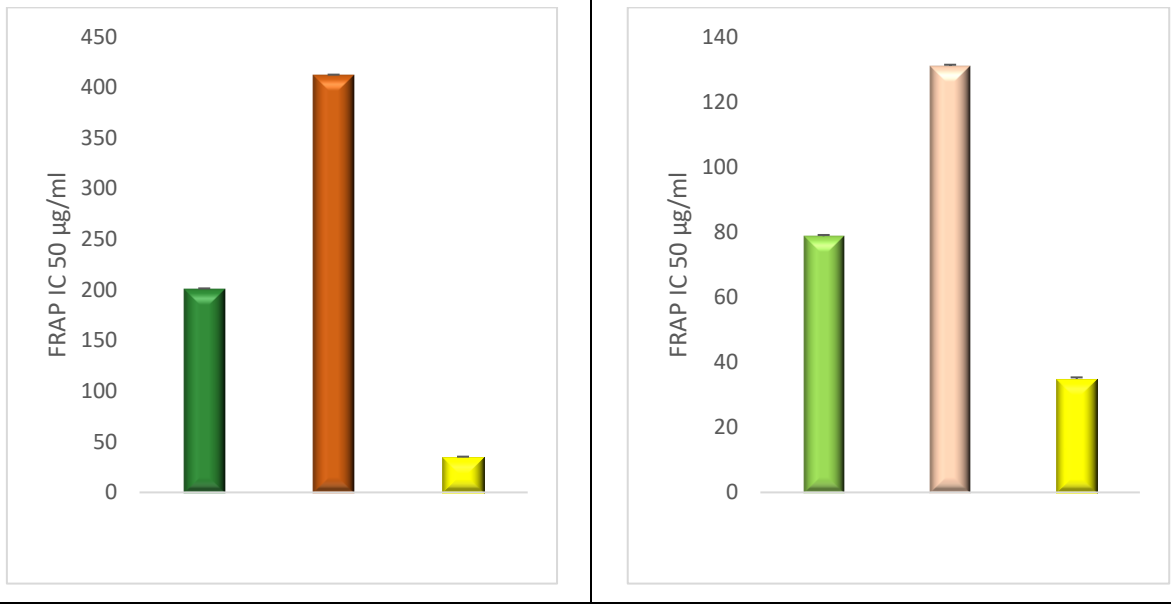

Figure 20: IC_{50} values of the antioxidant activity, using FRAP assay, of the plant extract (A) and the plant-based CuNPs (B).

I.3.2. Anti-inflammatory Activity

Figure 21 shows the IC_{50} values of the anti-inflammatory activity of both plant's parts and their phyto-synthesized copper nanoparticles, corresponding to the potential of inhibiting protein from denaturation. The plant-based Cu NPs exhibits the lowest values of IC_{50} which refers to their power in preventing BSA from denaturation. On the other hand, results of the hemolysis assay (Figure 22) realized using human erythrocytes reveals the plant potential in fighting the red blood cells' lysis. Results of the samples reveal an important anti-inflammatory power compared to the standard.

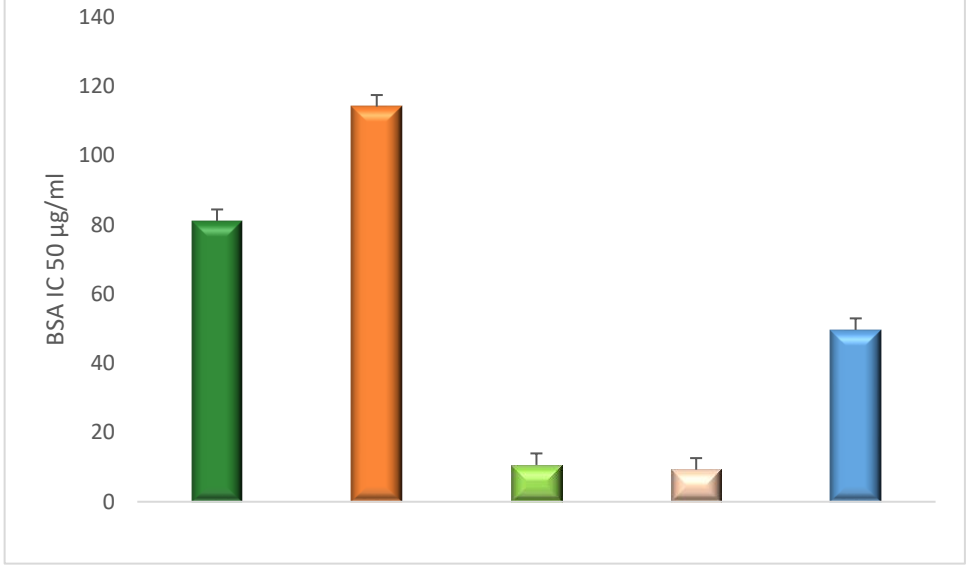

Figure 21: IC_{50} values of the anti-inflammatory activity, using BSA assay.

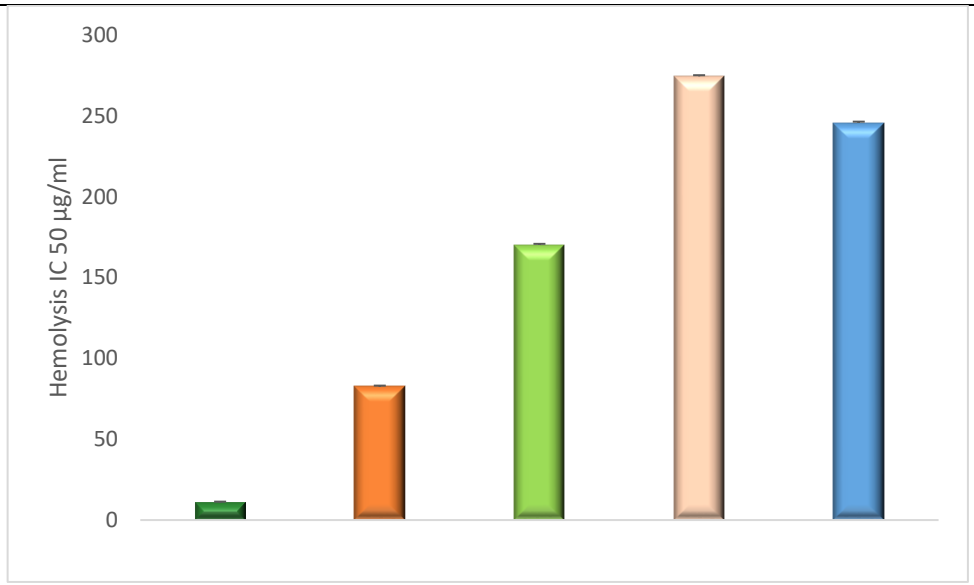

Figure 22: IC_{50} values of the anti-inflammatory activity, using hemolysis assay.

I.3.3. Antibacterial Activity

Table 07 shows the antibacterial activity of both plant-based CuNPs (LP-CuNPs and RP-CuNPs) and three standard antibiotics against four bacterial strains (Gram + and Gram -). The activity is measured as the diameter of the inhibition zone formed around the disc. The diameter of the disc itself is 6mm, so any measurement greater than this indicates antibacterial activity.The largest inhibition zone was recorded against *B. subtilis* at 40 µg/ml concentration for LP-CuNPs (Figure 21). Both plant-based CuNPs have a considerable antibacterial activity against *E. coli* even at low concentrations. However, the phyto-synthesized Cu NPs seem to have a slight antibacterial activity against *Klebsiella pneumoniae* and *Staphylococcus aureus*.

Table 08: Inhibition zone values (mm) of the tested bacterial strains and their corresponding antibiotics.

	E. coli				**K. pneumoniae**				**S. aureus**				**B. subtilis**			
Concentration (µg/ml)	5	10	20	40	5	10	20	40	5	10	20	40	5	10	20	40
	8	8.5	9	10	6.8	6.9	6.5	7	6.1	6.5	6.8	8	/	7	9	14
	9	8	8	9	6.1	6.2	6.6	7.2	6.2	6.1	7	8	/	/	/	/
Ampicillin	16				7				39				25			
Kanamycin	18				/				/				26			
Gentamycin	/				17				19				/			

LP-CuNPs	RP-CuNPs	Antibiotics (Ampicillin/ Gentamicyn/ Kanamycin)

E. coli

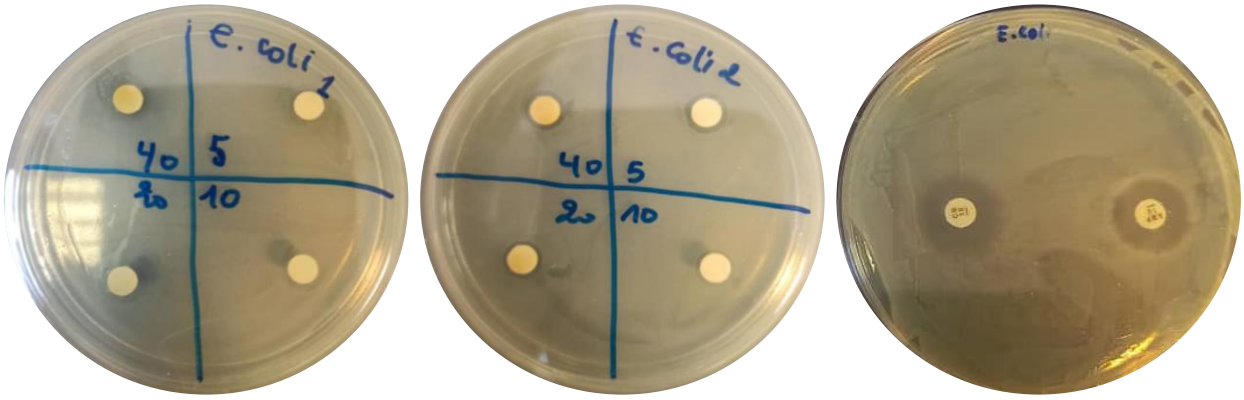

Klebsiella pneumoniae

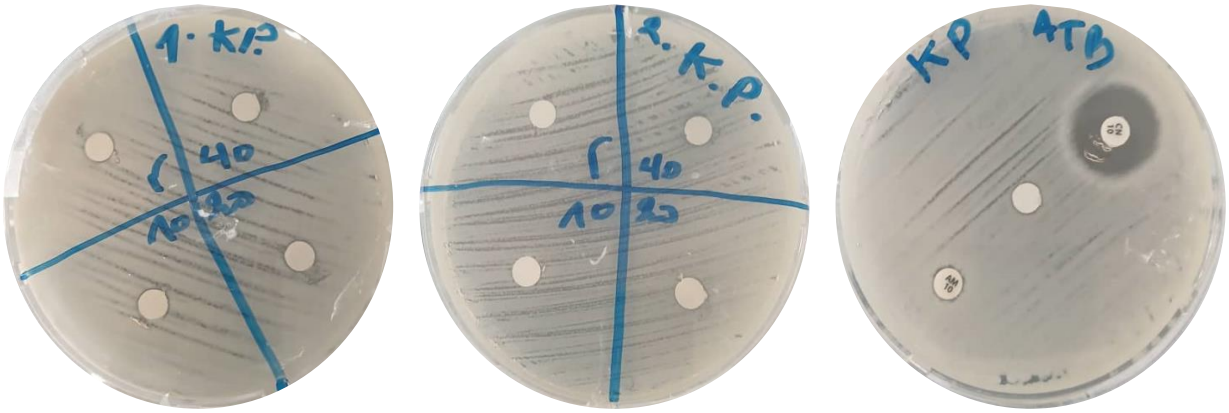

Staphylococcus aureus

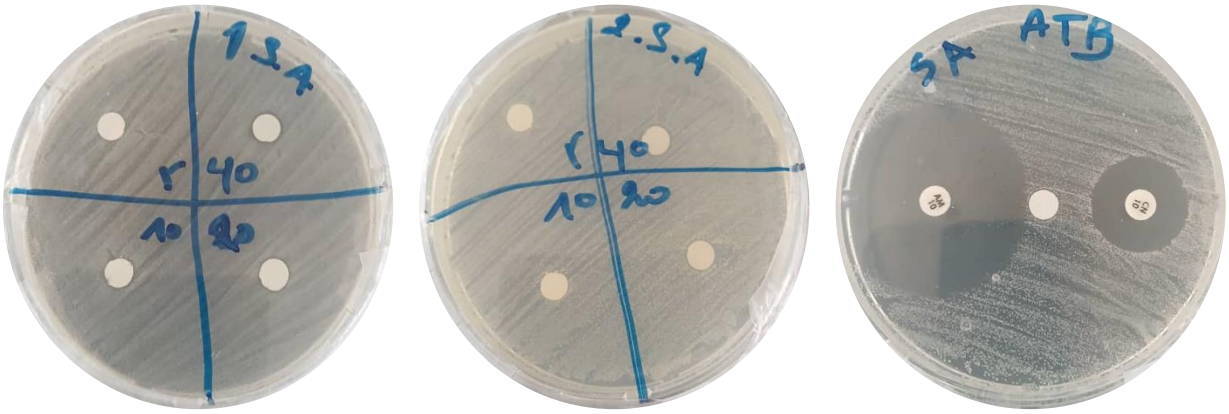

Bacillus subtilis

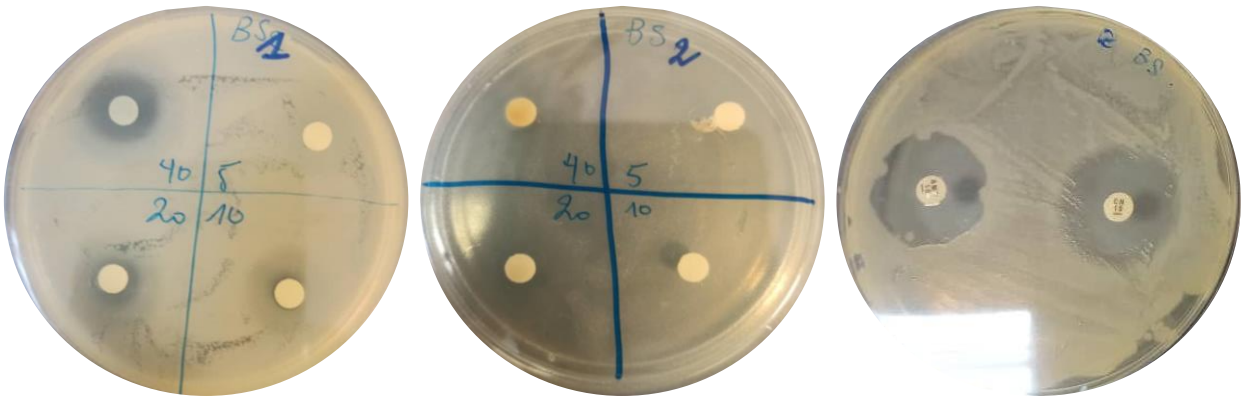

Figure 23: Anti-bacterial activity of both leaf and rhizome-based Cu NPs against gram (+) and gram (-) bacterial strains.

I.3.4. Cytotoxic Activity

As illustrated in Figure 24 and Figure 25, the cytotoxic effects of our green copper nanoparticles (CuNPs) on the MCF-7 cell line exhibit a dose-dependent relationship. The IC_{50} value, defined as the concentration at which the viability of 50% of cancer cells is compromised, is determined to be approximately 3.53 µg/ml for leaf-based CuNPs and 2,28µg/ml for rhizome-based CuNPs. Additionally, microscopic sections demonstrate the proliferative status of cancer cells where it is clear that once treated with Cu NPs, tumoral cells shrank and lost their cell-to-cell contact.

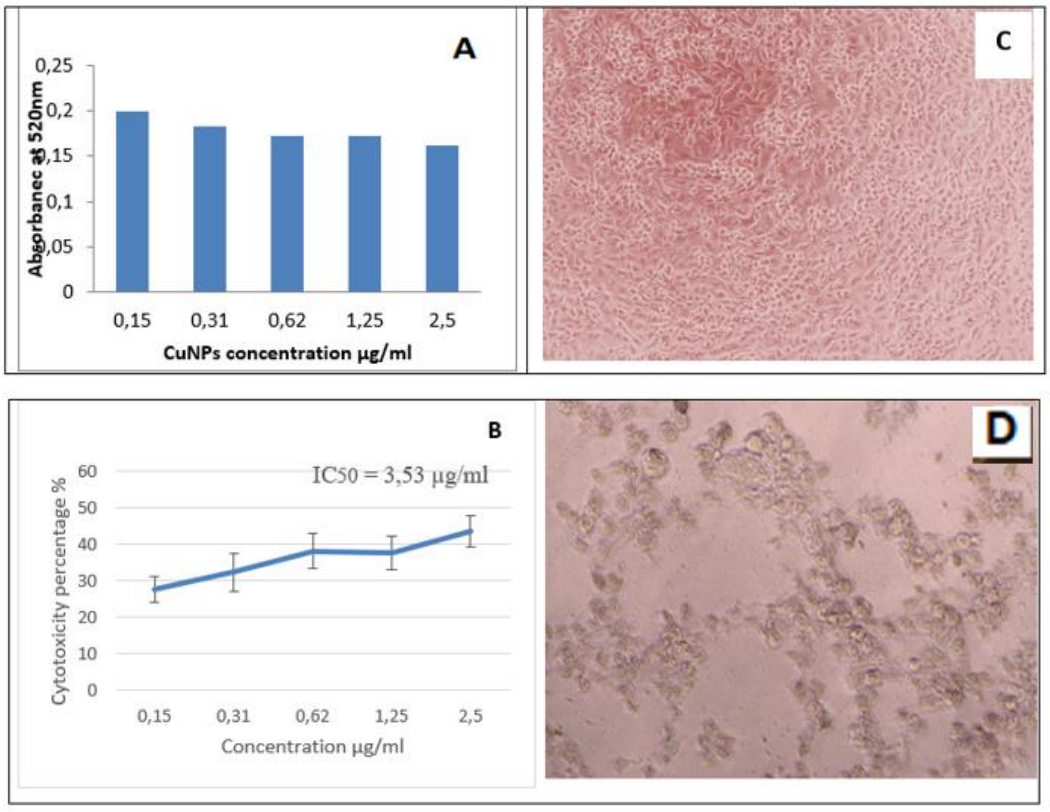

Figure 24: Absorbance variation (A), cytotoxicity percentage (B) and microscopic section of anti-proliferative activity of leaf extract-based CuNP (D) against MCF-7cells line compared to untreated cells (C).

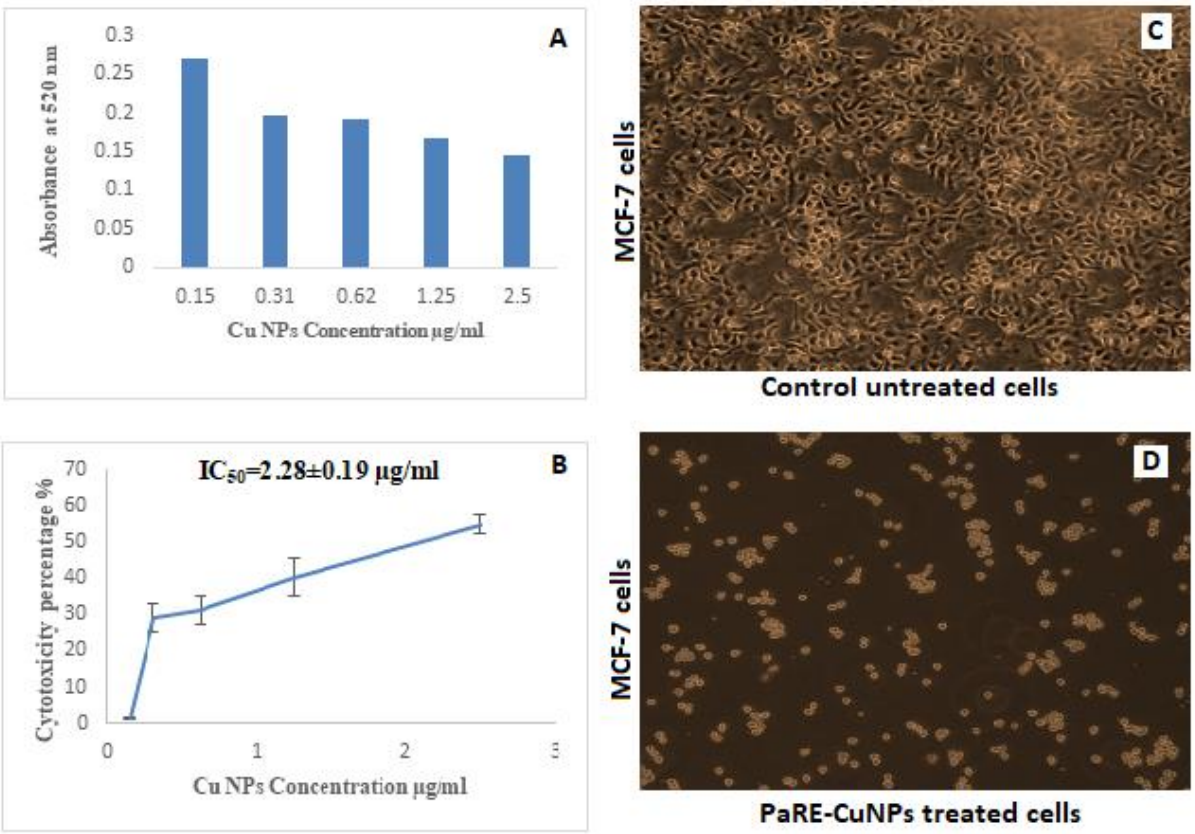

Figure 25: Absorbance variation (A), cytotoxicity percentage (B) and microscopic section of anti-proliferative activity of rhizome extract-based CuNP (D) against MCF-7cells line compared to untreated cells (C).

II. Part Two: *In Vivo* Study

II.1. Acute Toxicity Test of *P.australis*-based CuNPs

Table 08 recapitulates the birds' behavior for 24h after the green CuNPs injection. None of the animals exhibited any signs of toxicity. Their behavior remained normal, and no mortality was observed.

Table 09: Birds' behavior within 24 hours

	30 min post-injection			4 hours post-injection			24 hours post-injection		
Mortality	N	N	N	N	N	N	N	N	N
Food and water consumption	N	N	N	N	N	N	N	N	N
Diarrhea	N	N	N	N	N	N	N	N	N
Convulsion	N	N	N	N	N	N	N	N	N

N, Normal

- **Body weight and relative weights**

Body weights and organ relative weights of animals subject to acute toxicity test with different doses of Cu NPs were approximately similar to control group as presented in Table 09.

Table 10: Body weight and relative weight of broilers.

Body weight (g)	2.34±0.02	2.35±0.05 NS	2.40±0.02 NS	2.13±0.15 NS	2.41±0.09 NS
	3.07±0.02	2.44±0.10 NS	2.54±0.07 NS	2.87±0.32 NS	3.14±0.23 NS
	0.43±0.02	0.39±0.001 NS	0.35±0.02 NS	0.44±0.06 NS	0.44±0.06 NS

NS, non-significant.

II.1.1 Hematological parameters

As presented in Table 10, while white blood cells in both treated groups increased significantly ($p<0,01$ and $p<0,001$) with both tested doses, platelet levels were highly decreased ($p<0,001$). Red blood cells, percentage of hematocrite and mean corpuscular volume (MCV) increased significantly with RP-CuNPs25 dose and maintained without significant changes with RP-CuNPs50 dose. MCH levels decreased significantly with both doses.

Table 11: Hematological parameters of control and experimental groups.

	68.06±4.48	118.18±3.76***	127.64±6.60***	144.46±0.20 ***	114.21±8.56 **
	2.09 ±0.111	2.30±0.054*	2.49±0.080**	2.48±0.029 ***	2.30±0.092
	20.33±3.84	3.333±0.21***	2.000±0.37***	2.50±0.22***	4.50±0.67 ***
	8.23±0.59	7.43±0.16**	7.90±0.22	8.25±0.20	7.40±0.22*
	25.80±0.94	28.87±0.52**	30.70±0.89**	32.00±0.45 ***	28.65±1.14
	123.93±2.27	125.67±1.78	123.27±1.55	128.75±0.29 ***	124.3±0.04 ***
	39.33±0.95	32.37±0.40***	31.73±0.23***	33.15±0.42 ***	32.20±0.31 ***

Values are expressed as mean ± SE: Significance from control * $P<0.05$, ** $P<0.01$, *** $P<0.001$.

II.1.2. Biochemical parameters

Table 11 illustrates that there were no notable alterations in blood glucose, liver glycogen, and muscle glycogen when compared to the control group. Serum AST exhibited a significant increase across all samples; conversely, serum ALT and serum ALP demonstrated a significant

rise exclusively in conjunction with the RP-CuNP. Furthermore, serum urea showed an elevation with the dosage LP-CuNPs50, whereas serum uric acid experienced a significant decline with both synthesized copper nanoparticles.

Table 12: Biochemical parameters of treated and control groups.

	2.30±0.08	2.21±0.15	2.25±0.05	2.28±0.06	2.26±0.03
	26.36±0.0	25.71±0,2	26.30±0,04	26.33±0.03	25.98±0.36
	0.90±0.25	0.50±0.20	0.68±0.25	1.32± 0.09	1.09±0.14
	0.08±0.01	0.07±0.01	0.09±0.00*	0.06±0.0	0.08±0.01
	31.50±1.12	31.33±2.23	20.00±1.32 ***	19.50±0.67 ***	31.67±6.43
	9.50 ±0.66	15±1.15	13.5±1.44	10.50±0.67	19.33±1.48 **
	333.7±46.4	786.3±25.1 ***	709.7±71.8 **	471.5±10.5 ***	889.7±22.8 **
	1676±147	1535±123	1570±159.2	1928.0±16.7 ***	2640±315 *

Values are expressed as mean ± SE: Significance from control * $P<0.05$, ** $P<0.01$, *** $P<0.001$.

II.1.3. Oxidative Stress Evaluation

Figure 26, 27, 28 demonstrate the oxidative status of different organs. The injection of *P. australis*-based Cu NPs significantly increased the MDA levels of all studied organs. GSH levels have significantly increased in the kidney and the muscle; however, they decreased significantly in the liver and the heart. SOD activity decreased significantly in liver and kidney, while it was increased significantly in heart and muscle.

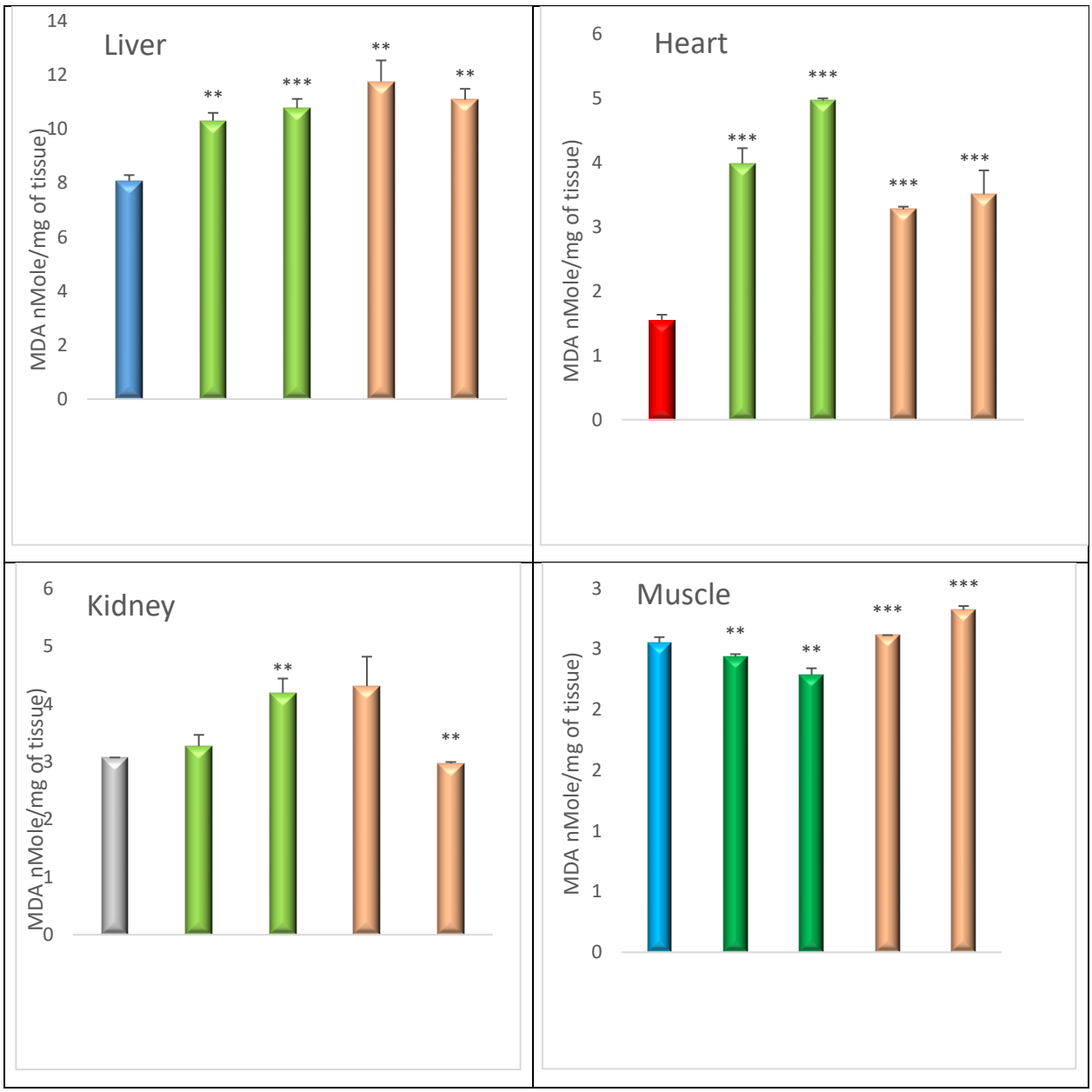

Figure 26: MDA levels in different organs.

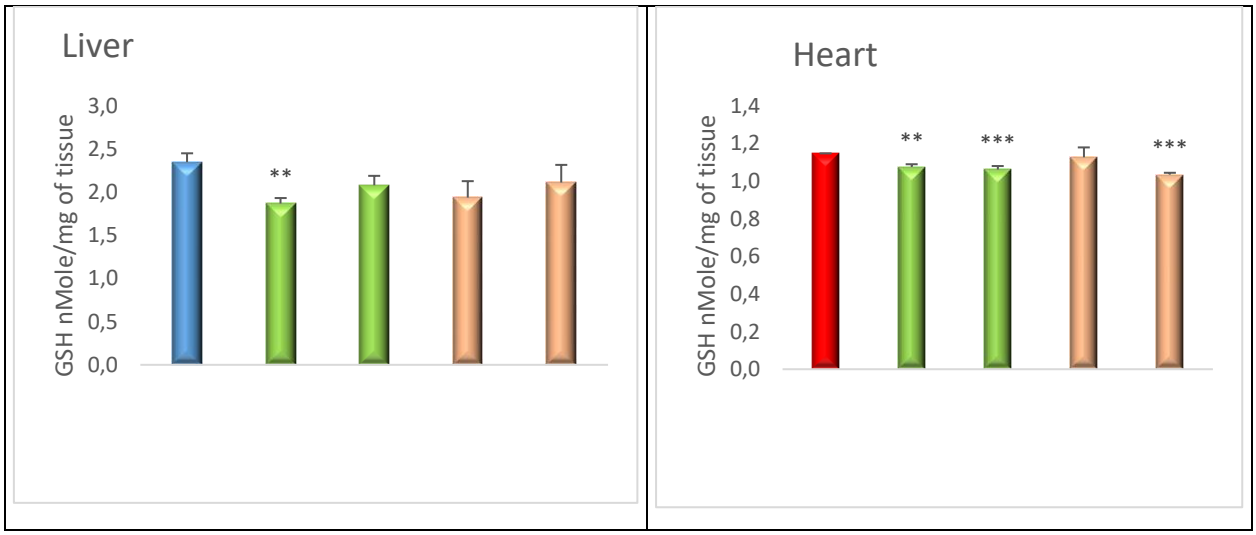

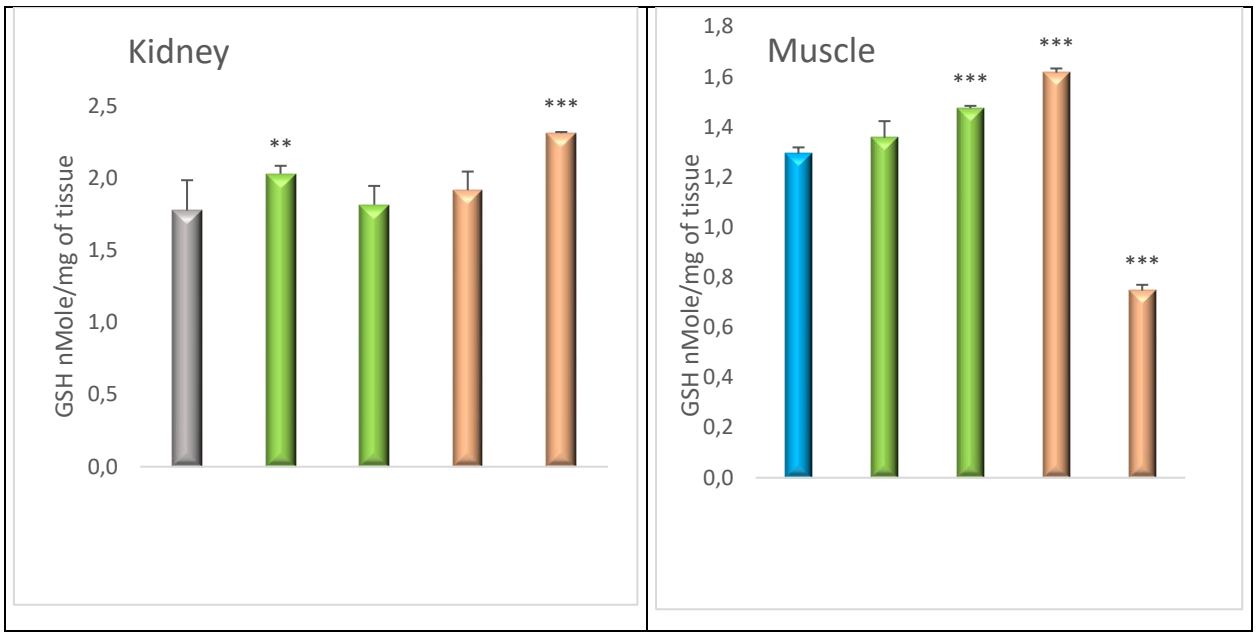

Figure 27: GSH levels in different organs.

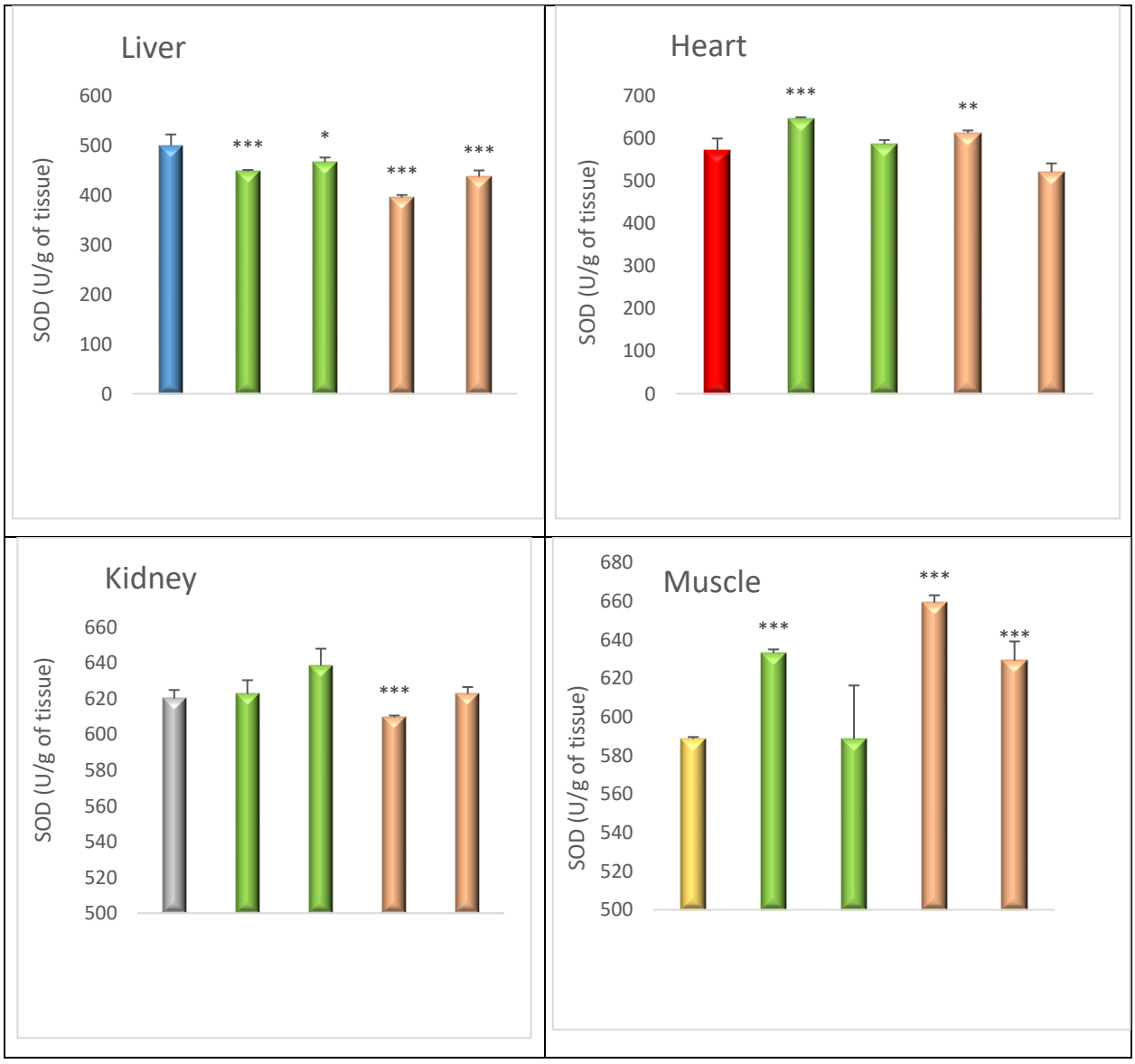

Figure 28: SOD levels in different organs.

Values are expressed as mean ± SE: Significance from control * $P<0.05$, ** $P<0.01$, *** $P<0.001$.

II.1.4. Liver Histopathological Examination

Figure 29 presents the photomicrographs of the control and treated groups in two magnifications. The control photo micrograph revealed a normal histological aspect of hepatocytes, whereas the treated groups' microscopic examination presented disproportionate signs of inflammation with eosinophilic infiltration and hemorrhagic foci.

10X10 **40X10**

Control

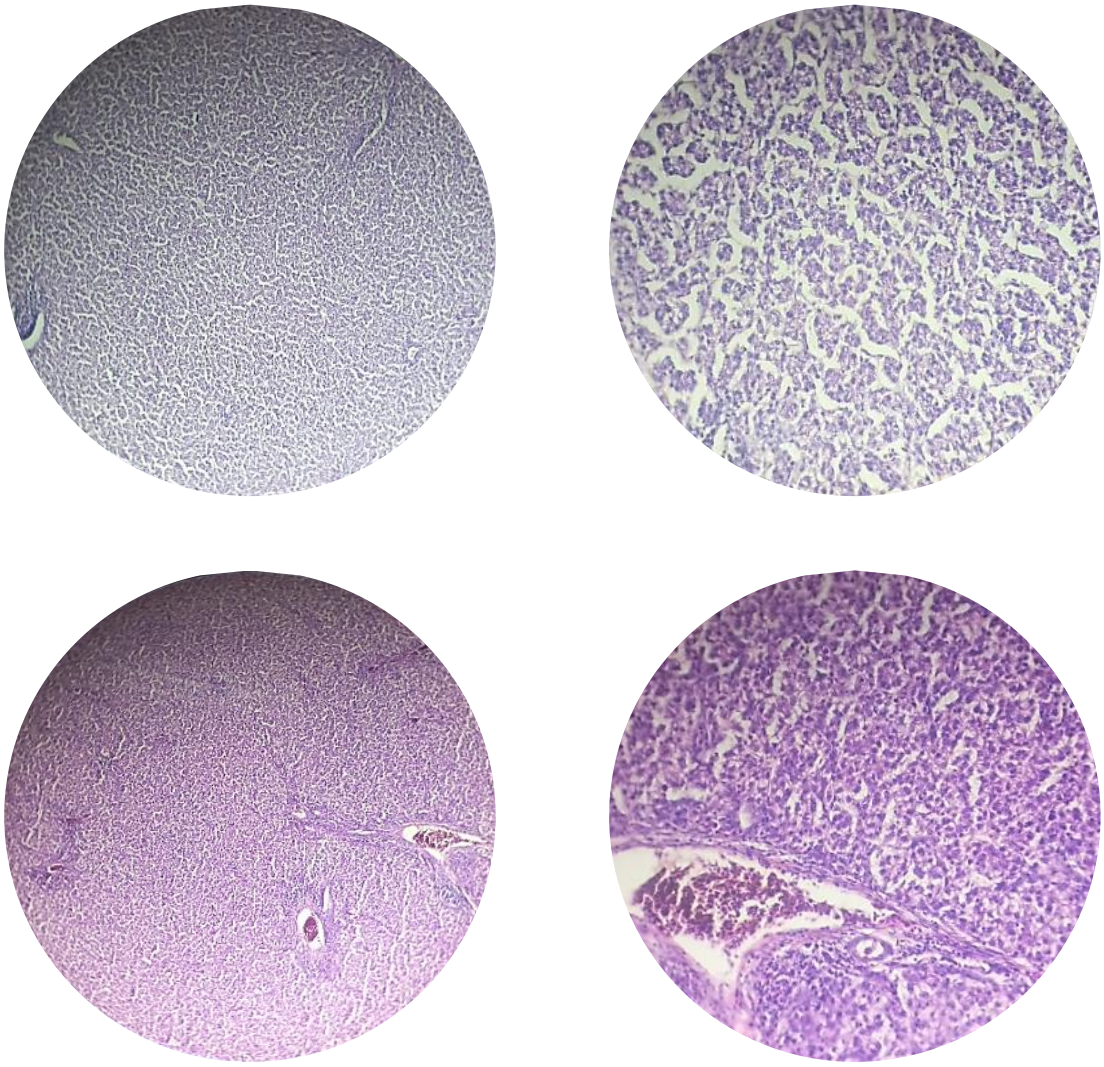

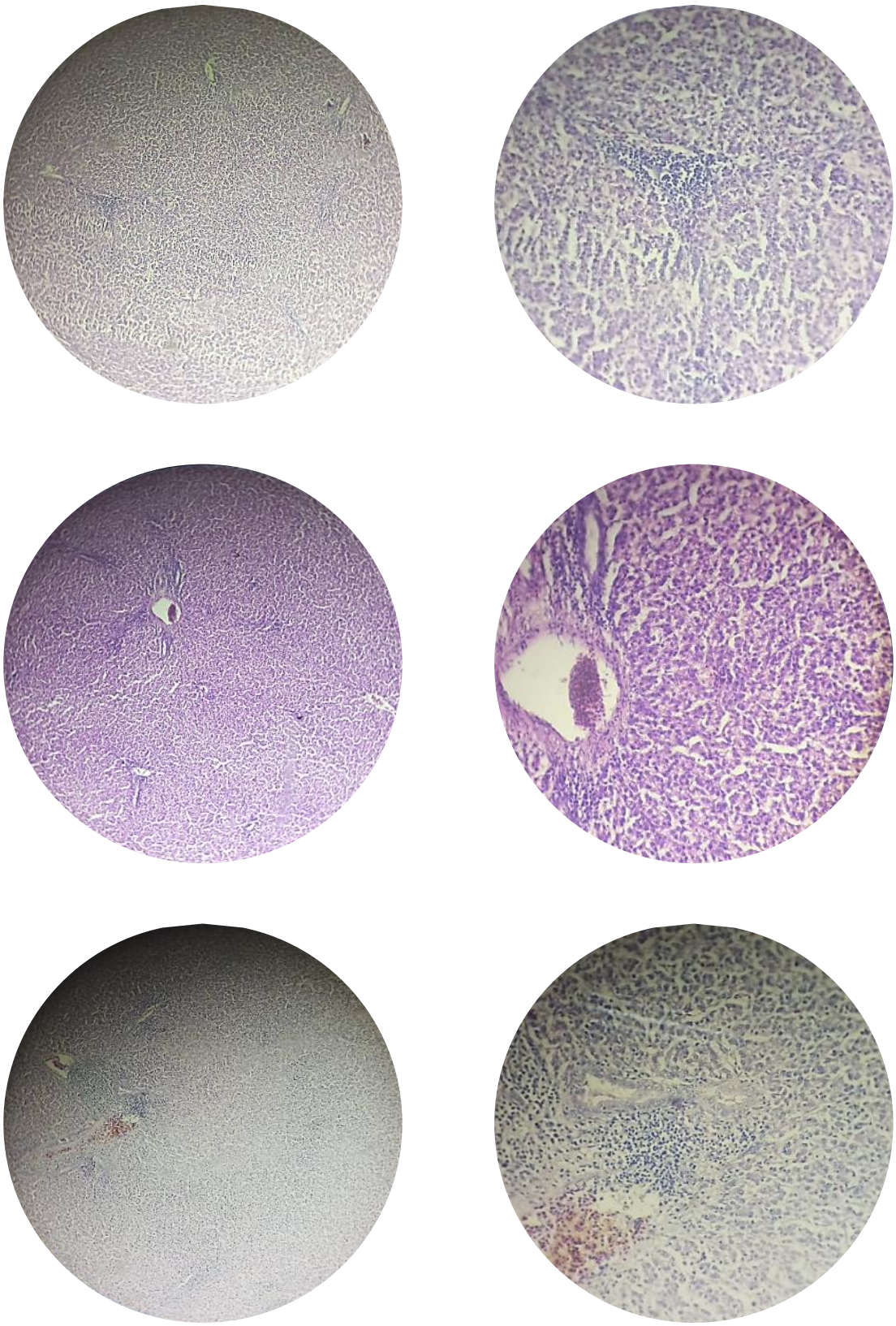

Figure 29: Histological examination of the liver of control and treated groups stained with hematoxylin (X10 and X40).

II.2. Biovaccination Effect

- **Hematological Parameters**

The results of the hematological analysis conducted on broiler chickens are illustrated in Figure 30. The ANOVA results were used to assess the differences in hematological parameters among the five experimental groups, indicating significant variances among the samples. Broilers that received treatment with RP-CuNPs displayed the most diminished concentrations of leukocytes. Furthermore, despite all groups subjected to various Cu NPs demonstrating elevated levels of erythrocytes, hemoglobin concentration, and hematocrit percentage, they concurrently exhibited the least number of platelets. Moreover, there is a variability in the MCV values across the groups, but some overlap exists. On the other hand, MCH values show overlapping groupings for most samples, suggesting limited variability in MCH values.

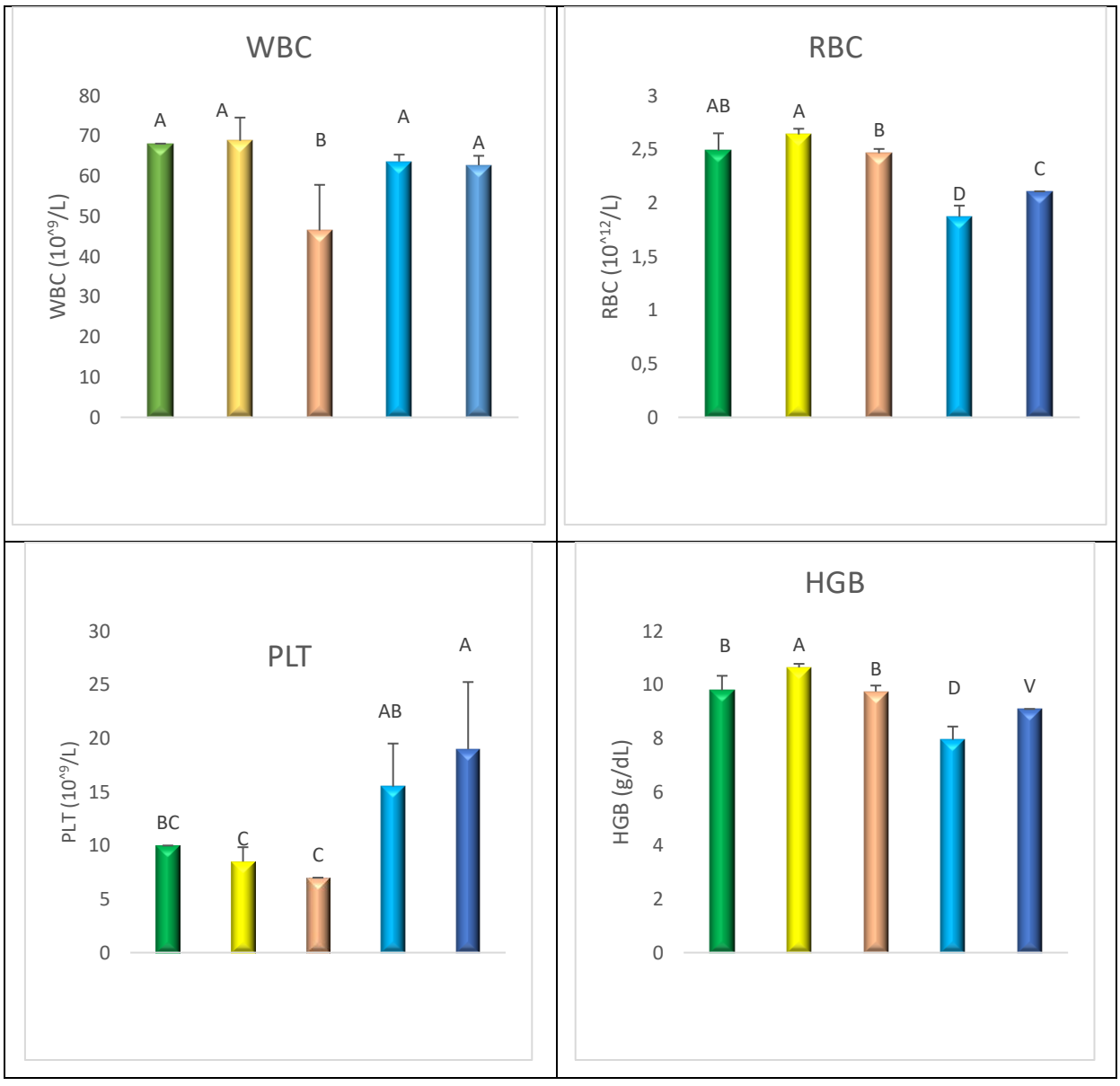

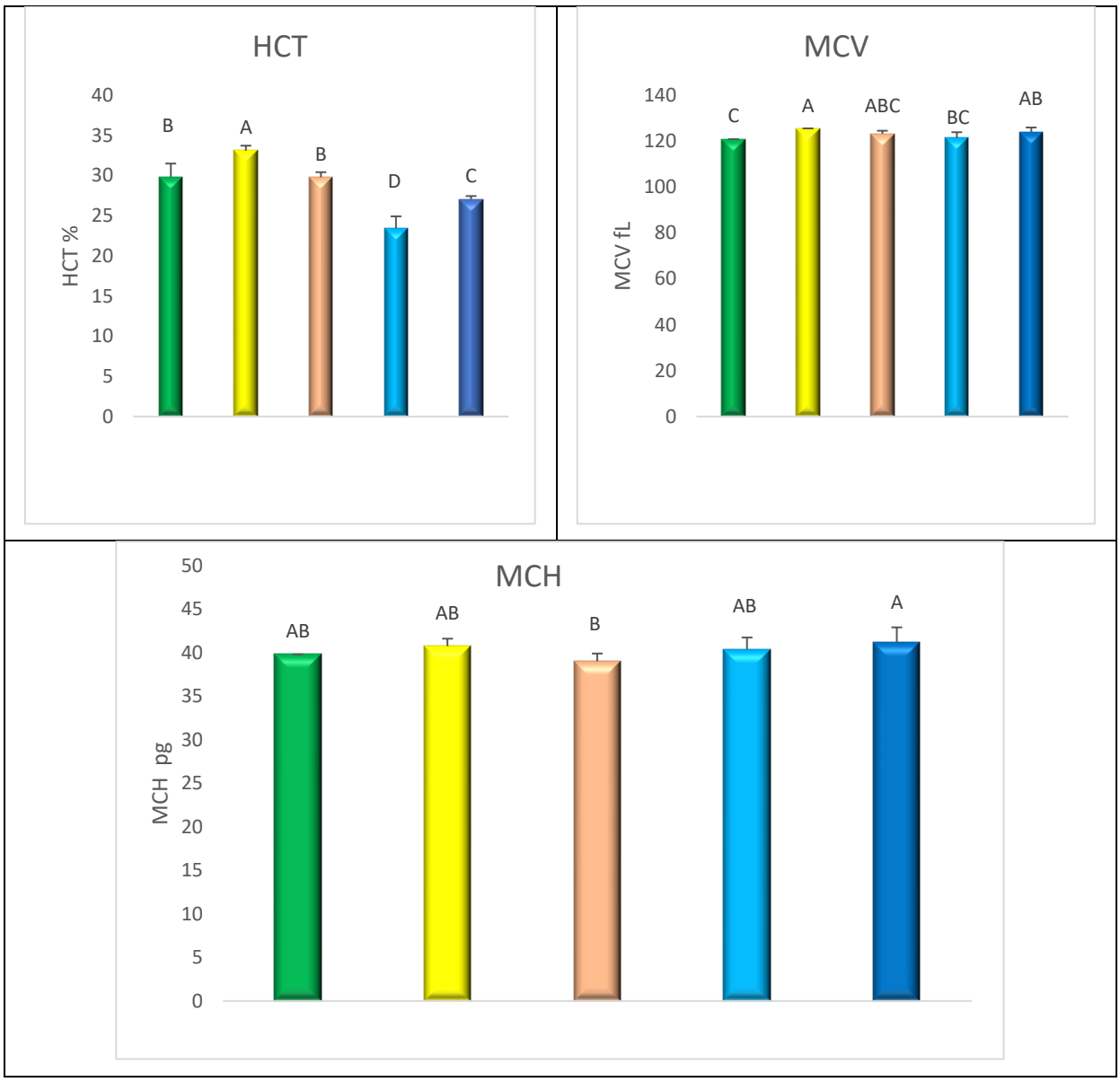

Figure 30: Hematological parameters of different groups analyzed using ANOVA.

- **Lipid Peroxidation Evaluation**

MDA levels in muscle (breast and thigh) as well as in the liver as presented in Figure 31 exhibit statistical differences. The chickens that received no treatment exhibited the lowest levels of malondialdehyde (MDA) in the breast muscle while displaying the highest levels in the thigh muscle. In comparison, the group that received vaccination demonstrated elevated values relative to the aforementioned group. Nevertheless, the treatments involving copper nanoparticles (Cu NPs) showed no statistically significant difference in the thigh muscle while manifesting variable effects in the breast muscle, with the LP-Cu NPs treatment presenting the lowest MDA level among the treatments. In the liver, the lowest MDA levels were attributed to the Cu NPs treatments.

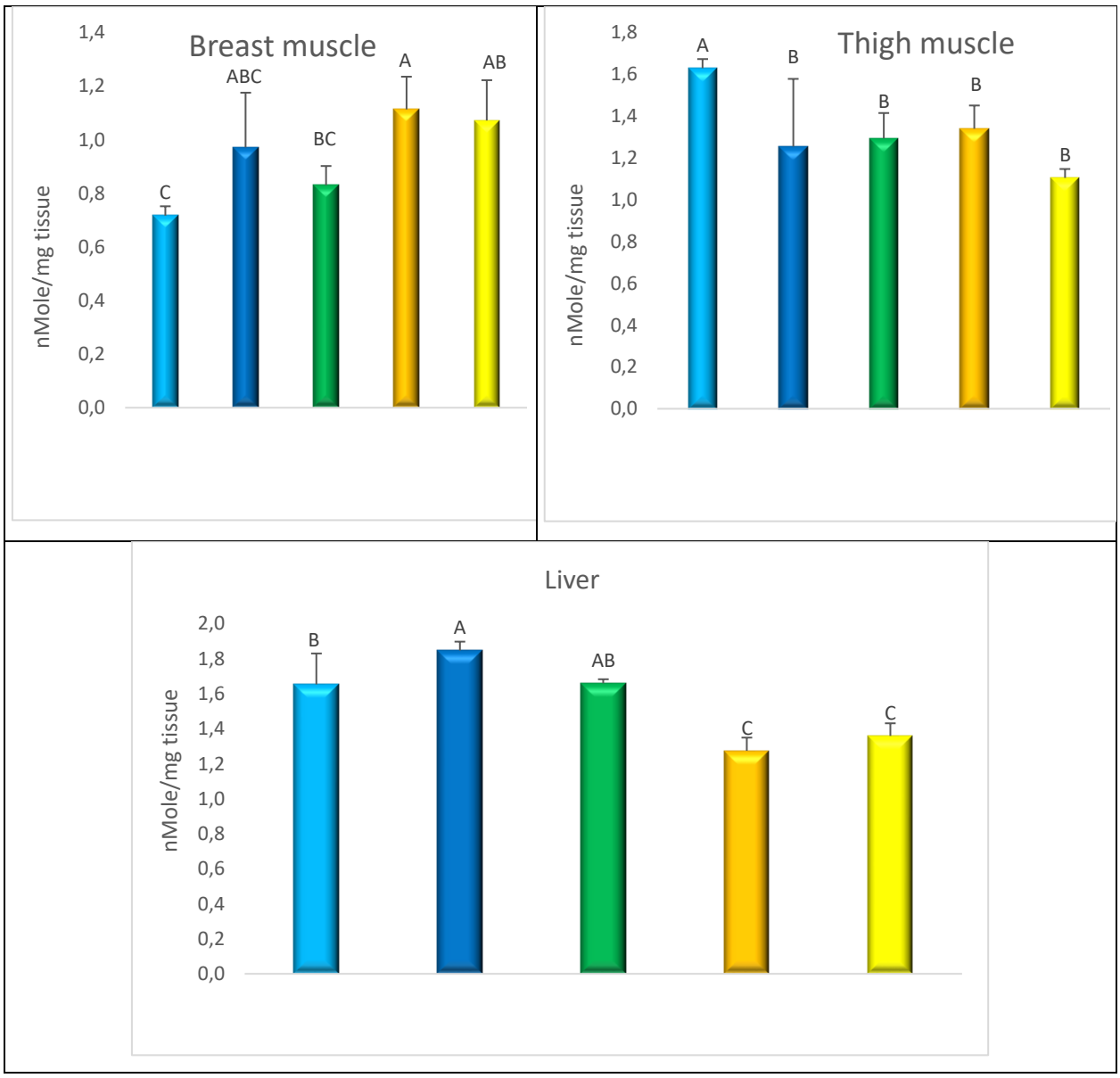

Figure 31: MDA levels in muscle and liver.

- **Muscle and Liver Glycogen**

Figure 32 represents glycogen levels in muscle (breast and thigh) and liver. ANOVA test results show statistically significant differences between the groups. The breast muscle glycogen presents no significant difference between the groups labelled as None, Conv, and LP-CuNPs on one side, and no significant difference between the groups labelled as RP-CuNPs and MP-CuNPs on the other side. On the other hand, MP-CuNPs presents the highest level of thigh muscle glycogen, while LP-CuNPs presents the lowest. The highest liver glycogen content is attributed to the group that has received no treatment and the ones receiving a mixture of both synthesized Cu NPs. The lowest is attributed to the groups receiving LP-CuNPs; however, LP-CuNPs group and RP-CuNPs group are not significantly different. Also, the Conv. group and RP-CuNPs group are not significantly different.

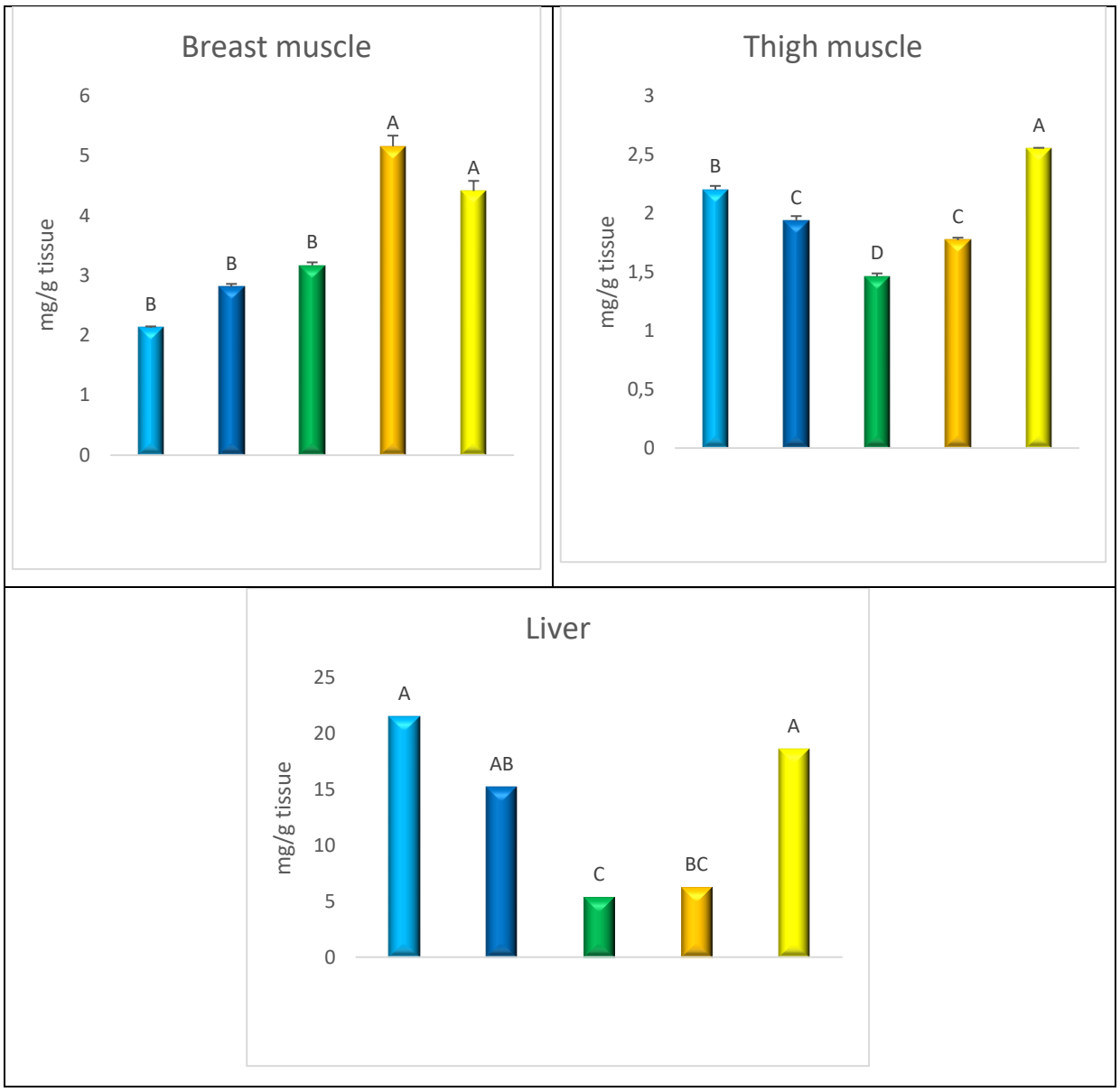

Figure 32: Glycogen values in muscle and liver.

- **Liver Histology**

As illustrated in Figure 33, the experimental groups administered phyto-nanoparticles exhibit a significantly reduced extent of hepatic tissue injury, characterized by minimal and localized inflammatory responses. The group receiving a mixture of both parts of *P. australis* demonstrates a tissue architecture that is nearly indistinguishable from normalcy. Conversely, the group subjected to conventional treatment and vaccination, referred to as Conv, reveals many distinct foci of periportal inflammation.

X 10

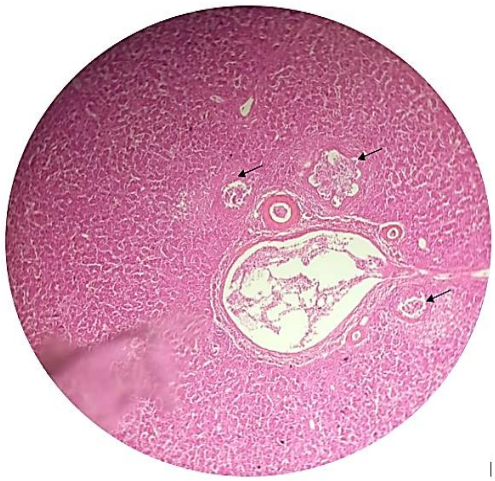

X 40

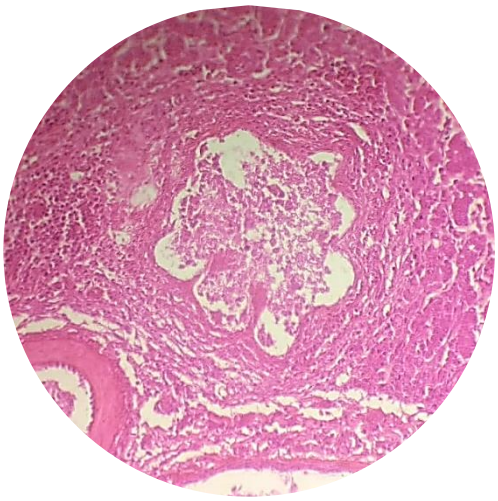

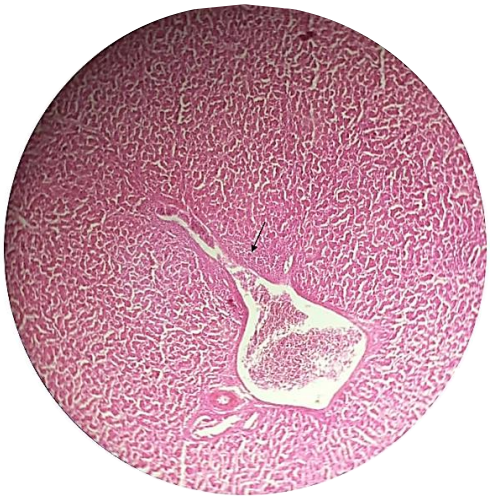

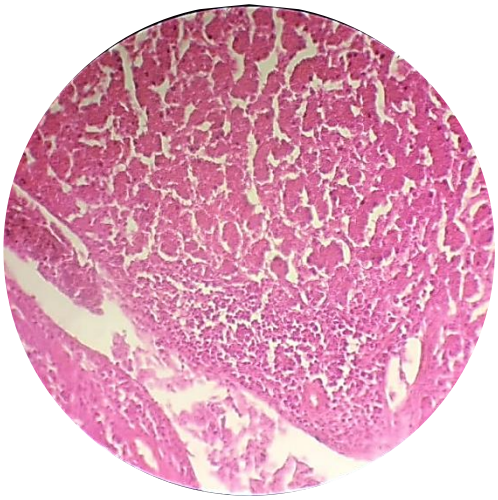

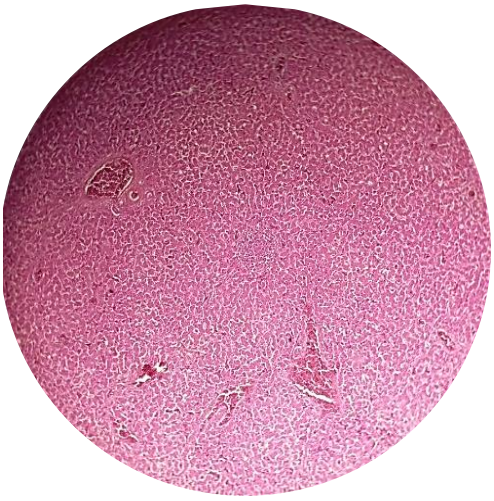

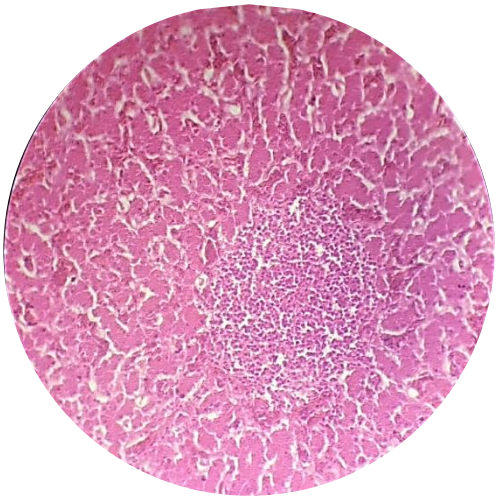

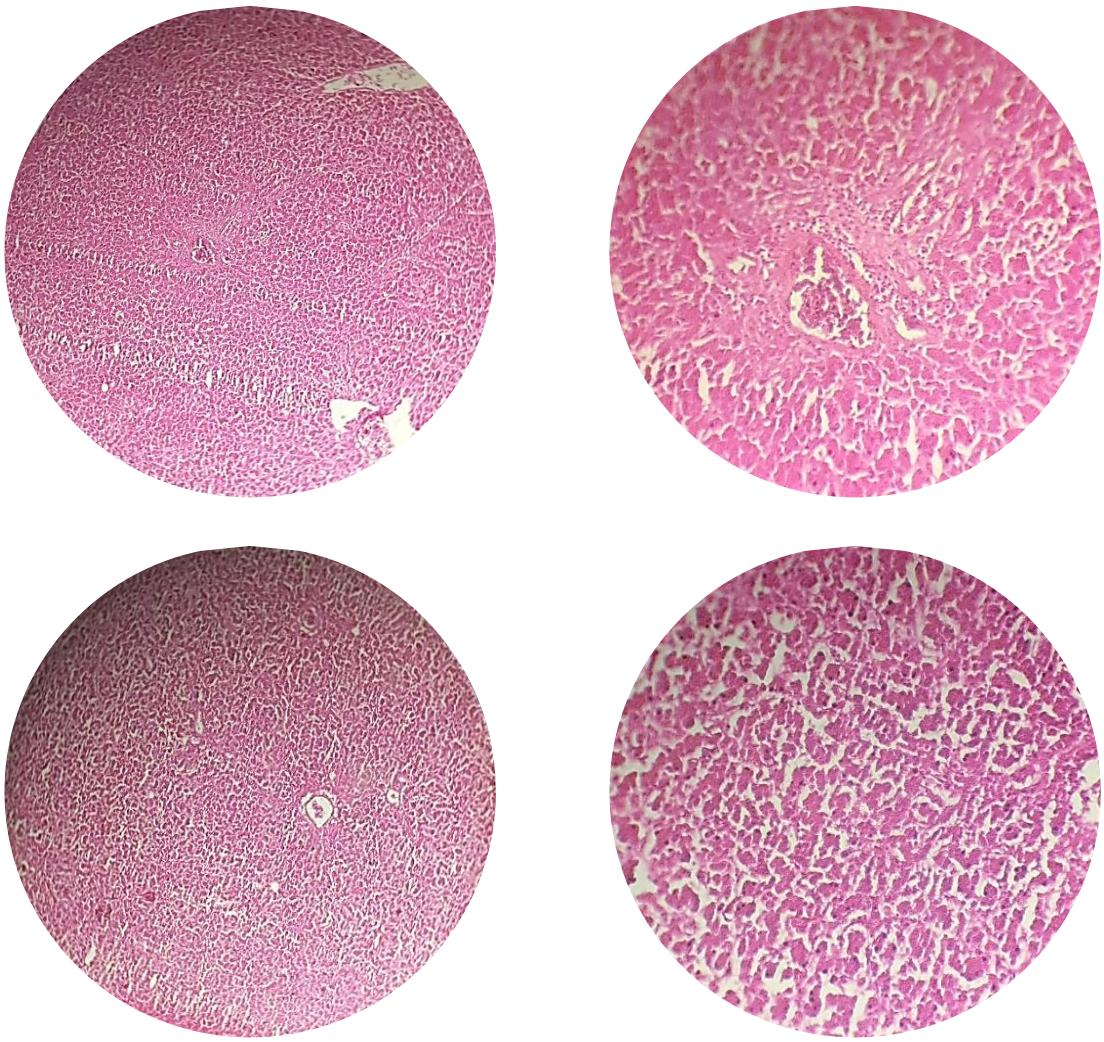

Figure 33: Photomicrographs of the liver of different groups stained with hematoxylin (X10, X40).

- **Final Weight**

Following the sacrifice of four birds from each designated experimental group, the residual chickens were maintained under controlled environmental conditions until the culmination of their rearing period at 43 days. The weights of the subjects were meticulously documented (Figure 34), revealing that the MP-CuNPs group exhibited the most significant weight gain, followed by the Conventional treated group. The LP-CuNPs and RP-CuNPs groups demonstrated nearly equivalent weight measurements, whereas the untreated cohort recorded the least weight gain. Furthermore, the mortality rates across all groups, except for the untreated group, remained within acceptable parameters. However, the chickens that received no treatment, medication, or vaccination exhibited a markedly elevated mortality rate, surpassing fifty percent of the total population (Figure 35).

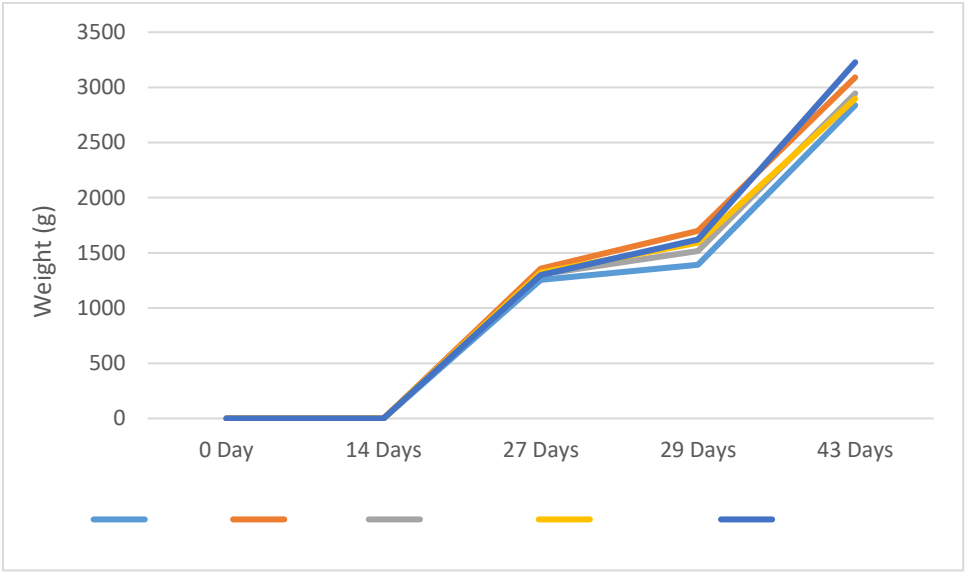

Figure 34:

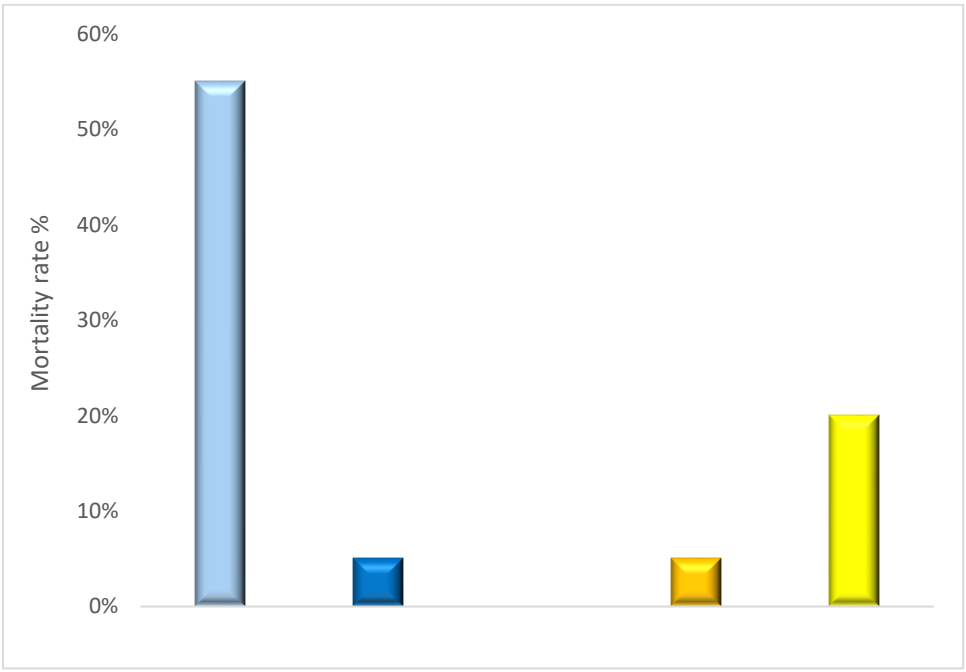

Figure 35:

Chapter III
Discussion

Part One: *In Vitro* Study

Qualitative, Quantitative, and Biological Activity Study of *Phragmites australis*

After the phytochemical screening, numerous bioactive components, including phenolics, terpenoids, tannins, alkaloids, carbohydrates, and flavonoids, were identified in *P. australis* aqueous extracts. The study of phenolic compounds and flavonoids in *Phragmites australis*, particularly in its leaves and rhizomes, reveals significant insights into their phytochemical composition and potential applications. TPC in leaf extract was found to be 70,74±1,94 mg GA eq/ g dry extract, which is much higher than what other studies have found (Unuofin et al., 2024); however, in rhizome extract, it was 30± 0.54 mg GA eq/ g dry extract, which is approximately the same value found by Derouiche *et al.* (Derouiche, Azzi, et al., 2019). On the other hand, TFC in rhizome extract was more important than in leaf extract (5.92± 1.01 mg Q eq/ g dry extract and 3,64±0,98 mg Q eq/ g dry extract, respectively). The richness of the extracts of those compounds, known also as secondary metabolites, contributes to various biological activities. The high concentration of phenolics and flavonoids is indicative of the plant's potential as a source of natural antioxidants and its role in scavenging free radicals (Unuofin et al., 2024). Hydroxyl groups (-OH) that characterize polyphenols and flavonoid structure serve as the basis for free radical scavenging and antioxidant activity (Kaouachi & Derouiche, 2018). Moreover, flavonoids are recognized to have anti-inflammatory properties via decreasing the production of transcription factors and regulatory enzymes responsible for inflammation (Yeshi, Turpin, Jamtsho, & Wangchuk, 2022). Furthermore, the extract derived from the rhizome has demonstrated hepatoprotective properties in various experimental models, indicating its prospective application in the management of liver-associated pathologies (S. Chen et al., 2013). While the presence of phenolic and flavonoid compounds in the leaves and rhizomes of *Phragmites australis* is extensively documented in the literature, it remains crucial to acknowledge the variability of these phytochemicals as a result of environmental influences and the methodologies employed in their extraction. The potency and concentration of these bioactive constituents may be affected by various determinants, including the developmental stage of the plant, climatic conditions, and the particular extraction protocols implemented (Pabón-Baquero, Otálvaro-Álvarez, Fernández, & Chaparro-González, 2018).

GC-MS analysis indicated that more than 200 components were identified in *P. australis* extracts which are dominated by 1-Dodecanol, Pyrazine, tetramethyl, Heptadecane, 2,6,10,15-tetramethyl, Cyclopentasiloxane, decamethyl, Cyclotetrasiloxane, octamethyl and Phthalic acid.1-Dodecanol also known as lauryl alcohol which is organic fatty alcohol (Veerakumar & Sreekumar, 2020). Studies have shown that 1-dodecanol has antibacterial activity against *S. aureus* with a MIC of 6.25 µg/ml (Chatterjee, Karmakar, Azmi, & Barik, 2017). It is also shown to be an

antimycobacterial agent (Mukherjee, Tribedi, Mukhopadhyay, & Sil, 2013). Pyrazine, tetramethyl also called ligustrazine, is an organic volatile compound that many studies have been conducted to investigate its medical usefulness, including the decrease of platelet aggregation, renal ischemia/reperfusion damage, and the prevention of atherosclerosis (Feng et al., 2011). Another study revealed its antioxidant activity (A. Wang, Zhang, & Li, 2012). Tetramethylpyrazine's effects on improving postoperative adhesion of tissues have been reported in pharmacological investigations and therapeutic applications (Yan, Yue, Zong, & Zeng, 2019). Heptadecane, 2,6,10,15-tetramethyl is a compound that has demonstrated antituberculous activity (Poongulali & Sundararaman, 2016) and anti-inflammatory activity (Naik et al., 2022). As for cyclopentasiloxane, decamethyl and cyclotetrasiloxane, octamethyl, they are well-known antimicrobial substances derived from many plant species (Keskın, Ceyhan, Uğur, & Dbeys, 2012; Rasyid & Putra, 2023). Finally, phthalic acid has been reported to have allelopathic, insecticidal, antibacterial and other biological actions (Huang et al., 2021).

The antioxidant activity done by DPPH assay increases when DPPH interacts with an antioxidant in the tested sample that might supply hydrogen. The color goes from deep violet to pale yellow (Sohaib et al., 2022). The potential of scavenging free radicals is expressed by IC_{50} values which is the extract concentration capable of blocking 50% of DPPH free radicals (Gheraissa, Chemsa, Elsharkawy, & Cherrada, 2022), the lower is IC_{50} value, the higher the antioxidant power and vice versa (Kaouachi & Derouiche, 2018). FRAP test is about reducing power related to a compound's capacity to transfer electrons, it can be used to anticipate its future antioxidant activity. This is due to the extract's polyphenols' predisposition to transfer electrons (Laib & Boutlelis, 2022). Our findings indicate that the extract derived from leaves exhibits a higher antioxidant capacity relative to that of the rhizome extract; nevertheless, both extracts are classified as possessing moderate activity when juxtaposed with the antioxidative potential of vitamin C. This observation stands in contrast to a prior investigation that illustrated a pronounced efficacy in scavenging free radicals, surpassing the performance of silver nanoparticles synthesized from the extract (PA-AgNPs) in analytical assays such as ABTS, DPPH, and FRAP. (Unuofin et al., 2024).

Regarding the anti-inflammatory properties, inflammation constitutes a complex pathological mechanism that represents a protective response of living tissues in conjunction with the vascular system to the detrimental effects of inflammatory agents (Zhou et al., 2020). The predominant limitation associated with the currently accessible potent synthetic anti-inflammatory pharmacological agents is their inherent toxicity and the reemergence of symptoms after cessation of use. Consequently, individuals are reverting to natural products in pursuit of enhanced safety

and security (Banerjee, Chanda, Adhikari, Das, & Biswas, 2014). Furthermore, the objective of employing plant extracts is to augment the likelihood of achieving a synergistic effect among all their constituents; otherwise, such an effect may be diminished when each component is utilized in isolation. Numerous pharmaceutical investigations, inclusive of those assessing anti-inflammatory efficacy, have substantiated this assertion (Ouidad, Sara, & Samir, 2020). Results of the anti-inflammatory tests presented in Figure 19 and Figure 20 expressed by the IC_{50} levels reveal a distinguished anti-inflammatory effect, *P. australis* aqueous extracts have protected red blood cells from hemolysis effectively ($IC_{50\ Leaf\ extract}$ = 10,73 µg/ml) as well as inhibiting BSA from denaturation ($IC_{50\ Rhizome\ extract}$ = 9,26±0,76 µg/ml). Our results are consistent with Zhu *et al.* who deduced that *P. australis* the crude extract has strongly repressed macrophages responsible for inflammation (Zhu et al., 2017).

Copper Nanoparticles Study

Characterization

The technique employed for the synthesis of nanoparticles holds significant importance, as the selected methodology serves as a pivotal factor influencing the morphological characteristics of the resultant particles, including attributes such as dimension, surface area, and geometric configuration. Variables including the selection of plant species, duration of the reaction, molar ratio of reagents, environmental temperature, and pH levels during the synthesis process must be meticulously established to achieve nanoparticles that exhibit the desired characteristics (Ghotekar, Pansambal, Bilal, Pingale, & Oza, 2021; Kocabas, Attar, Yuka, & Yapaoz, 2023).

The current investigation elucidates that the incorporation of the aqueous leaf extract and rhizome extract of *P. australis* into the copper sulfate solution precipitates a chromatic transition from blue to a dark green hue, thereby signifying the synthesis of copper nanoparticles. The findings are in alignment with prior studies concerning the green synthesis of Cu NPs (Nasrollahzadeh & Sajadi, 2015).

UV–Vis spectroscopy enabled the detection of peaks at 312 nm and 300 nm (for leaf extract-based Cu NPs and rhizome extract-based Cu NPs respectively), characteristic of Cu NPs. Other studies showed peaks at 300 nm (Ouidad et al., 2020) and 327 nm (Vasantharaj et al., 2019). According to Mie's theory, nanoparticle form determines the number of SPR bands, with spherical nanoparticles typically having a single band (Salopek, Krasic, & Filipovic, 1992). FT-IR spectroscopy performed on both plant extract and plant-based formulated Cu NPs shows different peaks with different intensities. The previously stated functional groups do exist in the structure of polyphenols. Their lower intensity in green synthesized Cu NPs is the proof of their role in reducing copper ions and stabilizing the produced Cu NPs. The sharp and intense peak detected at

608 cm^{-1} for leaf extract-based Cu NPs and at 600 cm^{-1} for rhizome extract-based Cu NPs are attributed to vibrations of CuO validating the formation of copper nanoparticles [105]. The TEM analysis revealed the presence of exceptionally fine nanoparticles exhibiting sizes ranging from 7,59 nm and 16,61 nm and from 7.22 nm to 30.05 nm (leaf-based Cu NPs and rhizome-based Cu NPs respectively). Other studies have found similar results to ours (Berra et al., 2018; Murthy, Desalegn, Kassa, Abebe, & Assefa, 2020). For XRD analysis, results demonstrate an average size of 18,06 nm and 18,25 nm (leaf extract-based Cu NPs and rhizome extract-based Cu NPs respectively). The result is in accordance with the TEM size finding. Other studies have found similar results to ours (Berra et al., 2018; Murthy et al., 2020). Regarding the stability analysis, Zeta potential measurement is of paramount importance in nanomedicine research; to ascertain the surface charge of the NPs and thus their stability in a colloidal suspension (Bhattacharjee, 2016). The stability determined by electrokinetic potential is categorized as extremely unstable when zeta values fall within the range of ±0–10 mV, relatively stable at zeta values of ±10–20 mV, moderately stable at values within the intervals of ±20–30 mV, and considered highly stable when zeta values exceed ±30 mV (Eid et al., 2023). The electrokinetic scanning was conducted over an extensive range to ascertain the charges present on the surfaces of nanoparticles (NPs). In this context, the spectrum indicated that all particles, in all samples, exhibited highly negative zeta potential values, with the lowest (most stable) being -45.38 mV for leaf-based Cu NPs and - 97.56 mV for rhizome-based Cu NPs., implying that the particles will persist in a divergent and repulsive state, thereby preventing their aggregation. Furthermore, the stability of the plant-derived NPs can be attributed to the presence of capping agents which are the phytochemical constituents within *Phragmites australis* extracts (leaves and rhizomes) such as flavonoids and alkaloids, which enhance the electrostatic interactions among the particles. A negative charge on the surface of the phytosynthesized Cu NPs is a significant indicator of the stability of colloidal Cu NPs solutions (Eid et al., 2023; Hosny, Fawzy, El-Borady, & Mahmoud, 2021; Unuofin et al., 2024). Johne *et al.*(John et al., 2021) recorded a Zeta value ranging from -23,2 mV to -33,8 mV of the biosynthesized Cu NPs via a bacterial strain. Khatoon *et al*. (Khatoon, Velidandi, & Rao, 2024) synthesized Cu NPs using sodium borohydride as a reducing agent which showed a zeta potential of −42.1 mV, whereas Eid *et al*. (Eid et al., 2023) when synthesizing Cu NPs using the aqueous extract of *Portulaca oleracea*, they recorded a zeta potential value of −24.6 mV. It is worth mentioning that the surface charge, as denoted by the zeta potential, significantly influences the manner in which nanoparticles engage with biological membranes and proteins. This interaction can subsequently affect their cellular uptake and their comprehensive biological activity, encompassing properties related to antimicrobial efficacy and drug delivery (John et al., 2021).

Biological Activity

Regarding the antioxidant activity, both tests revealed an important scavenging power of the green Cu NPs. IC_{50} values of Cu NPs and vitamin C as found by DPPH test are 4.62 µg/ml and 0.31 µg/ml respectively. While IC_{50} values of Cu NPs and vitamin C found by FRAP test are 78.99 µg/ml and 35.24 µg/ml respectively. It is known that the lower the IC_{50} level is, the highest the antioxidant activity. Our findings align with the majority of existing literature (Djamila, Eddine, Abderrhmane, Nassiba, & Barhoum, 2022; Ouidad et al., 2020).

The outcomes of the anti-inflammatory assessments revealed the intriguing efficacy of green Cu NPs in safeguarding both erythrocytes and proteins against haemolysis and denaturation, exhibiting levels surpassing those of the standard reference. The protective mechanism conferred upon erythrocytes against haemolysis may be attributed to the capacity of anti-inflammatory agents to enhance the stability of the red blood cell membrane, thereby preventing the release of their intracellular constituents at sites of inflammation. Al-Jubouri *et al*. reported analogous findings; however, the percentage of inhibition attributed to Aspirin, utilized by them as a positive control, demonstrated a greater efficacy relative to the Cu NPs synthesized from *Myrtus communis* leaf extract (Al-Jubouri, Al-Saadi, & Kadhim, 2022).

The antibacterial efficacy was assessed through the quantification of the inhibition zone measured in millimeters around the disc, with the results meticulously measured. *P. australis*-based Cu NPs exhibited notable antibacterial activity against different bacterial strains, mainly *E. coli* and *B. subtilis*, while they have little to no effect on *K. pneumoniae* and *S. aureus*. A research investigation employing water caltrop pod for the biosynthesis of copper nanoparticles has yielded analogous findings; however, it has demonstrated enhanced levels of bacterial inhibition, particularly against *Staphylococcus aureus* (Khatri et al., 2024). In the present study, it was determined that RP-Cu NPs exhibited no significant influence on *Bacillus subtilis*, which is advantageous for chickens since *Bacillus subtilis* promotes the health of the intestinal microbiota in these avian species and it is used as a probiotic supplementation (S. Khan et al., 2023). The observed variations in the antibacterial efficacy of nanoparticles, even when employing distinct parts of the same plant as reducing and capping agents, can be elucidated by the notion that the activity of nanoparticles is modulated by a multitude of factors, including their synthesis methodology, size, morphology, and even their surface charge. Research has demonstrated that diminutive nanoparticles exhibit an augmented surface area-to-volume ratio, which facilitates their interaction with bacterial cells and amplifies their antibacterial potency (El-Habib et al., 2024; Ershov & Ershov, 2024). Furthermore, the surface charge of nanoparticles significantly affects their engagement with bacterial cell membranes. Nanoparticles with a positive charge display

greater efficacy against bacterial cells due to electrostatic attractions towards the negatively charged membranes of bacteria, resulting in membrane disruption (Girma et al., 2024; Jiang et al., 2024). In addition, modifications such as capping agents or surface coatings can enhance both the stability and antibacterial characteristics of nanoparticles (Hassan & Abd, 2023; Shoudho, Uddin, Rumon, & Shakil, 2024). Moreover, the employment of biological methodologies for the synthesis of nanoparticles, often referred to as 'green' technology, has the potential to yield nanoparticles with distinctive properties that augment their antibacterial activity while possibly diminishing toxicity (Mani et al., 2023). Nanoparticles exhibit antibacterial activity through several mechanisms. One key method is the production of reactive oxygen species (ROS), which damage bacterial DNA, proteins, and lipids, ultimately leading to cell death (Hassan & Abd, 2023). Another mechanism involves membrane disruption, where nanoparticles directly interact with bacterial membranes, causing leakage of cellular contents; this is particularly effective against Gram-negative bacteria due to their complex cell wall structure (Dzuvor, Shen, Haritos, & He, 2024). Additionally, some nanoparticles, such as silver nanoparticles, release metal ions that interfere with bacterial cellular processes, resulting in cell death (Ershov & Ershov, 2024). The susceptibility of bacteria to these mechanisms is influenced by bacterial factors, such as the Gram type. Gram-negative bacteria, with their additional outer membrane, often require nanoparticles with enhanced penetration capabilities to overcome their structural defenses (Girma et al., 2024).

Concerning the anti-cancer activity of the plant-based formulated Cu NPs, the MTT assay relies on the activity of succinate dehydrogenase, a mitochondrial enzyme, to transform the yellow tetrazolium dye into purple formazan crystals. The rate of formazan crystal formation is directly proportional to cell viability, which is quantified by measuring optical density (Spinner, 2001). Figure 19 and Figure 20 show that the cytotoxicity effect on MCF-7 cell line is dose-dependent. The IC_{50} level, which is the concentration value to decrease the viability of 50% of cancer cells, is found to be about 3,53 µg/ml for leaf extract-based Cu NPs, and 2,28 µg/ml for rhizome extract-based Cu NPs. Many other studies have reported plant-based synthesized Cu NPs' anticancer potential against different cancer cell lines. In the study conducted by Shobha et *al*. the IC_{50} was 133,2 µg/ml (Shobha, Sagar, Shashidhara, Mahadimane, & Ananda, 2019), Ramaswamy et *al*. found that brown algae-mediated Cu NPs had a significant anticancer effect on the MCF-7 cell line where cells were inhibited by 93% at a dosage of 100 µg/ml (Ramaswamy, Narendhran, & Sivaraj, 2016). Studies indicate that nanoparticles should be smaller than 100 nm to pass through endothelial cells. Spherical nanoparticles ranging from 20 to 200 nm are more effective for drug delivery and *in vivo* applications (Santhosh et al., 2023). Cu NPs' antitumor effect against cancer cell lines is likely due to oxidative stress, lipid peroxidation, cellular breakage, membrane function loss, involvement in some interactions with intracellular macromolecules, DNA fragmentation, and chromosomal aberrations (Akintelu, Folorunso, Folorunso, & Oyebamiji, 2020).

Part Two: *In Vivo* Study

Acute Toxicity Test of *P.australis*-based CuNPs

Behaviour and Body Weight

The evaluation of specific behaviors and factors in toxicological control, such as eye health, mobility, sleep patterns, diarrhea, and mortality (DEROUICHE, 2020), revealed that the administration of both doses of Cu NPs (leaf-based and rhizome-based) caused no mortality or evidence of toxicity during the first 24 hours. Additionally, the post-mortem weight of organs like liver and heart showed no significant changes compared to the control group. The toxicity of nanoparticles synthesized using green methods is generally lower compared to those produced through chemical or physical methods alongside their enhanced biodegradability (Somya, Varshney, & Khan, 2025). Moreover, those green nanoparticles are more stable and biocompatible, making them ideal for applications in therapeutic and medical fields (Parmar, 2024).

Study of Hematological Analysis

Blood is recognized for demonstrating pathological alterations prior to the emergence of any overt clinical manifestations of toxicity. Hematological and plasma biochemical metrics serve as critical components in toxicological investigations, as indicators of disease, and ecological stressors (Z.-H. Li et al., 2011). In other words, the hematological and biochemical characteristics of blood can yield significant insights regarding the organism's internal milieu (Z.-H. Li et al., 2011). Hematotoxicity is a critical factor in drug development, and hematological analysis plays a key role in detecting adverse effects at an early stage of the process (Long et al., 2022).

Our acute toxicity test results revealed disturbance in hematological parameters of treated groups. The most conspicuous modification is the elevation in the leukocyte count (leukocytosis) alongside a pronounced reduction in the platelet count (thrombocytopenia). Both of these alterations provide insights into the condition of the immune system.

The synthesis of reactive metabolites within hepatic tissues can lead to hepatocellular injury, which may subsequently trigger immune responses such as leukocytosis. This phenomenon is particularly relevant in the context of immunoallergic hepatitis, wherein the pharmaceutical agent or its metabolites act as haptens, modifying proteins and eliciting an immune response (Dansette et al., 1998; Pessayre & Larrey, 1988). Similar findings regarding leukocytosis were found in other studies (K Ognik et al., 2016).

The liver plays a pivotal role in regulating the synthesis of platelets by producing thrombopoietin (TPO). By utilizing the Ashwell-Morell receptor (AMR), the liver interacts with desialylated platelets, thereby activating the JAK2-STAT3 signaling cascade to enhance TPO secretion. This regulatory feedback mechanism is essential for maintaining platelet homeostasis,

and any impairment of liver function can interfere with this system, leading to atypical platelet levels (Grozovsky et al., 2015). Drug-induced hepatitis has the potential to influence both the count and functionality of platelets through immune-mediated mechanisms and alterations in platelet production and longevity, necessitating intricate interactions among the liver, the immune system, and platelets. The phenomenon of drug-induced thrombocytopenia may arise via immune-mediated pathways in which drug-dependent antibodies specifically target platelets for elimination. This mechanism entails the formation of complexes comprising drugs, platelets, and antibodies, which are subsequently eliminated by the immune system, resulting in diminished platelet counts (Christie & Aster, 1982; Kenney & Stack, 2009). In a comparable manner, in the context of immunoallergic hepatitis, drug metabolites have the potential to generate neoantigens that elicit an immune response, resulting in hepatic injury and the synthesis of antibodies that similarly target platelets, thereby exacerbating thrombocytopenia (Dansette et al., 1998). Mean corpuscular hemoglobin (MCH) and hemoglobin (HGB) levels have significantly decreased. A research investigation utilizing silver nanoparticles administered at a dosage of 5 mg/kg body weight (BW) via oral route, revealed alterations in hematological parameters, including a reduction in hemoglobin content, which may be attributable to the elicitation of oxidative stress and inflammatory responses in broiler chickens (K Ognik et al., 2016). Conversely, an alternative investigation employing Zinc oxide nanoparticles (ZONPs) has been documented to elevate hemoglobin concentration and enhance red blood cell counts in broilers, indicating a plausible beneficial impact on hematological parameters (Hatab et al., 2024). Additionally, red blood cells (RBC) and mean corpuscular volume levels (MCV) have significantly increased, which may be the reason why the hematocrit (HCT) percentage has also increased. In an investigation concerning silver-curcumin nanoparticles, noteworthy elevations in packed cell volume and red blood cell count were documented in broilers administered elevated concentrations of these nanoparticles (2mg/L of drinking water). Nevertheless, there was an absence of significant variation in mean corpuscular volume (MCV) among the various treatment groups (Al-Zuhairi, Al-Salhie, & AlAbdullah, 2023). Another study reported an increase in hemoglobin concentration and red blood cell counts in broilers after zinc nanoparticle administration, suggesting a potential positive effect on blood parameters (Hatab et al., 2024). Nevertheless, within the framework of our acute toxicity assessment, this augmentation may also signify a compensatory mechanism aimed at enhancing the oxygen transport capacity, given that the administered dosages are exceedingly elevated.

Study of Biochemical Analysis

Our acute toxicity test seems to have no significant effect on broilers' glucose metabolism and glycogen storage, which are interconnected and crucial processes in maintaining energy homeostasis in the body, since glycemia values, livre glycogen, and muscle glycogen levels were kept stable compared to the control group, suggesting that the tested doses did not affect the insulin signaling pathways which facilitates the uptake of glucose by the cells and its conversion into glycogen for storage. Another investigation revealed that broilers' supplementation with Cr-CNPs resulted in a reduction of serum glucose concentrations and liver glycogen reserves, while not influencing the levels of muscle glycogen (Tahir et al., 2019). Separate studies indicated that broilers that were nourished with Ag NPs and Cu NPs demonstrated diminished plasma glucose concentrations (Abdullah et al., 2022; Saleh & El-Magd, 2018).

Elevated concentrations of alanine transaminase (ALT) and aspartate transaminase (AST) in broiler chickens may be ascribed to a multitude of determinants, encompassing oxidative stress, environmental parameters, and nutritional factors. These enzymes function as indicators of hepatic health, and their increased levels frequently signify hepatic injury or impairment (Thakur, Kumar, Das, Sharma, & Mehta, 2024). Oxidative stress constitutes a critical factor in the pathophysiology of hepatocellular injury in broiler chickens, culminating in increased serum levels of ALT and AST. This phenomenon may arise from accelerated growth patterns and susceptibility to infectious pathogens, which adversely affect hepatic functionality and overall physiological well-being (Srinivasan et al., 2017). Moreover, elevated ambient temperatures and unrestricted feeding practices have been associated with heightened levels of AST and ALT, signifying hepatic necrosis and metabolic imbalance. Empirical research indicates that broiler chickens exposed to thermal stress demonstrate marked elevations in these hepatic enzymes, thereby implying a direct relationship between environmental stressors and hepatic well-being (Senanayake, Ranasinghe, Waduge, Nizanantha, & Alexander, 2015). Additionally, The incorporation of specific nutritional supplements, such as lead acetate, has been demonstrated to markedly augment levels of ALT and AST, thereby suggesting the presence of hepatotoxic effects (Khanam et al., 2016). Research findings demonstrate that broiler chickens administered ZONPs at dosages of 40 and 60 mg/kg displayed markedly elevated levels of AST and ALT in comparison to the control group. The augmentation of hepatic enzymes was notably more significant at increased dosages, indicating a potential relationship between nanoparticle concentration and the activity of liver enzymes (Hatab et al., 2024). These results are consistent with our own. While elevated levels of AST and ALT are frequently suggestive of hepatic injury, it is crucial to acknowledge that not every increase is harmful, some studies have demonstrated an absence of substantial hepatic damage, implying that

the rise in enzyme levels may not correlate directly with adverse health implications (Yusof, Mohamad, Zaidan, Arshad, & Samsudin, 2023).

In the context of our experimental study, serum alkaline phosphatase (ALP) concentrations exhibited a notable elevation associated with the administration of RP-Cu nanoparticles at a dosage of 50 mg/kg body weight. However, it is pertinent to acknowledge that hepatic pathology is frequently recognized as a contributing factor to elevated ALP levels in various species: any pharmacological agent that exerts hepatotoxic effects or precipitates cholestasis has the potential to markedly elevate serum alkaline phosphatase (ALP) concentrations (Safdar et al., 2024). In avian broilers, however, the liver is less commonly identified as the predominant source of increased ALP concentrations (Kuan, Martin, & Patrick, 1966). Studies on broilers have shown that dietary supplementation with zinc oxide nanoparticles (ZONPs) increases alkaline phosphatase (ALP) activity, which is linked to enhanced bone metabolism and liver function due to the high bioavailability of ZONPs. This effect is dose-dependent, with the greatest ALP activity observed at higher concentrations, as confirmed by significant ALP increases at 10, 20, 40, and 60 mg/kg ZONP supplementation levels (Fathi, Haydari, & Tanha, 2016; Hatab et al., 2024).

Regarding the nephrotoxicity signs, unlike humans and other mammals, which exhibit ureotelism (Adomako & Moe, 2023), broilers demonstrate uricotelism, signifying that the principal end product of nitrogen metabolism in these avian species is uric acid (UA) rather than urea (Kumar, Gupta, Kumar, & Rana, 2024). The limited production of urea in broilers can be attributed to the diminished activity of arginase in the liver, an enzyme that plays a crucial role in urea synthesis (Stevens, 1997) The concentration of uric acid in avian plasma is influenced by factors such as age, sex, reproductive status, and nutritional state. Birds lack uricase, an enzyme essential for uric acid breakdown, making plasma uric acid (PUA) and excreted uric acid reliable indicators of its production (Hevia & Clifford, 1977). Efficient elimination of uric acid from the bloodstream is crucial to prevent its accumulation, which could lead to gout due to its insolubility and tendency to form crystals in joints, tissues, and kidneys (Donsbough, 2008).

The acute toxicity test results regarding uric acid and urea show a slight increase in serum urea and a decreased level of uric acid. A study revealed that starvation decreases the entry rates of uric acid and urea into the system. However, it enhances their degradation, suggesting that the body increases the breakdown of these compounds during periods of food scarcity, which may explain our results since the chickens were fasted hours before their sacrifice. The same study found that the duration of urea turnover and the degree of degradation within the urea pool were elevated. In contrast, the urea excretion rate was diminished compared to that of uric acid (Emmanuel & Howard, 1978). On the other hand, it is known that elevated serum uric acid level

indicates renal injury (Bideshki, Karimi-Dehkordi, & Gholami-Ahangaran, 2023), which may allow us to say that our green Cu NPs have no adverse effect on the kidney.

Study of Oxidative Stress Markers

The administration of *P. australis*-based copper nanoparticles at 25 and 50 mg/Kg BW (leaves and rhizomes) in broiler chickens has increased the levels of malondialdehyde (MDA), a byproduct of membrane lipid peroxidation (Derouiche, Serouti, & Rezzagmohcen, 2019), in various tissues including liver, heart, kidney, and muscle, thereby indicating the presence of oxidative stress. This finding aligns with the research conducted by BaoHua et *al.* (Yang BaoHua, Lei RongHui, & Wu ChunQi, 2009) and Lei et *al*. (Lei et al., 2008), in which it was demonstrated that the levels of MDA exhibited an increase in a dose-dependent manner, with elevated concentrations of copper nanoparticles (CuNPs) inducing more significant oxidative injury and lipid peroxidation within hepatic tissues in rat models. A separate investigation undertaken on broilers corroborated the aforementioned results; nevertheless, this study employed chemically synthesized CuO nanoparticles (Morsy, Hussien, Ibrahim, Farroh, & Hassanen, 2021).

SOD constitutes the principal enzymatic antioxidant within the cellular mechanisms that mitigate free radical activity (Hatab et al., 2024). It plays a crucial role in maintaining the redox equilibrium of avian immune systems through the detoxification of reactive oxygen species (Noor, Mittal, & Iqbal, 2002).

The increase in SOD activity across tissues (heart and kidney) indicates an adaptative response induced by the high doses of Cu NPs. RP-CuNPs appear to have a more consistent and stronger impact than LP-CuNPs, especially at the higher dose, suggesting greater bioactivity. Conversely, the decrease in SOD activity within hepatic and renal tissues may serve as a biomarker for oxidative stress, which represents an imbalance between the generation of reactive oxygen species and the organism's capacity to neutralize these deleterious intermediates (BOULAARES, DEROUICHE, & GUEMARI, 2024a), given that these two organs are recognized as pivotal sites for the detoxification processes of the entire organism (Apte & Krishnamurthy, 2011). This is supported by findings where increased free radical activity correlates with decreased SOD levels in broilers infected with pathogens or exposed to toxic substances (DZ Guo, Yang, Wu, & Li, 2000).

Glutathione (GSH) is a key intracellular antioxidant that protects cells from oxidative damage by neutralizing reactive oxygen species (Forman, Zhang, & Rinna, 2009). It also preserves cellular homeostasis, facilitates the elimination of toxins and ROS generated during the metabolism of xenobiotics, and modulates the activity of proteins and other biomolecules. Moreover, glutathione serves as a critical element in numerous biochemical processes

(Mangkalopakorn, Segsarnviriya, Keeratipranon, & Maiprasert, 2025; Pompella, Visvikis, Paolicchi, De Tata, & Casini, 2003). A reduction in GSH levels indicates increased oxidative stress, which can lead to cellular toxicity, organ dysfunction, and apoptosis (Zou et al., 2012). In this study, only the LP-CuNPs 25 group showed a significant (**p < 0.01) reduction in the liver GSH levels, while the higher dose and RP-CuNPs groups did not show significant changes. This suggests that the hepatic antioxidant system is capable of counteracting CuNP-induced oxidative stress at these exposure levels. It is known that the liver, recognized as the principal organ for detoxification, typically exhibits remarkable resilience against oxidative injury owing to its comprehensive antioxidant defense mechanisms (Jaeschke, McGill, & Ramachandran, 2012). Moreover, the significant depletion of heart's GSH in LP-CuNPs 25, LP-CuNPs 50, and RP-CuNPs 50 groups (**p < 0.01, (***p < 0.001, (**p < 0.01 respectively) suggests increased ROS production, which can impair cardiac function. The heart exhibits a pronounced vulnerability to oxidative stress, attributable to its elevated metabolic activity and comparatively diminished antioxidant defenses (Boulaares, Derouiche, & Guemari, 2024b). However, in the kidney and muscle, GSH levels increased significantly following CuNP administration. This suggests a possible compensatory antioxidant response rather than direct depletion. Notwithstanding, the RP-CuNPs50 induced a decrease in GSH level in muscle and hence provoking oxidative stress. This may suggest that muscles could be more sensitive to higher doses of RP-CuNPs, which may be due to differences in nanoparticle synthesis and the capping agents involved, affecting their size, shape, and surface reactivity, which influence their bioavailability and toxicity (Lira et al., 2024; Miao et al., 2024).

Our investigation into the oxidative stress biomarkers concerning the acute toxicity assessment indicates that elevated concentrations of *P. australis*-based copper nanoparticles can elicit oxidative stress across various tissues, accompanied by the activation of a compensatory mechanism. Similar findings have been reported in other studies where high doses of Cu NPs led to increases in MDA levels, DNA fragmentation, and histopathological alterations in broilers indicating cytotoxic and genotoxic effects (Morsy et al., 2021) with the alteration of the antioxidant status (Katarzyna Ognik et al., 2018)

Histopathological Study

The liver histopathological study, after administrating a high concentration of the plant-based Cu NP for the aim of evaluating its acute toxicity, revealed the presence of a slight to moderate level of inflammatory response and eosinophilic prominence which are the most common patterns of drug-induced hepatitis (Dansette et al., 1998). A separate study unveiled dose-dependent pathological modifications in both breast and thigh musculature, as well as in all the

examined organs (namely, the heart, liver, kidneys, and spleen) within the groups that have been administered CuO-NPs (Morsy et al., 2021). The most significant lesions identified in the aforementioned study included cellular cytoplasmic vacuolization, cellular swelling, necrosis, hemorrhage, and inflammatory response. These hepatic lesions could be related to oxidative stress triggered by nanoparticles (NPs). A key factor in the mechanism of NP toxicity is their propensity to generate free radicals (H. Yang, Liu, Yang, Zhang, & Xi, 2009). The excessive production of reactive oxygen species (ROS) and the resulting oxidative stress play a significant role in the development of numerous diseases, as they can harm essential cellular components such as DNA, proteins, and lipids. ROS are produced as by-products of normal cellular metabolism and can also arise from drug-induced oxidative stress. While ROS serve critical physiological functions in many cells, excessive ROS generation can surpass the cell's internal defense mechanisms, leading to cellular damage (Akbarian et al., 2016; H. Yang et al., 2009). These findings elucidate the ramifications associated with elevated MDA concentrations identified within hepatic tissue, in conjunction with the augmented presence of leukocytes and the diminished count of thrombocytes.

Biovaccination Effect of *P.australis*-based CuNPs

Hematological Parameters

Hematological analysis is a key method for assessing the physiological condition and the impact of xenobiotics. Combined with biochemical and histopathological analyses, it provides a thorough understanding of physiological changes, offering the advantage of being cost-effective and not requiring specialized equipment (Witeska, Kondera, & Bojarski, 2023). Our ANOVA test results indicate the effects of different *P. australis* Cu NPs (synthesized with leaf extract, rhizome extract, and a mixture of both) treatments on various hematological parameters. The higher WBC counts suggest an immune response, which could be due to mild inflammatory reactions (K Ognik et al., 2016) or immune system stimulation (Al-Zuhairi et al., 2023). The RBC counts observed in groups subjected to treatment with varying *P. australis*-based Cu NPs demonstrate elevated levels, indicative of enhanced oxygenation attributed to improved erythropoiesis. This aligns with the observed elevated HGB, HCT, and MCH values. Furthermore, the augmentation in the aforementioned hematological parameters may be associated with the pivotal role of copper in the synthesis of hemoglobin through its function in iron metabolism (Mroczek-Sosnowska et al., 2013).

Lipid Peroxidation Marker

MDA is a marker of lipid peroxidation, associated with oxidative stress and tissue damage (Gaweł, Wardas, Niedworok, & Wardas, 2004). The higher MDA levels in the vaccinated group suggest that immune activation leads to oxidative stress, as previously reported by Surai *et al*.

(Surai, Kochish, Fisinin, & Kidd, 2019). The LP-Cu NPs treatments resulted in the lowest MDA levels, in breast muscle, among the other Cu NPs treatments, suggesting its potential anti-oxidant effect. There were no significant differences among Cu NPs treatments in the thigh muscle. This indicates that Cu NPs did not significantly alter lipid peroxidation. The plant-based Cu NPs treatments resulted in the lowest MDA levels in the liver, indicating their potential to reduce lipid peroxidation, possibly due to improved bioavailability and anti-oxidant capacity of these nanoparticles (Katarzyna Ognik et al., 2018).

Liver and Muscle Glycogen

Liver glycogen is a crucial energy reserve, particularly in poultry, as it reflects metabolic adaptations to stress, disease, and nutritional interventions (Mannuthy, 2000). Despite variations among groups, the fact that the MP-Cu NPs group maintains glycogen levels similar to the group that has not been provided with any medications suggests that the Cu NPs synthesized using both extracts of P. australis (leaves and rhizomes) do not disrupt glycogen metabolism. While the hepatic glycogen levels in the LP-Cu NPs and RP-Cu NPs cohorts appear to be diminished in comparison to the other experimental groups, indicating a potential manifestation of oxidative stress, the diminished concentrations of MDA in the previously mentioned cohorts contradict this assertion. In contrast, the elevated concentrations of hepatic glycogen observed in the vaccinated cohort do not provide a definitive understanding of the favorable glycogen storage equilibrium, given the concomitant elevation of MDA levels. Furthermore, MP-Cu NPs and RP-Cu NPs seem to promote higher glycogen levels, especially in breast muscle. This could be due to enhanced glucose uptake by muscle cells via improved insulin sensitivity or increased glycogen synthase activity (Sharma et al., 2016).

Liver Histology

Our histological analysis of the hepatic slides of all groups administered with *P. australis*-based Cu NPs indicates a significant enhancement in comparison to the slides obtained from the acute toxicity evaluation. The occurrence of mild and minimal inflammatory foci is an unavoidable phenomenon in the liver of a living organism, given that this organ serves as the central hub for detoxification throughout the entire body. The MP-Cu nanoparticles groups demonstrate a nearly normal hepatic architecture, whereas the vaccinated cohort exhibits multiple and extensive foci of periportal inflammation, which may reflect the repercussions of xenobiotic agents (such as vaccines, growth-promoting substances, anti-stress compounds, etc.) that are consistently administered throughout the rearing period. These findings are in concordance with our observations regarding oxidative stress markers. In other words, reduced inflammation or

oxidative stress in the liver tissues may validate the biocompatibility of our green-synthesized Cu NPs.

Final Body Weight

The findings of our research indicate that the administration of *P. australis*-based copper nanoparticles yields a beneficial impact on the growth and weight gain of chickens. Notably, the group receiving MP-Cu NPs presented the highest weight metrics compared to all other experimental groups, including those comprising chickens that had undergone vaccination against numerous diseases and were supplemented with multivitamins and anti-stress compounds. This particular cohort demonstrated an almost exemplary condition of hepatic tissue, which is indicative of the overall health status of the chickens. The observed mortality rate fell within an acceptable range, as it is widely recognized among veterinary professionals that a mortality percentage of approximately 11% is deemed normal. Conversely, the significantly elevated mortality rate in the group raised without any form of medication or dietary supplementation can be rationalized, as only those chickens exhibiting robust immunity and resilience survived. These findings imply, when juxtaposed with conventional rearing methodologies that encompass vaccination, vitamin and trace elements supplementation, and antibiotic treatment in the event of disease occurrence, the prospective advantages of employing green nanoparticles in broiler production, given that a single molecule, namely the nanoparticle, may function as an antiviral, antibacterial, and growth-promoting agent while also being environmentally sustainable and cost-efficient.

The enhancement observed in hematological parameters was correlated with a diminution in oxidative stress and inflammation, which subsequently resulted in enhanced growth performance and improved health outcomes. Many other studies have found similar results (Al-Saeedi & Al-Khafaji, 2024; Basharat et al., 2023).

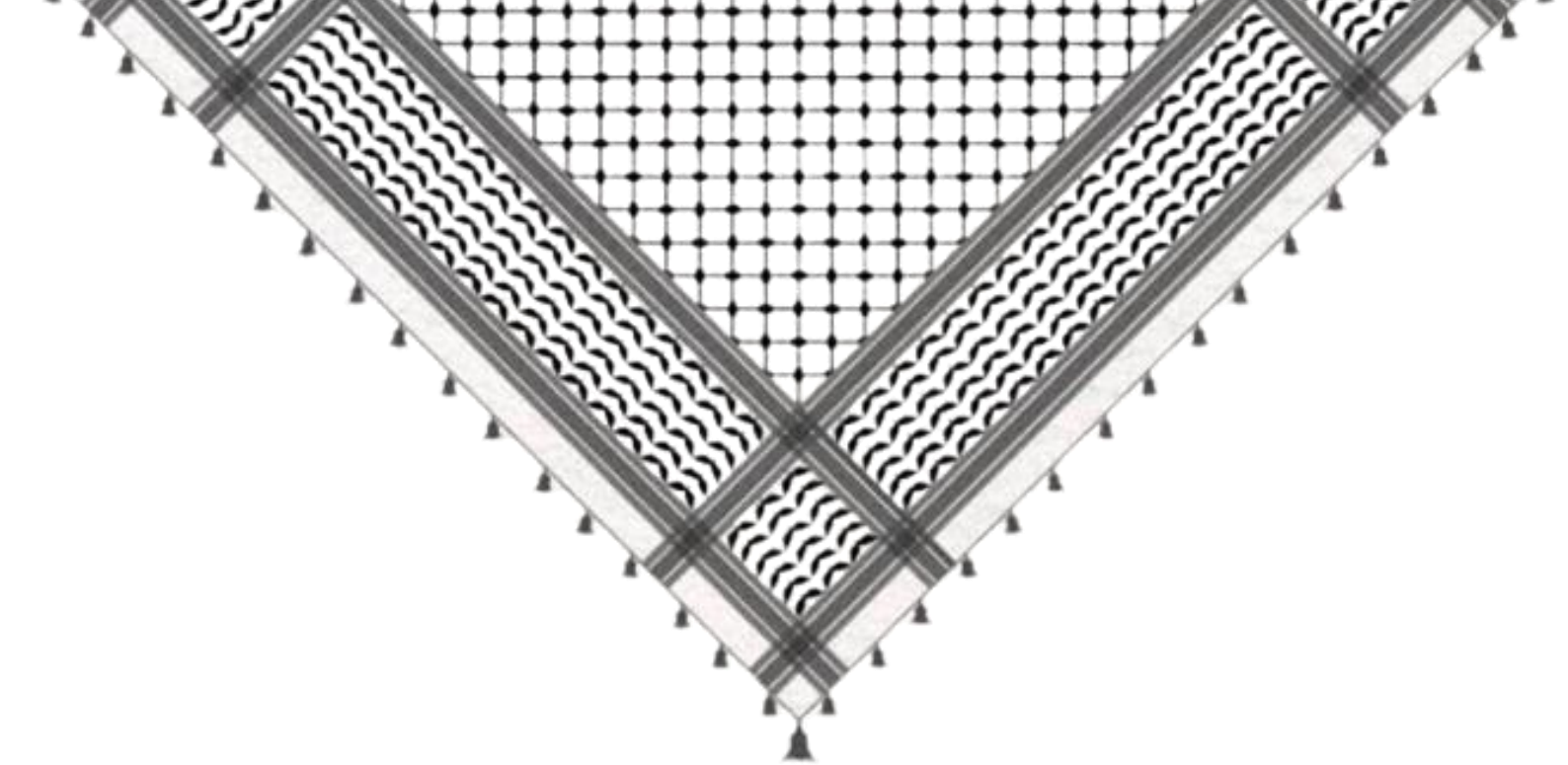

Conclusion & Perspectives

Conclusion

By employing green synthesis methods, such as using plant-based or biological materials, green nanotechnology offers an eco-friendlier alternative to traditional nanofabrication techniques, paving the way for the development of safer, more efficient drug delivery systems, diagnostic tools, and therapeutic agents. In alignment with our *in vitro* and *in vivo* investigations, we are positioned to draw the subsequent inferences:

- ✓ Leaves and rhizomes of the studied plant, *Phragmites australis*, are a rich source of bioactive compounds such as phenols, flavonoids, and terpenoids, as evidenced by quantitative and qualitative phytochemical screening. These secondary metabolites are known to fight against ROS and disorders caused by them.
- ✓ The GC-MS analysis revealed significant semi-volatile compounds, further supporting the plant's potential therapeutic applications.
- ✓ Leaves and rhizomes of *Phragmites australis* have successfully reduced copper sulfate to copper nanoparticles.
- ✓ The greenly synthesized copper nanoparticles, characterized by techniques such as SEM, TEM, UV-Vis spectroscopy, FTIR, XRD and Zeta potential, exhibited fine-sized and very stable particles and promising *in vitro* biological activities, including potent antioxidant, anti-inflammatory, anti-bacterial, and anti-cancer effects.

These findings highlight the plant's value as a source of bioactive compounds acting as reducing and capping agents for the green synthesis of copper nanoparticles which is a viable option for therapeutic development, paving the way for further research into their applications in veterinary medicine and pharmacology.

- ✓ Our *In vivo* acute toxicity assessments indicate that these nanoparticles are non-toxic, with only slight alterations in biochemical and hematological markers, at very high doses, underscoring their safety for potential biomedical applications.
- ✓ Our investigation demonstrates notable improvements in hematological parameters, oxidative stress levels, growth metrics, and health-related outcomes.
- ✓ The histological evidence supports the use of green-synthesized Cu NPs as a safer and more effective alternative to conventional treatments in broiler.
- ✓ The weight of chickens at the end of the rearing period along with the low mortality rate of our biovaccinated groups allow us to conclude the growth promoting effect of the green synthesized Cu NPs.

Perspectives

Given the significance of broiler poultry production; these findings unveil alternative viewpoints, encompassing:

- ✓ Evaluation of the antiviral effect of *P. australis*-based Cu NPs.
- ✓ Conducting further comprehensive assays to ascertain the impact of *P. australis*-based Cu NPs administered via alternative routes.
- ✓ Exploration of new drugs and strategies to reduce antibiotic use and expensive vaccines.
- ✓ Investigating the potential of *P. australis*-based Cu NPs in enhancing meat quality and improving its shelf-life.
- ✓ Assessment of the effect of bioaccumulation of the nanoparticles.

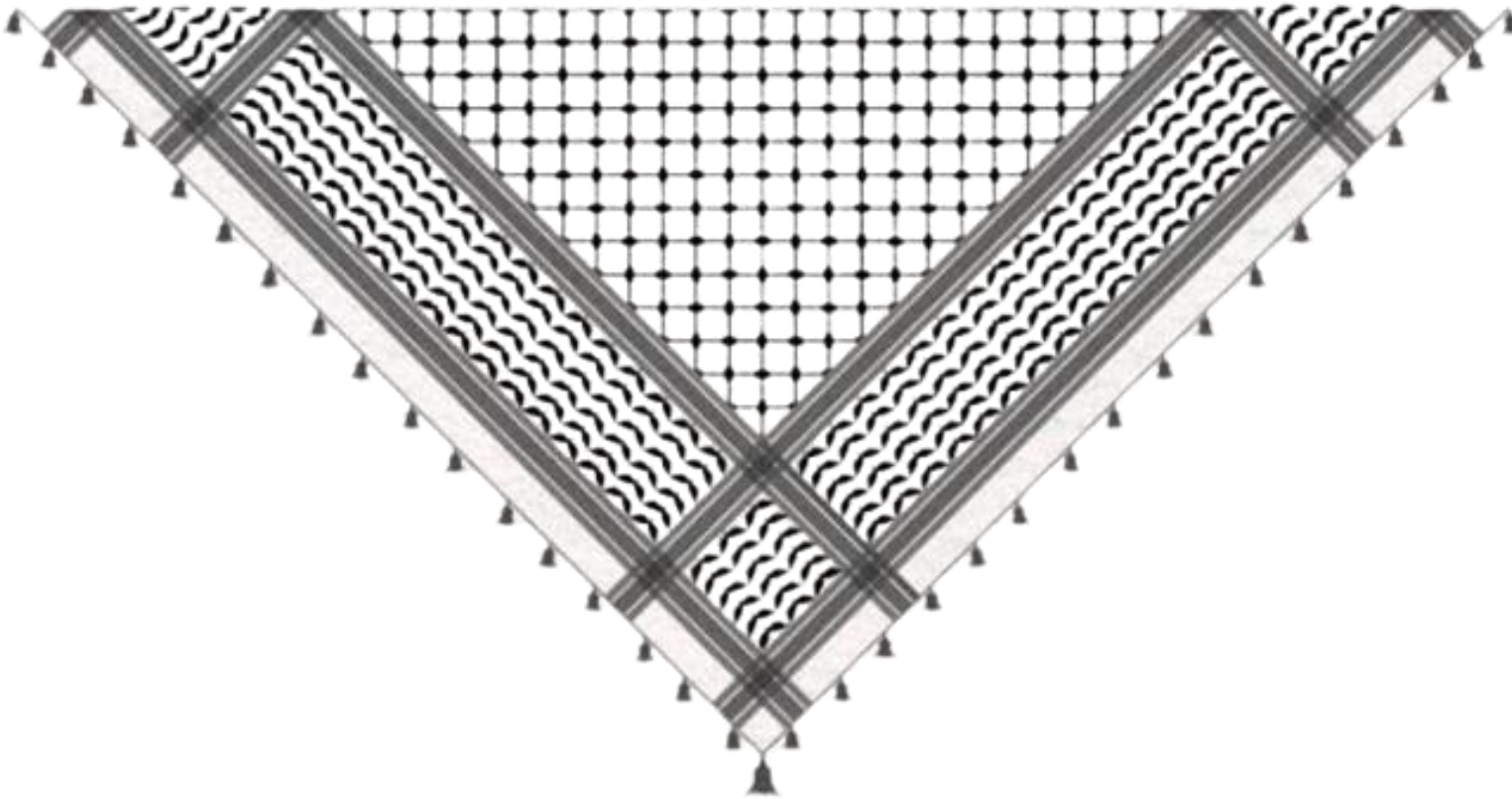

References

Abdel-Azeem, A., Nada, A. A., O'Donovan, A., Thakur, V. K., & Elkelish, A. (2020). Mycogenic silver nanoparticles from endophytic Trichoderma atroviride with antimicrobial activity. *Journal of renewable Materials, 8*(2), 171-185.

Abdullah, S. S., Masood, S., Zaneb, H., Rabbani, I., Akbar, J., Kuthu, Z., . . . Vargas-Bello-Pérez, E. (2022). Effects of copper nanoparticles on performance, muscle and bone characteristics and serum metabolites in broilers. *Brazilian journal of biology, 84*, e261578.

Abu Hafsa, S. H., Ibrahim, S. A., Eid, Y. Z., & Hassan, A. A. (2020). Effect of dietary Moringa oleifera leaves on the performance, ileal microbiota and antioxidative status of broiler chickens. *Journal of Animal Physiology and Animal Nutrition, 104*(2), 529-538.

Adomako, E. A., & Moe, O. W. (2023). Uric acid transport, transporters, and their pharmacological targeting. *Acta Physiologica, 238*(2), e13980.

Afzal, S., Abdul Manap, A. S., Attiq, A., Albokhadaim, I., Kandeel, M., & Alhojaily, S. M. (2023). From imbalance to impairment: the central role of reactive oxygen species in oxidative stress-induced disorders and therapeutic exploration. *Frontiers in Pharmacology, 14*, 1269581.

Ahmad, S., Munir, S., Zeb, N., Ullah, A., Khan, B., Ali, J., . . . Salman, S. M. (2019). Green nanotechnology: A review on green synthesis of silver nanoparticles—An ecofriendly approach. *International journal of nanomedicine*, 5087-5107.

Akbarian, A., Michiels, J., Degroote, J., Majdeddin, M., Golian, A., & De Smet, S. (2016). Association between heat stress and oxidative stress in poultry; mitochondrial dysfunction and dietary interventions with phytochemicals. *Journal of animal science and biotechnology, 7*, 1-14.

Akintelu, S. A., Folorunso, A. S., Folorunso, F. A., & Oyebamiji, A. K. (2020). Green synthesis of copper oxide nanoparticles for biomedical application and environmental remediation. *Heliyon, 6*(7).

Akue, A., Lare, L., & Talaki, E. (2023). Eucalyptus globulus as an Alternative to Antibiotics for Isa brown Laying Hens during the Starter Phase. *Journal of World's Poultry Research, 13*(4), 394-405.

Akyildiz, S., & Denli, M. (2016). Application of plant extracts as feed additives in poultry nutrition. *Anim. Sci, 59*(2393), 2260.

Al-Jubouri, A., Al-Saadi, N., & Kadhim, M. (2022). Anti-Inflammatory and Anti-Bacterial Activity of Copper Nanoparticles Synthesized from Myrtus Communis Leaves Extract. *Iraqi Journal of Agricultural Sciences, 53*(3), 698-711.

Al-Saeedi, M. K. I., & Al-Khafaji, F. R. A. (2024). *Productive Response for Adding Copper Nanoparticles Synthesized by Green Method to Broiler Chickens Diet.* Paper presented at the IOP Conference Series: Earth and Environmental Science.

Al-Zuhairi, S. K., Al-Salhie, K. C., & AlAbdullah, Z. T. (2023). Effect of Adding Different Levels of Silver-Curcumin Nanoparticles on Some Productive Traits, Blood Parameters and Antioxidant Status of Broiler Chickens. *Jornal of Al-Muthanna for Agricultural Sciences, 10*(2).

Alabi, O. J., Makinde, O. J., Egena, S., Mbajiorgu, F. E., & Adewara, O. (2024). Antibiotics in broilers chicken production: a review of impacts, challenges and potential alternatives: https://doi. org/10.12982/VIS. 2024.039. *Veterinary Integrative Sciences, 22*(2), 559-578.

Alghuthaymi, M. A., Hassan, A. A., Kalia, A., Sayed El Ahl, R. M., El Hamaky, A. A., Oleksak, P., . . . Abd-Elsalam, K. A. (2021). Antifungal nano-therapy in veterinary medicine: Current status and future prospects. *Journal of Fungi, 7*(7), 494.

Ali, A. S., Lawson, M. A., Tauson, A.-H., Fris Jensen, J., & Chwalibog, A. (2007). Influence of electrical stunning voltages on bleed out and carcass quality in slaughtered broiler chickens. *Archiv fur Geflugelkunde, 71*(1), 35-40.

Altammar, K. A. (2023). A review on nanoparticles: characteristics, synthesis, applications, and challenges. *Frontiers in microbiology, 14*, 1155622.

Amaral, A. B., Silva, M. V. d., & Lannes, S. C. d. S. (2018). Lipid oxidation in meat: mechanisms and protective factors–a review. *Food Science and Technology, 38*, 1-15.

Apte, U., & Krishnamurthy, P. (2011). Detoxification functions of the liver. *Molecular pathology of liver diseases*, 147-163.

Arsène, M. M. J., Davares, A. K. L., Viktorovna, P. I., Andreevna, S. L., Sarra, S., Khelifi, I., & Sergueïevna, D. M. (2022). The public health issue of antibiotic residues in food and feed: Causes, consequences, and potential solutions. *Veterinary world, 15*(3), 662.

Bacou, E., Walk, C., Rider, S., Litta, G., & Perez-Calvo, E. (2021). Dietary oxidative distress: A review of nutritional challenges as models for poultry, swine and fish. *Antioxidants, 10*(4), 525.

Balasooriya, E. R., Jayasinghe, C. D., Jayawardena, U. A., Ruwanthika, R. W. D., Mendis de Silva, R., & Udagama, P. V. (2017). Honey mediated green synthesis of nanoparticles: new era of safe nanotechnology. *Journal of Nanomaterials, 2017*.

Banerjee, S., Chanda, A., Adhikari, A., Das, A., & Biswas, S. (2014). Evaluation of phytochemical screening and anti inflammatory activity of leaves and stem of Mikania scandens (L.) wild. *Annals of medical and health sciences research, 4*(4), 532-536.

Basharat, S., Tahir, S. K., Majeed, K. A., Yousaf, M. S., Hussain, K. K., Rashid, M. A., . . . Rehman, H. (2023). Effects of Iron Oxide Nanoparticle Supplementation on the Growth Performance, Serum Metabolites, Meat Quality, and Jejunal Basal Morphology in Broilers. *Animals, 14*(1), 99.

Bayda, S., Adeel, M., Tuccinardi, T., Cordani, M., & Rizzolio, F. (2019). The history of nanoscience and nanotechnology: from chemical–physical applications to nanomedicine. *Molecules, 25*(1), 112.

Beauchamp, C., & Fridovich, I. (1971). Superoxide dismutase: improved assays and an assay applicable to acrylamide gels. *Analytical biochemistry, 44*(1), 276-287.

Beaudette, A. M. (2020). *Estimating the Onset and Extent of Dieback of Phragmites Australis Using the Normalized Difference Vegetation Index and Remotely Sensed Land Cover Classifications*: Louisiana State University and Agricultural & Mechanical College.

Berra, D., Laouini, S., Benhaoua, B., Ouahrani, M., Berrani, D., & Rahal, A. (2018). Green synthesis of copper oxide nanoparticles by Pheonix dactylifera L leaves extract. *Digest Journal of Nanomaterials and Biostructures, 13*(4), 1231-1238.

Bharathala, S., & Sharma, P. (2019). Biomedical applications of nanoparticles *Nanotechnology in modern animal biotechnology* (pp. 113-132): Elsevier.

Bhattacharjee, S. (2016). DLS and zeta potential–what they are and what they are not? *Journal of controlled release, 235*, 337-351.

Bideshki, A., Karimi-Dehkordi, M., & Gholami-Ahangaran, M. (2023). Relationship between serum biochemical parameters and kidney lesions in broiler chickens with acute tubular necrosis. *Indian Journal of Animal Sciences, 93*(6), 578-582.

Boizot, N., & Charpentier, J.-P. (2006). Méthode rapide d'évaluation du contenu en composés phénoliques des organes d'un arbre forestier. *Le Cahier des Techniques de l'INRA, In: Numéro spécial*, 79-82.

BOULAARES, I., DEROUICHE, S., & GUEMARI, I. Y. (2024a). Hepatoprotective effect of Ocimum basilicum aqueous extract against doxorubicin-induced hepatic damage in albino rats. *Asian Journal of Tropical Biotechnology, 21*(2).

Boulaares, I., Derouiche, S., & Guemari, I. Y. (2024b). lmpact of Doxorubicin Chemotherapy on Oxidative Stress Status in Heart and Liver: An experimental Study on Rats. *Pharmaceutical Sciences & Analytical Research Journal 6*(3), 180067.

Cai, K., Shao, W., Chen, X., Campbell, Y., Nair, M., Suman, S., . . . Schilling, M. (2018). Meat quality traits and proteome profile of woody broiler breast (pectoralis major) meat. *Poultry science, 97*(1), 337-346.

Chatterjee, S., Karmakar, A., Azmi, S. A., & Barik, A. (2017). Antibacterial activity of long-chain primary alcohols from Solena amplexicaulis leaves. *Proceedings of the Zoological Society, 71*, 313-319. doi: 10.1007/s12595-017-0208-0

Chen, S., Ju, M., Luo, Y., Chen, Z., Zhao, C., Zhou, Y., & Fu, J. (2013). Hepatoprotective and antioxidant activities of the aqueous extract from the rhizome of Phragmites australis. *Zeitschrift für Naturforschung C, 68*(11-12), 439-444.

Chen, Z., Xing, T., Li, J., Zhang, L., Jiang, Y., & Gao, F. (2022). Oxidative stress impairs the meat quality of broiler by damaging mitochondrial function, affecting calcium metabolism and leading to ferroptosis. *Animal bioscience, 35*(10), 1616.

Chetehouna, S., Boulaares, I., Atoussi, O., Guemari, I. Y., & Derouiche, S. (2024). Green nanoparticles as a Novel application of nanotechnology in medicine: study of zinc, copper and magnesium nanoparticles. *Records of Pharmaceutical and Biomedical Sciences, 8*(3), 109-120.

Choi, J., Kong, B., Bowker, B. C., Zhuang, H., & Kim, W. K. (2023). Nutritional strategies to improve meat quality and composition in the challenging conditions of broiler production: a review. *Animals, 13*(8), 1386.

Chowdhury, M. A. H., Ashrafudoulla, M., Mevo, S. I. U., Mizan, M. F. R., Park, S. H., & Ha, S. D. (2023). Current and future interventions for improving poultry health and poultry food safety and security: A comprehensive review. *Comprehensive Reviews in Food Science and Food Safety, 22*(3), 1555-1596.

Christie, D. J., & Aster, R. H. (1982). Drug-antibody-platelet interaction in quinine-and quinidine-induced thrombocytopenia. *The Journal of Clinical Investigation, 70*(5), 989-998.

Dahman, Y. (2017). *Nanotechnology and functional materials for engineers*: Elsevier.

Dahman, Y., Nasr, E. J., Prekh, D., Alhamami, M., & Kaur, R. (2018). Nanotechnology and its Applications in Biomedical Engineering *NanoBioEngineering* (pp. 1-26): CRC Press.

Dansette, P., Bonierbale, E., Minoletti, C., Beaune, P., Pessayre, D., & Mansuy, D. (1998). Drug-induced immunotoxicity. *European journal of drug metabolism and pharmacokinetics, 23*, 443-451.

Dehpour, A. A., Ebrahimzadeh, M. A., Fazel, N. S., & Mohammad, N. S. (2009). Antioxidant activity of the methanol extract of Ferula assafoetida and its essential oil composition. *Grasas y aceites, 60*(4), 405-412.

DEROUICHE, S. (2020). Characterization and acute toxicity evaluation of the MgO Nanoparticles Synthesized from Aqueous Leaf Extract of Ocimum basilicum L. *Algerian journal of Biosciences, 1*(1), 1-6.

Derouiche, S., Azzi, M., & Hamida, A. (2019). Phytochemical analysis and antioxidant property of rhizome extracts aqueous of Phragmites australis in alloxan diabetic rats. *Asian Journal of Pharmacy and Technology, 9*(4), 249. doi: 10.5958/2231-5713.2019.00041.2

Derouiche, S., Chetehouna, S., & Atoussi, W. (2022). The effects of aqueous leaf extract of *Portulaca oleracea* on haemato-biochemical and histopathological changes induced by sub-chronic aluminium toxicity in male wistar rats. *Pharmacological Research-Modern Chinese Medicine, 3*, 100101. doi: https://doi.org/10.1016/j.prmcm.2022.100101

Derouiche, S., Degachi, O., & Gharbi, K. (2020). The effect of purslane and aquilaria malaccensis on insulin-resistance and lipid peroxidation in high-fructose diet rats. *Romanian Journal of Diabetes Nutrition and Metabolic Diseases, 27*(4), 357-365.

Derouiche, S., Djermoun, M., & Abbas, K. (2017). Beneficial Effect of Zinc on diabetes induced kidney damage and liver stress oxidative in rats. *J Adv Biol, 10*(1), 2050-5055.

Derouiche, S., & Kechrid, Z. (2013). Influence of calcium supplements on zinc status, carbohydrate metabolism and the liver activity of detoxifying glutathione enzymatic system in alloxan-induced diabetic rats. *J Exp Biol, 1*, 6.

Derouiche, S., Serouti, A., & Rezzagmohcen, O. (2019). Risk of Metribuzin (Triazinone herbicide) on hematological and renal structure and function of pregnancy rabbits. *Asian Journal of Biological Sciences, 12*, 192-198.

Desbruslais, A., & Wealleans, A. L. (2022). Oxidation in poultry feed: impact on the bird and the efficacy of dietary antioxidant mitigation strategies. *Poultry, 1*(4), 246-277.

DeSimone, J. M., Gratton, S., Guo, J., Kelly, J. Y., Murphy, A. J., & Napier, M. E. (2013). Discrete size and shape specific pharmaceutical organic nanoparticles: Google Patents.

Dinda, G., Halder, D., Vazquez-Vazquez, C., Lopez-Quintela, M. A., & Mitra, A. (2015). Green synthesis of copper nanoparticles and their antibacterial property. *J. Surf. Sci. Technol, 31*, 117-122.

Djamila, B., Eddine, L. S., Abderrhmane, B., Nassiba, A., & Barhoum, A. (2022). In vitro antioxidant activities of copper mixed oxide (CuO/Cu.

Donsbough, A. L. (2008). *The use of serum uric acid as an indicator of amino acid utilization in diets for broilers*: Louisiana State University and Agricultural & Mechanical College.

Dukare, S., Mir, N. A., Mandal, A. B., Dev, K., Begum, J., Rokade, J., . . . Bhanja, S. (2021). A comparative study on the antioxidant status, meat quality, and mineral deposition in broiler chicken fed dietary nano zinc viz-a-viz inorganic zinc. *Journal of Food Science and Technology, 58*, 834-843.

Duvhåteau, G., & Florkin, M. (1959). Sur la tréhalosémie des insectes et sa signification. *Archives Internationales de Physiologie et de Biochimie, 67*(2), 306-314.

Dzuvor, C. K., Shen, H.-H., Haritos, V. S., & He, L. (2024). Coassembled Multicomponent Protein Nanoparticles Elicit Enhanced Antibacterial Activity. *ACS nano, 18*(5), 4478-4494.

Ebrahimi, R., Ebrahimi, M., & Shakeri, M. (2023). Mitigating the adverse effects of lead and cadmium heavy metals-induced oxidative stress by phytogenic compounds in poultry. *Poultry, 2*(2), 235-251.

Echiegu, E. A. (2017). Nanotechnology applications in the food industry. *Nanotechnology: Food and Environmental Paradigm*, 153-171.

Edebali, S., Oztekin, Y., & Arslan, G. (2018). Metallic engineered nanomaterial for industrial use *Handbook of Nanomaterials for Industrial Applications* (pp. 67-73): Elsevier.

Eid, A. M., Fouda, A., Hassan, S. E.-D., Hamza, M. F., Alharbi, N. K., Elkelish, A., . . . Salem, W. M. (2023). Plant-based copper oxide nanoparticles; biosynthesis, characterization, antibacterial activity, tanning wastewater treatment, and heavy metals sorption. *Catalysts, 13*(2), 348.

El-Habib, I., Maatouk, H., Lemarchand, A., Dine, S., Roynette, A., Mielcarek, C., . . . Azouani, R. (2024). Antibacterial size effect of ZnO nanoparticles and their role as additives in emulsion waterborne paint. *Journal of Functional Biomaterials, 15*(7), 195.

Emmanuel, B., & Howard, B. R. (1978). Endogenous uric acid and urea metabolism in the chicken. *British Poultry Science, 19*(3), 295-301. doi: 10.1080/00071667808416479

Ershov, V. A., & Ershov, B. G. (2024). Effect of Silver Nanoparticle Size on Antibacterial Activity. *Toxics, 12*(11), 801.

Estévez, M. (2011). Protein carbonyls in meat systems: A review. *Meat science, 89*(3), 259-279.

Estévez, M. (2015). Oxidative damage to poultry: from farm to fork. *Poultry science, 94*(6), 1368-1378.

Falowo, A. B., Fayemi, P. O., & Muchenje, V. (2014). Natural antioxidants against lipid–protein oxidative deterioration in meat and meat products: A review. *Food research international, 64*, 171-181.

Farouk, O. Y., Fahim, J. R., Attia, E. Z., & Kamel, M. S. (2023). Phytochemical and biological profiles of the genus Phragmites (Family Poaceae): a review. *South African Journal of Botany, 163*, 659-672.

Fathi, M., Haydari, M., & Tanha, T. (2016). Effects of zinc oxide nanoparticles on antioxidant status, serum enzymes activities, biochemical parameters and performance in broiler chickens. *Journal of Livestock Science and Technologies, 4*(2), 7-13.

Fawzy, M., Khairy, G. M., Hesham, A., Rabaan, A. A., El-Shamy, A. G., & Nagy, A. (2021). Nanoparticles as a novel and promising antiviral platform in veterinary medicine. *Archives of virology, 166*, 2673-2682.

Feng, L., Ke, N., Cheng, F., Guo, Y., Li, S., Li, Q., & Li, Y. (2011). The protective mechanism of ligustrazine against renal ischemia/reperfusion injury. *Journal of Surgical Research, 166*(2), 298-305.

Forman, H. J., Zhang, H., & Rinna, A. (2009). Glutathione: overview of its protective roles, measurement, and biosynthesis. *Molecular aspects of medicine, 30*(1-2), 1-12.

Fúnez, A. Á., Duaso, A. I. H., & Gómez, P. M. (2016). Nanotecnología en la industria alimentaria II: evaluación del riesgo y legislación. *Revista complutense de ciencias veterinarias, 10*(2), 18-40.

Gaweł, S., Wardas, M., Niedworok, E., & Wardas, P. (2004). Malondialdehyde (MDA) as a lipid peroxidation marker. *Wiadomosci lekarskie (Warsaw, Poland: 1960), 57*(9-10), 453-455.

Gheraissa, N., Chemsa, A. E., Elsharkawy, E. R., & Cherrada, N. (2022). Phenolic compound profile, and evaluation of biological properties of Bassia muricata (L.) Asch. aerial part. *International Journal of Secondary Metabolite, 9*(3), 335-347.

Ghernaout, D., Alghamdi, A., Touahmia, M., Aichouni, M., & Ait Messaoudene, N. (2018). Nanotechnology phenomena in the light of the solar energy. *Journal of Energy, Environmental & Chemical Engineering, 3*(1), 1.

Ghotekar, S., Pansambal, S., Bilal, M., Pingale, S. S., & Oza, R. (2021). Environmentally friendly synthesis of Cr2O3 nanoparticles: characterization, applications and future perspective─ a review. *Case Studies in Chemical and Environmental Engineering, 3*, 100089.

Girma, A., Mebratie, G., Mekuye, B., Abera, B., Bekele, T., & Alamnie, G. (2024). Antibacterial Capabilities of Metallic Nanoparticles and Influencing Factors. *Nano Select, 5*(12), e202400049.

Glezer, A. (2011). Structural classification of nanomaterials. *Russian Metallurgy (Metally), 2011*(4), 263-269.

Goesmann, H., & Feldmann, C. (2010). Nanoparticulate functional materials. *Angewandte Chemie International Edition, 49*(8), 1362-1395.

Goluch, Z., Słupczyńska, M., Okruszek, A., Haraf, G., Wereńska, M., & Wołoszyn, J. (2023). The energy and nutritional value of meat of broiler chickens fed with various addition of wheat germ expeller. *Animals, 13*(3), 499.

Gorenflot, R. (1976). Le complexe polyploïde du Phragmites australis (Cav.) Trin. ex Steud.(= P. communis Trin.). *Bulletin de la Société botanique de France, 123*(5-6), 261-271.

Grozovsky, R., Begonja, A. J., Liu, K., Visner, G., Hartwig, J. H., Falet, H., & Hoffmeister, K. M. (2015). The Ashwell-Morell receptor regulates hepatic thrombopoietin production via JAK2-STAT3 signaling. *Nature medicine, 21*(1), 47-54.

Guo, D., Xie, G., & Luo, J. (2013). Mechanical properties of nanoparticles: basics and applications. *Journal of physics D: applied physics, 47*(1), 013001.

Guo, D., Yang, S., Wu, J., & Li, J. (2000). The level of MDA and activities of SOD in broiler infected with newcastle disease virus. *Chin. J. Preventive Vet. Med, 22*(5), 365-367.

Gupta, D., Boora, A., Thakur, A., & Gupta, T. K. (2023). Green and sustainable synthesis of nanomaterials: recent advancements and limitations. *Environmental Research, 231*, 116316.

Gupta, S. K., Talati, M., & Jha, P. K. (2008). *Shape and size dependent melting point temperature of nanoparticles.* Paper presented at the Materials Science Forum.

Hameed, H., Waheed, A., Sharif, M. S., Saleem, M., Afreen, A., Tariq, M., . . . Ahmad, S. (2023). Green Synthesis of Zinc Oxide (ZnO) Nanoparticles from Green Algae and Their Assessment in Various Biological Applications. *Micromachines, 14*(5), 928.

Haque, M. H., Sarker, S., Islam, M. S., Islam, M. A., Karim, M. R., Kayesh, M. E. H., . . . Anwer, M. S. (2020). Sustainable antibiotic-free broiler meat production: Current trends, challenges, and possibilities in a developing country perspective. *Biology, 9*(11), 411.

Harborne, A. (1998). *Phytochemical methods a guide to modern techniques of plant analysis*: springer science & business media.

Harborne, J. B. (1973). *A guide to modern techniques of plant analysis*: Chapman and hall.

Haslam, S. (1972). Phragmites communis Trin.(Arundo phragmites L.,? Phragmites australis (Cav.) Trin. ex Steudel). *The journal of ecology*, 585-610.

Hassan, D., & Abd, F. (2023). Antibacterial Activity of Nanoparticle Biosynthesis by Bacteria. *Journal of University of Babylon for Pure and Applied Sciences, 31*(2), 146-160.

Hatab, M. H., Badran, A. M., Elaroussi, M. A., Rashad, E., Taleb, A. M. A., & Elokil, A. A. (2024). Effect of zinc oxide nanoparticles as feed additive on blood indices, physiological, immunological responses, and histological changes in broiler chicks. *Biological trace element research, 202*(5), 2279-2293.

Hevia, P., & Clifford, A. (1977). Protein intake, uric acid metabolism and protein efficiency ratio in growing chicks. *The Journal of Nutrition, 107*(6), 959-964.

Hidayat, C., Sadarman, S., Adli, D. N., Rusli, R. K., Bakrie, B., Ginting, S. P., . . . Zainal, H. (2024). Comparative effects of dietary zinc nanoparticle and conventional zinc supplementation on broiler chickens: A meta-analysis. *Veterinary World, 17*(8), 1733.

Holmberg, R. J., Aharen, T., & Murugesu, M. (2012). Paramagnetic nanocrystals: remarkable lanthanide-doped nanoparticles with varied shape, size, and composition. *The Journal of Physical Chemistry Letters, 3*(24), 3721-3733.

Horikoshi, S., & Serpone, N. (2013). *Microwaves in nanoparticle synthesis: fundamentals and applications*: John Wiley & Sons.

Hosny, M., Fawzy, M., El-Borady, O. M., & Mahmoud, A. E. D. (2021). Comparative study between Phragmites australis root and rhizome extracts for mediating gold nanoparticles synthesis and their medical and environmental applications. *Advanced Powder Technology, 32*(7), 2268-2279.

Huang, L., Zhu, X., Zhou, S., Cheng, Z., Shi, K., Zhang, C., & Shao, H. (2021). Phthalic acid esters: Natural sources and biological activities. *Toxins, 13*(7), 495.

Hubert, S. M., & Athrey, G. (2020). Energy metabolism and sources of oxidative stress in wooden breast-a review. *F1000Research, 9*, 319.

Hurley, O., Lynn, A., DeVries, A., Reid, C., & Elsey-Quirk, T. (2024). Return of the Phrag-i: evaluating sexual reproduction mechanisms amenable to dieback recovery and potential invasiveness across Phragmites australis haplotypes. *Wetlands Ecology and Management*, 1-15.

Iravani, S. (2011). Green synthesis of metal nanoparticles using plants. *Green Chemistry, 13*(10), 2638-2650.

Jaeschke, H., McGill, M. R., & Ramachandran, A. (2012). Oxidant stress, mitochondria, and cell death mechanisms in drug-induced liver injury: lessons learned from acetaminophen hepatotoxicity. *Drug metabolism reviews, 44*(1), 88-106.

Jiang, Z., Yang, R., Sheng, Y., Sun, Y., Li, J., Bradley, M., & Zhang, R. (2024). Preparation and antibacterial ability of photodynamic antibacterial nanoparticles with ammonium cationic groups. *Journal of Bioactive and Compatible Polymers, 39*(5), 301-316.

John, M. S., Nagoth, J. A., Zannotti, M., Giovannetti, R., Mancini, A., Ramasamy, K. P., . . . Pucciarelli, S. (2021). Biogenic synthesis of copper nanoparticles using bacterial strains isolated from an antarctic consortium associated to a psychrophilic marine ciliate: characterization and potential application as antimicrobial agents. *Marine drugs, 19*(5), 263.

Kachungwa Lugata, J., Ortega, A. D. S. V., & Szabó, C. (2022). The role of methionine supplementation on oxidative stress and antioxidant status of poultry-a review. *Agriculture, 12*(10), 1701.

Kaouachi, A., & Derouiche, S. (2018). Phytochemical analysis, DPPH antioxidant activity and Acute toxicity of bark aqueous extracts of Pinus halepensis. *Research Journal of Chemical and Environmental Sciences, 6*(3), 86-91.

Kenney, B., & Stack, G. (2009). Drug-induced thrombocytopenia. *Archives of pathology & laboratory medicine, 133*(2), 309-314.

Keskın, D., Ceyhan, N., Uğur, A., & Dbeys, A. D. (2012). Antimicrobial activity and chemical constitutions of West Anatolian olive (Olea europaea L.) leaves. *Journal of Food, Agriculture & Environment, 10*(2), 99-102.

Khan, I., Saeed, K., & Khan, I. (2019). Nanoparticles: Properties, applications and toxicities. *Arabian journal of chemistry, 12*(7), 908-931.

Khan, S., Chand, N., Hafeez, A., Ali, M., Qattan, S. Y. A., Alam, M., . . . Kamal, M. (2023). Impact of Bacillus subtilis probiotic on growth, visceral and lymphatic organ weights, intestinal histo-morphology, and pathogenic bacteria of broilers. *Annals of Animal Science, 0*(0). doi: 10.2478/aoas-2024-0084

Khanam, F., Iqbal, M. N., Ashraf, A., Alam, S., Muhammad, A., Xiao, S., . . . Mumtaz, H. (2016). Evaluation of Changes in Liver Enzymes in Broiler Chicks (Gallous domesticus). *PSM Veterinary Research, 1*(1), 26-31.

Khatib, J., ElKhatib, L., Assaad, J., & El Kordi, A. (2023). Properties of mortar containing Phragmites Australis Ash. *Journal of Engineering, Design and Technology*.

Khatoon, U. T., Velidandi, A., & Rao, G. N. (2024). Nano-sized copper particles: Chemical synthesis, characterization, and their size and surface charge dependent antibacterial potential. *Results in Chemistry, 7*, 101258.

Khatri, F. A., Solangi, I. B., Memon, G. Z., Khattak, M. I., Bhatti, M. A., Keerio, F. A., & Farooque, M. (2024). Antibacterial Application of Copper Nanoparticles Biosynthesized by Water Caltrop Pod. *Journal of Applied Research in Plant Sciences, 5*(02), 288-296.

Kocabas, B. B., Attar, A., Yuka, S. A., & Yapaoz, M. A. (2023). Biogenic synthesis, molecular docking, biomedical and environmental applications of multifunctional CuO nanoparticles mediated Phragmites australis. *Bioorganic Chemistry, 133*, 106414.

Konomi, B. A., Dhavala, S. S., Huang, J. Z., Kundu, S., Huitink, D., Liang, H., . . . Mallick, B. K. (2013). Bayesian object classification of gold nanoparticles.

Kralik, G., & Kralik, Z. (2017). Poultry products enriched with nutricines have beneficial effects on human health. *Medicinski Glasnik, 14*(1).

Kryger, K. N., Thomsen, K., Whyte, M., & Dissing, M. (2010). Smallholder poultry production–livelihoods, food security and sociocultural significance. *FAO Smallholder Poultry Production Paper, 4*, 1-67.

Kuan, S., Martin, W., & Patrick, H. (1966). Alkaline Phosphatases of the Chick. Partial Characterization of the Tissue Isozymes. *Proceedings of the Society for Experimental Biology and Medicine, 122*(1), 172-177.

Kumar, S., Gupta, M. K., Kumar, S., & Rana, T. (2024). Comparative studies of xanthine oxidase inhibitors viz. allopurinol and febuxostat against induced hyperuricaemia in a poultry model. *Avian Pathology, 53*(1), 80-89.

Laib, I., & Boutlelis, D. A. (2022). Phytochemical investigation of *Helianthemum lippii* L. aerial Dum. Cours part and evaluation for its antioxidant activities. *International Journal of Secondary Metabolite, 9*(2), 229-237. doi: 10.21448/ijsm.999518

Lambertini, C., Sorrell, B. K., Riis, T., Olesen, B., & Brix, H. (2012). Exploring the borders of European Phragmites within a cosmopolitan genus. *AoB plants, 2012*, pls020.

Lei, R., Wu, C., Yang, B., Ma, H., Shi, C., Wang, Q., . . . Liao, M. (2008). Integrated metabolomic analysis of the nano-sized copper particle-induced hepatotoxicity and nephrotoxicity in rats: a rapid in vivo screening method for nanotoxicity. *Toxicology and applied pharmacology, 232*(2), 292-301.

Lekhisa, K., & Muroyiwa, B. (2024). Determinants of market participation for small scale broiler farmers in Leribe District of Lesotho. *International Journal of Research in Business and Social Science (2147-4478), 13*(4), 302-314.

Li, Y., Wang, K., & Li, C. (2024). Oxidative Stress in Poultry and the Therapeutic Role of Herbal Medicine in Intestinal Health. *Antioxidants, 13*(11), 1375.

Li, Z.-H., Velisek, J., Grabic, R., Li, P., Kolarova, J., & Randak, T. (2011). Use of hematological and plasma biochemical parameters to assess the chronic effects of a fungicide propiconazole on a freshwater teleost. *Chemosphere, 83*(4), 572-578.

Lira, C. N., Carpenter, A. P., Baio, J. E., Harper, B. J., Harper, S. L., & Mackiewicz, M. R. (2024). Size-and shape-dependent interactions of lipid-coated silver nanoparticles: an improved mechanistic understanding through model cell membranes and in vivo toxicity. *Chemical research in toxicology, 37*(6), 968-980.

Long, T.-Z., Shi, S.-H., Liu, S., Lu, A.-P., Liu, Z.-Q., Li, M., . . . Cao, D.-S. (2022). Structural analysis and prediction of hematotoxicity using deep learning approaches. *Journal of Chemical Information and Modeling, 63*(1), 111-125.

Mal, T. K., & Narine, L. (2004). The biology of Canadian weeds. 129. Phragmites australis (Cav.) Trin. ex Steud. *Canadian Journal of Plant Science, 84*(1), 365-396.

Mangan, M., & Siwek, M. (2024). Strategies to combat heat stress in poultry production—A review. *Journal of Animal Physiology and Animal Nutrition, 108*(3), 576-595.

Mangkalopakorn, P., Segsarnviriya, C., Keeratipranon, M., & Maiprasert, M. (2025). Glutathione Levels after Glutathione Supplementation: A Systematic Review and Meta-analysis. *Journal of Current Science and Technology, 15*(1), 90-90.

Mani, U., kumar Ponnala, A., Jayabharathi, T., Shanmugavel, M., Sujatha, D., & Ezhilarasan, D. (2023). Antibacterial Properties of Metal and Metal Oxide Nanoparticles-An Overview: Special Column on Microbial Nanotechnology. *Applied Microbiology: Theory & Technology*, 33-49.

Manjunatha, R., Naik, D., & Usharani, K. (2019). Nanotechnology application in agriculture: A review. *Journal of Pharmacognosy and Phytochemistry, 8*(3), 1073-1083.

Mannuthy, K. (2000). Correlation of blood glucose and liver glycogen profile of Japanese quail at different stages of growth. *Journal of Veterinary and Animal Sciences, 31*, 47-52.

Miao, C., Jia, P., Luo, C., Pang, J., Xiao, L., Zhang, T., . . . Sun, Z. (2024). The size-dependent in vivo toxicity of amorphous silica nanoparticles: A systematic review. *Ecotoxicology and Environmental Safety, 271*, 115910.

Mishra, B., & Jha, R. (2019). Oxidative stress in the poultry gut: Potential challenges and interventions. *Frontiers in veterinary science, 6*, 60.

Mohamed, A. A., Abu-Elghait, M., Ahmed, N. E., & Salem, S. S. (2021). Eco-friendly mycogenic synthesis of ZnO and CuO nanoparticles for in vitro antibacterial, antibiofilm, and antifungal applications. *Biological trace element research, 199*, 2788-2799.

Mohamed, A. S., Milošević, M., Mohany, M., Al-Rejaie, S. S., & Elwan, H. (2024). Heat stress relief for broiler chickens: organic selenium and a vitamin C and E blend can enhance growth, nutrient digestibility, and blood parameters. *Italian Journal of Animal Science, 23*(1), 275-287.

Morsy, E. A., Hussien, A. M., Ibrahim, M. A., Farroh, K. Y., & Hassanen, E. I. (2021). Cytotoxicity and genotoxicity of copper oxide nanoparticles in chickens. *Biological trace element research*, 1-15.

Mott, D., Galkowski, J., Wang, L., Luo, J., & Zhong, C.-J. (2007). Synthesis of size-controlled and shaped copper nanoparticles. *Langmuir, 23*(10), 5740-5745.

Mroczek-Sosnowska, N., Batorska, M., Lukasiewicz, M., Wnuk, A., Sawosz, E., Jaworski, S., & Niemiec, J. (2013). Effect of nanoparticles of copper and copper sulfate administered in ovo on hematological and biochemical blood markers of broiler chickens. *Annals of Warsaw University of Life Sciences-SGGW. Animal Science*(52).

Mujahid, A., Yoshiki, Y., Akiba, Y., & Toyomizu, M. (2005). Superoxide radical production in chicken skeletal muscle induced by acute heat stress. *Poultry science, 84*(2), 307-314.

Mukherjee, K., Tribedi, P., Mukhopadhyay, B., & Sil, A. K. (2013). Antibacterial activity of long-chain fatty alcohols against mycobacteria. *FEMS microbiology letters, 338*(2), 177-183.

Murthy, H., Desalegn, T., Kassa, M., Abebe, B., & Assefa, T. (2020). Synthesis of green copper nanoparticles using medicinal plant hagenia abyssinica (Brace) JF. Gmel. leaf extract: Antimicrobial properties. *Journal of nanomaterials, 2020*.

Murugan, K., Senthilkumar, B., Senbagam, D., & Al-Sohaibani, S. (2014). Biosynthesis of silver nanoparticles using Acacia leucophloea extract and their antibacterial activity. *International Journal of Nanomedicine*, 2431-2438.

Naik, N. M., Krishnaveni, M., Mahadevswamy, M., Bheemanna, M., Nidoni, U., Kumar, V., & Tejashri, K. (2022). Comparative analysis of supercritical fluid and Soxhlet Prosopis juliflora leaves extract with antifungal traits. *Research Square*, 1-15. doi: 10.21203/rs.3.rs-1676795/v1

Nair, G. M., Sajini, T., & Mathew, B. (2022). Advanced green approaches for metal and metal oxide nanoparticles synthesis and their environmental applications. *Talanta Open, 5*, 100080.

Nakyinsige, K., Fatimah, A., Aghwan, Z., Zulkifli, I., Goh, Y., & Sazili, A. (2014). Bleeding efficiency and meat oxidative stability and microbiological quality of New Zealand White rabbits subjected to halal slaughter without stunning and gas stun-killing. *Asian-Australasian journal of animal sciences, 27*(3), 406.

Nandeshwar, V. S., Kalkar, S. A., & Agrawal, P. S. (2022). Green synthesis of nanoparticles using plants as a bioreactor. *IJSRST*.

Nanjwade, B. K., Sarkar, A. B., & Srichana, T. (2019). Design and characterization of nanoparticulate drug delivery *Characterization and biology of nanomaterials for drug delivery* (pp. 337-350): Elsevier.

Nasrollahzadeh, M., & Sajadi, S. M. (2015). Green synthesis of copper nanoparticles using Ginkgo biloba L. leaf extract and their catalytic activity for the Huisgen [3+ 2] cycloaddition of azides and alkynes at room temperature. *Journal of colloid and interface science, 457*, 141-147.

Naumenko, S., Koshevoy, V., Matsenko, O., Miroshnikova, O., Zhukova, I., & Bespalova, I. (2023). Antioxidant properties and toxic risks of using metal nanoparticles on health and productivity in poultry. *Journal of World's Poultry Research, 13*(3), 292-306.

Nawaz, A. H., & Zhang, L. (2021). Oxidative stress in broiler chicken and its consequences on meat quality. *International Journal of Life Science Research Archive, 1*(1), 045-054.

Naz, S., Gul, A., Zia, M., & Javed, R. (2023). Synthesis, biomedical applications, and toxicity of CuO nanoparticles. *Applied Microbiology and Biotechnology, 107*(4), 1039-1061.

Nirala, R., Anjana, K., Mandal, K., & Jayachandran, C. (2018). Antibiotic residue-Food producing animal origin and its impact on human health. *International Journal of Livestock Research, 8*(10), 61-69.

Noor, R., Mittal, S., & Iqbal, J. (2002). Superoxide dismutase--applications and relevance to human diseases. *Medical science monitor: international medical journal of experimental and clinical research, 8*(9), RA210-215.

Nwidu, L. L., Elmorsy, E., Aprioku, J. S., Siminialayi, I., & Carter, W. G. (2018). In vitro anti-cholinesterase and antioxidant activity of extracts of Moringa oleifera plants from Rivers State, Niger Delta, Nigeria. *Medicines, 5*(3), 71.

Ognik, K., Cholewińska, E., Czech, A., Kozłowski, K., Wlazło, Ł., Nowakowicz-Dębek, B., . . . Tutaj, K. (2016). Effect of silver nanoparticles on the immune, redox, and lipid status of chicken blood.

Ognik, K., Sembratowicz, I., Cholewińska, E., Jankowski, J., Kozłowski, K., Juśkiewicz, J., & Zduńczyk, Z. (2018). The effect of administration of copper nanoparticles to chickens in their drinking water on the immune and antioxidant status of the blood. *Animal Science Journal, 89*(3), 579-588.

Ojha, S. (2022). Green synthesis of metallic nanoparticles: Advancements and future perspectives. *Biological Sciences, 2*(3), 262-268.

Oladipo, A. O., Iku, S. I., Ntwasa, M., Nkambule, T. T., Mamba, B. B., & Msagati, T. A. (2020). Doxorubicin conjugated hydrophilic AuPt bimetallic nanoparticles fabricated from Phragmites australis: Characterization and cytotoxic activity against human cancer cells. *Journal of Drug Delivery Science and Technology, 57*, 101749.

Oluwasanu, A. A., Oluwaseun, F., Teslim, J. A., Isaiah, T. T., Olalekan, I. A., & Chris, O. A. (2019). Scientific applications and prospects of nanomaterials: A multidisciplinary review. *African Journal of Biotechnology, 18*(30), 946-961.

Oshi, M. A., Haider, A., Siddique, M. I., Zeb, A., Jamal, S. B., Khalil, A. A. K., & Naeem, M. (2022). Nanomaterials for chronic inflammatory diseases: the current status and future prospects. *Applied Nanoscience, 12*(11), 3097-3110.

Ouidad, A., Sara, C., & Samir, D. (2020). Biological properties and Acute Toxicity Study of Copper oxide nanoparticles prepared by aqueous leaves extract of Portulaca oleracea (L). *Asian Journal of Pharmaceutical Research, 10*(2), 89-94.

Oyaizu, M. (1986). Studies on products of browning reaction antioxidative activities of products of browning reaction prepared from glucosamine. *The Japanese journal of nutrition and dietetics, 44*(6), 307-315.

Pabón-Baquero, L. C., Otálvaro-Álvarez, Á. M., Fernández, M. R. R., & Chaparro-González, M. P. (2018). Plant extracts as antioxidant additives for food industry. *Antioxidants in Foods and its Applications, 87*.

Parmar, J. (2024). A Review on Green Synthesis of Metallic Nanoparticles by Using Plant Extracts and Their Role in Cancer. *Journal of Natural Remedies*, 1909-1922.

Patra, A., & Lalhriatpuii, M. (2020). Progress and prospect of essential mineral nanoparticles in poultry nutrition and feeding—a review. *Biological trace element research, 197*(1), 233-253.

Pessayre, D., & Larrey, D. (1988). 8 Acute and chronic drug-induced hepatitis. *Baillière's Clinical Gastroenterology, 2*(2), 385-422.

Petroski, J. M., Green, T. C., & El-Sayed, M. A. (2001). Self-assembly of platinum nanoparticles of various size and shape. *The Journal of Physical Chemistry A, 105*(23), 5542-5547.

Pompella, A., Visvikis, A., Paolicchi, A., De Tata, V., & Casini, A. F. (2003). The changing faces of glutathione, a cellular protagonist. *Biochemical pharmacology, 66*(8), 1499-1503.

Poongulali, S., & Sundararaman, M. (2016). Antimycobacterial, anticandidal and antioxidant properties of Terminalia catappa and analysis of their bioactive chemicals. *International Journal of Pharmacy and Biological Sciences, 6*(2), 69-83.

Queenan, K., Cuevas, S., Mabhaudhi, T., Chimonyo, M., Slotow, R., & Häsler, B. (2021). A Qualitative Analysis of the Commercial Broiler System, and the Links to Consumers' Nutrition and Health, and to Environmental Sustainability: A South African Case Study. *Frontiers in sustainable food systems, 5*, 650469.

Radu-Rusu, R., Vacaru-Opris, I., & Usturoi, M. (2010). Contributions on the nutritional value knowledge for the meat produced by ROSS-308 chicken hybrid. *Lucrari Stiintifice Seria Zootehnie, 53*(15), 257-261.

Rafique, M., Tahir, M. B., Rafique, M. S., & Hamza, M. (2020). History and fundamentals of nanoscience and nanotechnology *Nanotechnology and photocatalysis for environmental applications* (pp. 1-25): Elsevier.

Ramaswamy, S. V. P., Narendhran, S., & Sivaraj, R. (2016). Potentiating effect of ecofriendly synthesis of copper oxide nanoparticles using brown alga: antimicrobial and anticancer activities. *Bulletin of Materials Science, 39*, 361-364.

Rasyid, A., & Putra, M. Y. (2023). Antibacterial and antioxidant activity of sea cucumber extracts collected from Lampung waters, Indonesia. *Kuwait Journal of Science, 50*(4), 615-621.

Razvarz, S., Chavez, L. F. G., & Vargas-Jarillo, C. (2020). *Nanotechnology applications in industry and heat transfer.* Paper presented at the Industrial and Robotic Systems: LASIRS 2019.

Rehman, Z. U., Meng, C., Sun, Y., Safdar, A., Pasha, R. H., Munir, M., & Ding, C. (2018). Oxidative stress in poultry: lessons from the viral infections. *Oxidative medicine and cellular longevity, 2018*(1), 5123147.

Riaz Rajoka, M. S., Thirumdas, R., Mehwish, H. M., Umair, M., Khurshid, M., Hayat, H. F., . . . Barba, F. J. (2021). Role of food antioxidants in modulating gut microbial communities: Novel understandings in intestinal oxidative stress damage and their impact on host health. *Antioxidants, 10*(10), 1563.

Rice, K. P., Saunders, A. E., & Stoykovich, M. P. (2012). Classifying the shape of colloidal nanocrystals by complex Fourier descriptor analysis. *Crystal growth & design, 12*(2), 825-831.

Sadhvi, B., Rajeshkumar, S., Roy, A., & Lakshmi, T. (2014). Copper oxide nanoparticles synthesis and characterization using UV-vis spectrophotometer and TEM. *Int J Res Pharm Sci, 10*(4), 2845-2848.

Safdar, K., Naz, R., Ullah, S., Khan, M. S., Abubakar, A. A., Mohammed, A. S., . . . Bhatti, F. (2024). EFFECT OF AQUEOUS HERBAL EXTRACTS, PROBIOTICS AND SIGANUS LURIDUS (UNANI DRUG) ON GROWTH PERFORMANCE AND RENAL FUNCTIONS OF BROILER CHICKS. *Health Sciences Journal, 2*(2), 57-62.

Saleh, A. A., & El-Magd, M. A. (2018). Beneficial effects of dietary silver nanoparticles and silver nitrate on broiler nutrition. *Environmental Science and Pollution Research, 25*, 27031-27038.

Salopek, B., Krasic, D., & Filipovic, S. (1992). Measurement and application of zeta-potential. *Rudarsko-geolosko-naftni zbornik, 4*(1), 147.

Santhosh, P., Mukhtar, L., Kamaraj, M., Nithya, T., Ganesh, M., Aswathy, K., . . . Lopes, B. S. (2023). Phytomediated synthesis of copper oxide nanoparticles from floating fern Salvinia cucullata R oxb. and their antibacterial, antioxidant, and anticancer potential. *Biomass Conversion and Biorefinery*, 1-15.

Santo-Orihuela, P. L., Desimone, M. F., & Catalano, P. N. (2023). Green Synthesis: A Land of Complex Nanostructures. *Current Pharmaceutical Biotechnology, 24*(1), 3-22.

Sayes, C. M., Smith, P. A., & Ivanov, I. V. (2013). A framework for grouping nanoparticles based on their measurable characteristics. *International journal of nanomedicine, 8*(sup1), 45-56.

Sellal, A., & Belattar, R. (2024). The traces elements absorption, accumulation and translocation ability of Phragmites australis. *International Journal of Phytoremediation, 26*(5), 618-625.

Senanayake, S., Ranasinghe, J., Waduge, R., Nizanantha, K., & Alexander, P. (2015). Changes in the serum enzyme levels and liver lesions of broiler birds reared under different management conditions.

Seomoon, K.-M., & Jang, I.-S. (2022). Application of plant flavonoids as natural antioxidants in poultry production.

Sharma, A. K., Kumar, A., Taneja, G., Nagaich, U., Deep, A., & Rajput, S. K. (2016). Synthesis and preliminary therapeutic evaluation of copper nanoparticles against diabetes mellitus and-induced micro-(renal) and macro-vascular (vascular endothelial and cardiovascular) abnormalities in rats. *RSC Advances, 6*(43), 36870-36880.

Shende, S., Ingle, A. P., Gade, A., & Rai, M. (2015). Green synthesis of copper nanoparticles by Citrus medica Linn.(Idilimbu) juice and its antimicrobial activity. *World Journal of Microbiology and Biotechnology, 31*, 865-873.

Shobha, G., Sagar, S., Shashidhara, K., Mahadimane, V., & Ananda, S. (2019). In vitro cytotoxicity study of green synthesized copper nanoparticles. *Res. J. Biotech., 14*, 105.

Shoudho, K. N., Uddin, S., Rumon, M. M. H., & Shakil, M. S. (2024). Influence of Physicochemical properties of Iron Oxide nanoparticles on their antibacterial activity. *ACS omega, 9*(31), 33303-33334.

Singh, G. (2003). Plant systematics: an integrated approach: Science Publishers.

Sohaib, M., Al-Barakah, F. N., Migdadi, H. M., & Husain, F. M. (2022). Comparative study among Avicennia marina, Phragmites australis, and Moringa oleifera based ethanolic-extracts for their antimicrobial, antioxidant, and cytotoxic activities. *Saudi Journal of Biological Sciences, 29*(1), 111-122.

Somya, A., Varshney, A. P., & Khan, A. (2025). Green Nanoparticles: Innovative Solutions for Sustainable Wastewater Treatment *Synthesizing and Characterizing Plant-Mediated Biocompatible Metal Nanoparticles* (pp. 91-112): IGI Global.

Spinner, D. M. (2001). MTT growth assays in ovarian cancer. *Ovarian Cancer: Methods and Protocols*, 175-177.

Srinivasan, C., Gangadevi, P., Ally, K., Ananth, D., Chacko, B., & Sathya, P. (2017). Effect of dietary supplementation of polyalthia longifolia leaf meal on alanine transaminase (ALT) and aspartate transaminase (AST) levels in broiler chicken. *Int J Curr Microbiol. Appl Sci, 6*, 887-889.

Stevens, L. (1997). Avian biochemistry and molecular biology. *General Pharmacology, 1*(28), 168.

Sudheer, S., Bai, R. G., Muthoosamy, K., Tuvikene, R., Gupta, V. K., & Manickam, S. (2022). Biosustainable production of nanoparticles via mycogenesis for biotechnological applications: A critical review. *Environmental research, 204*, 111963.

Surai, P. F., Kochish, I. I., Fisinin, V. I., & Kidd, M. T. (2019). Antioxidant defence systems and oxidative stress in poultry biology: An update. *Antioxidants, 8*(7), 235.

Tahir, S. K., Yousaf, M. S., Ahmad, S., Shahzad, M. K., Khan, A. F., Raza, M., . . . Rabbani, I. (2019). Effects of chromium-loaded chitosan nanoparticles on the intestinal electrophysiological indices and glucose transporters in broilers. *Animals, 9*(10), 819.

Thakur, S., Kumar, V., Das, R., Sharma, V., & Mehta, D. K. (2024). Biomarkers of Hepatic Toxicity: An Overview. *Current Therapeutic Research*, 100737.

Unuofin, J. O., Oladipo, A. O., More, G. K., Adeeyo, A. O., Mustapha, H. T., Msagati, T. A., & Lebelo, S. L. (2024). Phytochemical Profiling of Phragmites australis Leaf Extract and Its Nano-Structural Antioxidant, Antimicrobial, and Anticancer Activities. *Journal of Inorganic and Organometallic Polymers and Materials*, 1-15.

Utreja, P., Verma, S., Rahman, M., & Kumar, L. (2020). Use of nanoparticles in medicine. *Current Biochemical Engineering, 6*(1), 7-24.

Valli, C., & Kavitha, R. (2023). PHYTOBIOTICS AS AN ALTERNATIVE FEED ADDITIVE. *Indian Journal of Veterinary and Animal Sciences Research, 52*(4), 1-14.

Vasantharaj, S., Sathiyavimal, S., Saravanan, M., Senthilkumar, P., Gnanasekaran, K., Shanmugavel, M., . . . Pugazhendhi, A. (2019). Synthesis of ecofriendly copper oxide nanoparticles for fabrication over textile fabrics: characterization of antibacterial activity and dye degradation potential. *Journal of Photochemistry and Photobiology B: Biology, 191*, 143-149.

Veerakumar, C., & Sreekumar, A. (2020). Thermo-physical investigation and experimental discharge characteristics of lauryl alcohol as a potential phase change material for thermal management in buildings. *Renewable Energy, 148*, 492-503.

Vennila, K., Chitra, L., Balagurunathan, R., & Palvannan, T. (2018). Comparison of biological activities of selenium and silver nanoparticles attached with bioactive phytoconstituents: green synthesized using Spermacoce hispida extract. *Advances in Natural Sciences: Nanoscience and Nanotechnology, 9*(1), 015005.

Vinjamuri, S., Afshan, S., Shekar, S., & Saraswathi, V. (2015). Evaluation of hemolytic activity, ATPase inhibitory activity and antitumor activity of TLC extract of lemon grass (Cymbpogon citratus). *International Journal of Pharmacognosy and Phytochemical Research, 7*(4), 785-788.

Wadood, A., Ghufran, M., Jamal, S. B., Naeem, M., Khan, A., & Ghaffar, R. (2013). Phytochemical analysis of medicinal plants occurring in local area of Mardan. *Biochem anal biochem, 2*(4), 1-4.

Wang, A., Zhang, J., & Li, Z. (2012). Correlation of volatile and nonvolatile components with the total antioxidant capacity of tartary buckwheat vinegar: Influence of the thermal processing. *Food research international, 49*(1), 65-71.

Wang, R., Lei, C., Li, Z., Lei, Y., Luo, C., Shao, L., . . . Yang, P. (2022). Effects of a Diet of Phragmites australis instead of Triticum aestivum L. on Immune Performance and Liver Tissue Structure of Ctenopharyngodon idellus. *Fishes, 7*(6), 378.

Wasti, S., Sah, N., & Mishra, B. (2020). Impact of heat stress on poultry health and performances, and potential mitigation strategies. *Animals, 10*(8), 1266.

Watson, L., & Clifford, H. (1976). The major groups of Australasian grasses: a guide to sampling. *Australian Journal of Botany, 24*(4), 489-507.

Weckbecker, G., & Cory, J. G. (1988). Ribonucleotide reductase activity and growth of glutathione-depleted mouse leukemia L1210 cells in vitro. *Cancer letters, 40*(3), 257-264.

Witeska, M., Kondera, E., & Bojarski, B. (2023). Hematological and hematopoietic analysis in fish toxicology—a review. *Animals, 13*(16), 2625.

Xie, X. (2023). Application of Nanomedicine in Diagnostic Technology. *Highlights in Science, Engineering and Technology, 40*, 125-131.

Yagi, K. (1976). A simple fluorometric assay for lipoperoxide in blood plasma. *Biochemical medicine, 15*(2), 212-216.

Yan, S., Yue, Y.-z., Zong, Y., & Zeng, L. (2019). Tetramethylpyrazine improves postoperative tissue adhesion: a drug repurposing. *Chinese journal of integrative medicine, 25*(7), 554-560.

Yang BaoHua, Y. B., Lei RongHui, L. R., & Wu ChunQi, W. C. (2009). Oxidative damage in livers and kidneys induced by nano-copper particles in rats.

Yang, H., Liu, C., Yang, D., Zhang, H., & Xi, Z. (2009). Comparative study of cytotoxicity, oxidative stress and genotoxicity induced by four typical nanomaterials: the role of particle size, shape and composition. *Journal of applied Toxicology, 29*(1), 69-78.

Yang, W., Wang, L., Mettenbrink, E. M., DeAngelis, P. L., & Wilhelm, S. (2021). Nanoparticle toxicology. *Annual Review of Pharmacology and Toxicology, 61*(1), 269-289.

Yeshi, K., Turpin, G., Jamtsho, T., & Wangchuk, P. (2022). Indigenous uses, phytochemical analysis, and anti-inflammatory properties of Australian tropical medicinal plants. *Molecules, 27*(12), 3849.

Yusof, H. M., Mohamad, R., Zaidan, U. H., Arshad, M. A., & Samsudin, A. A. (2023). Effects of dietary zinc oxide nanoparticles supplementation on broiler growth performance, zinc

retention, liver health status, and gastrointestinal microbial load. *Journal of Trace Elements and Minerals, 4*, 100072.

Zhou, R., Cui, M., Wang, Y., Zhang, M., Li, F., & Liu, K. (2020). Isolation, structure identification and anti-inflammatory activity of a polysaccharide from Phragmites rhizoma. *International journal of biological macromolecules, 161*, 810-817.

Zhu, L., Zhang, D., Yuan, C., Ding, X., Shang, Y., Jiang, Y., & Zhu, G. (2017). Anti-Inflammatory and antiviral effects of water-soluble crude extract from Phragmites australis in vitro. *Pakistan journal of pharmaceutical sciences, 30*(4), 1357-1362.

Zou, X., Feng, Z., Li, Y., Wang, Y., Wertz, K., Weber, P., . . . Liu, J. (2012). Stimulation of GSH synthesis to prevent oxidative stress-induced apoptosis by hydroxytyrosol in human retinal pigment epithelial cells: activation of Nrf2 and JNK-p62/SQSTM1 pathways. *The Journal of nutritional biochemistry, 23*(8), 994-1006.

Annex

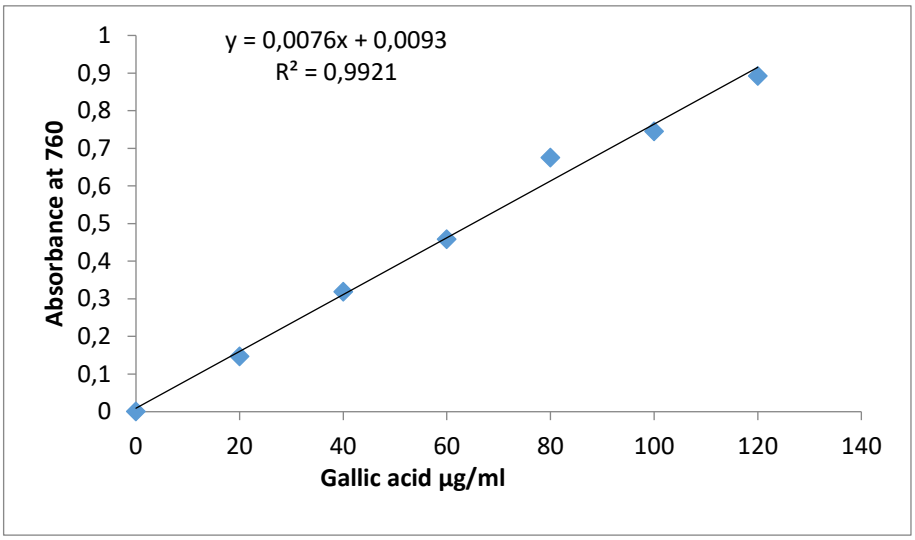

Annex 01: Gallic acid calibration curve for the determination of polyphenols

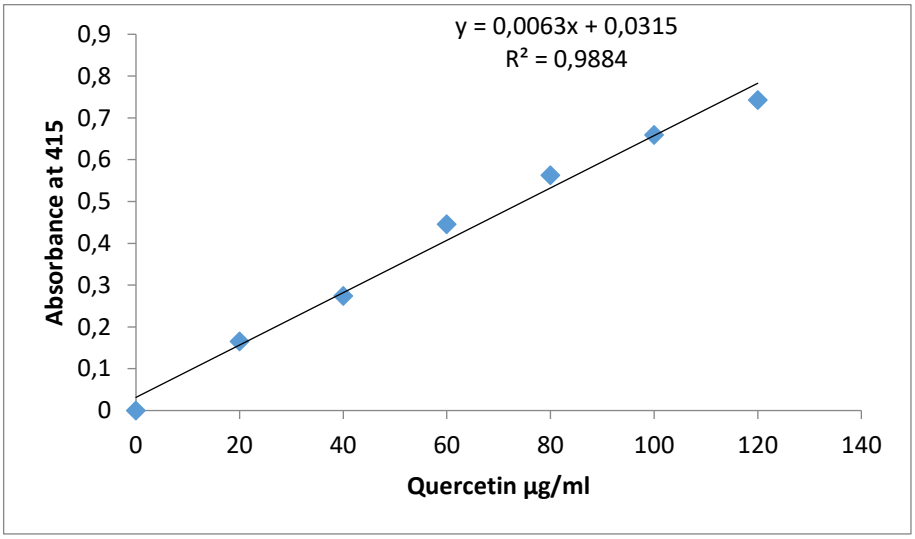

Annex 02: Quercetin calibration curve for flavonoid assays

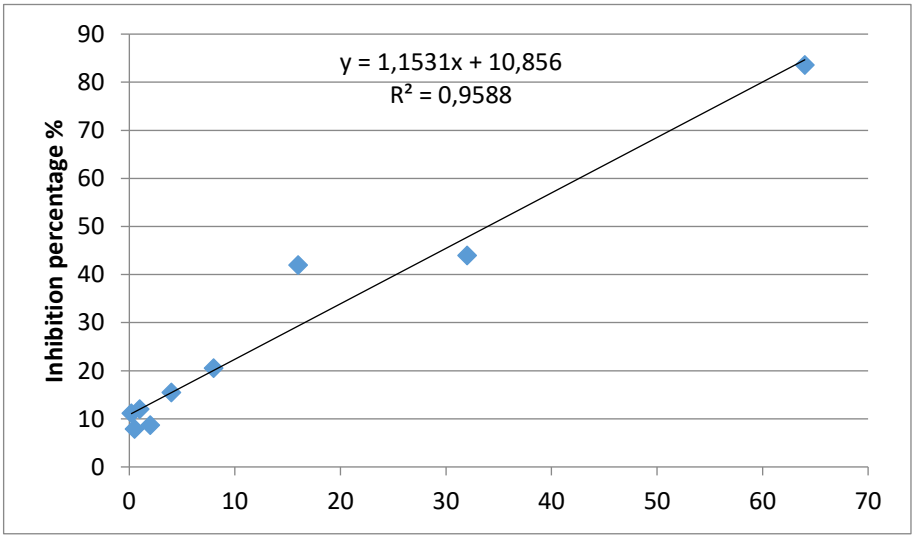

Annex 03: Inhibition percentage values of ascorbic acid (DPPH assay)

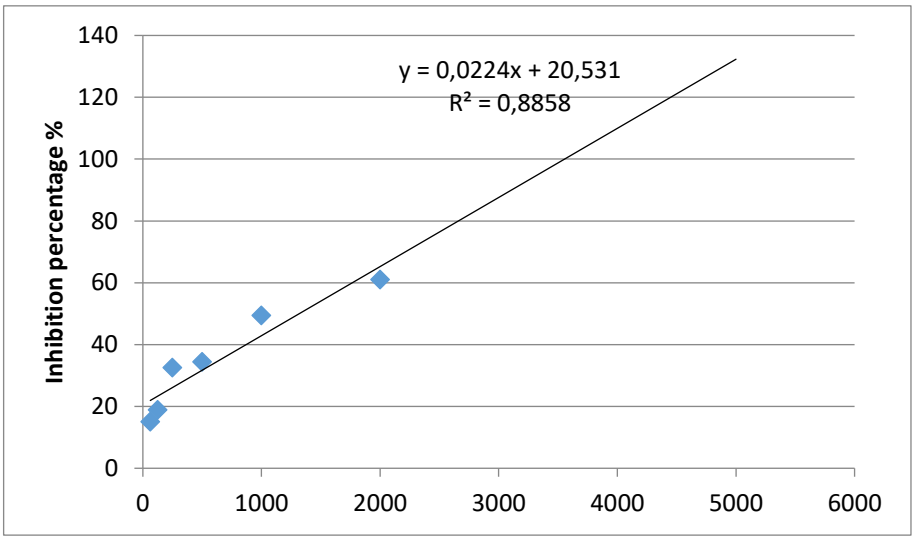

Annex 04: Inhibition percentage values of leaf extract (DPPH assay)

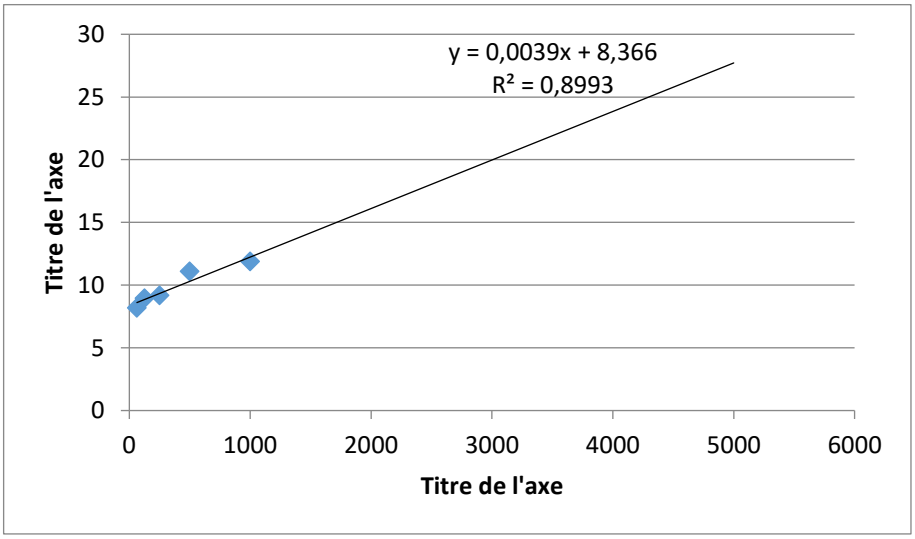

Annex 05: Inhibition percentage values of rhizome extract (DPPH assay)

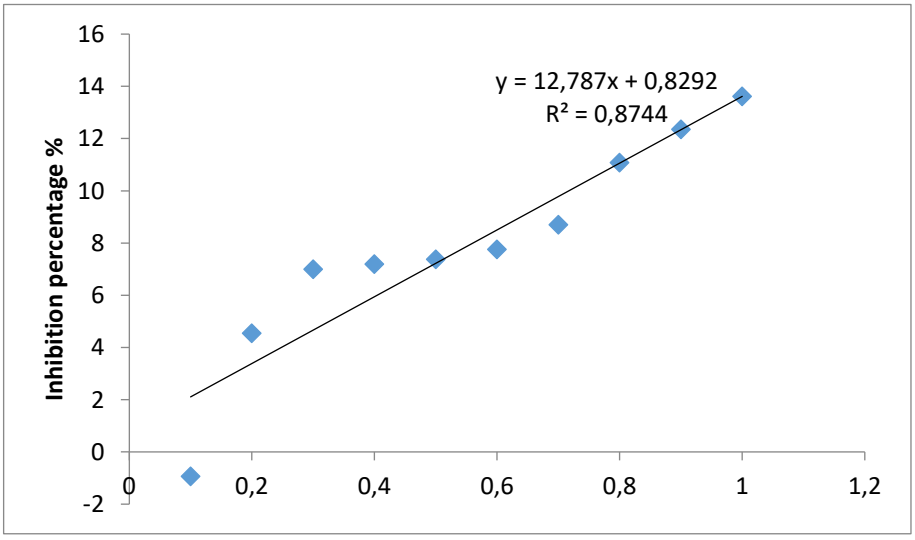

Annex 06: Inhibition percentage values of leaf-based Cu NPs (DPPH assay)

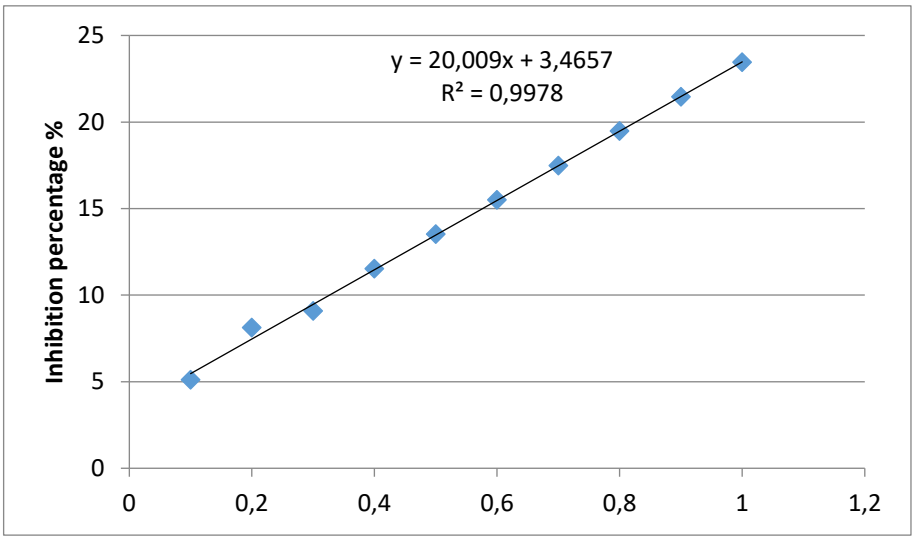

Annex 07: Inhibition percentage values of rhizome-based Cu NPs (DPPH assay)

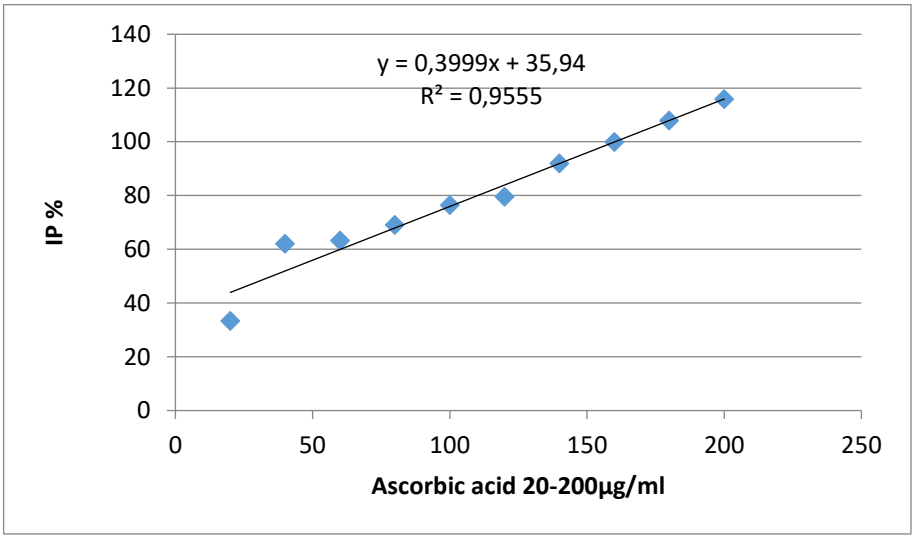

Annex 08: Inhibition percentage values of ascorbic acid (FRAP assay)

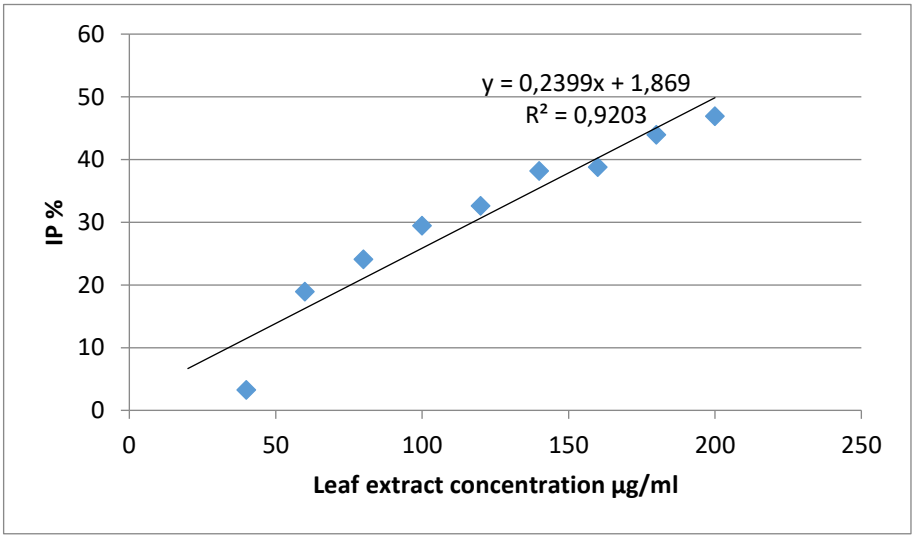

Annex 09: Inhibition percentage values of leaf extract (FRAP assay)

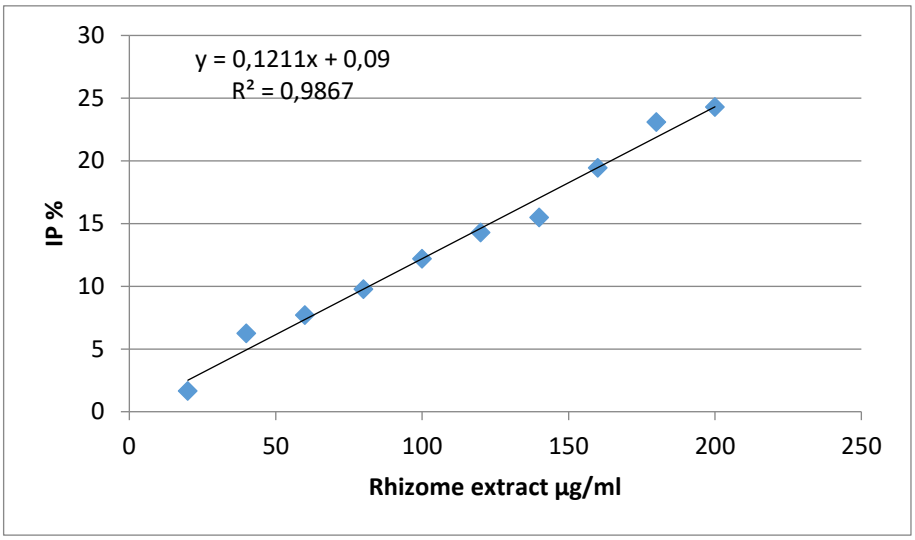

Annex 10: Inhibition percentage values of rhizome extract (FRAP assay)

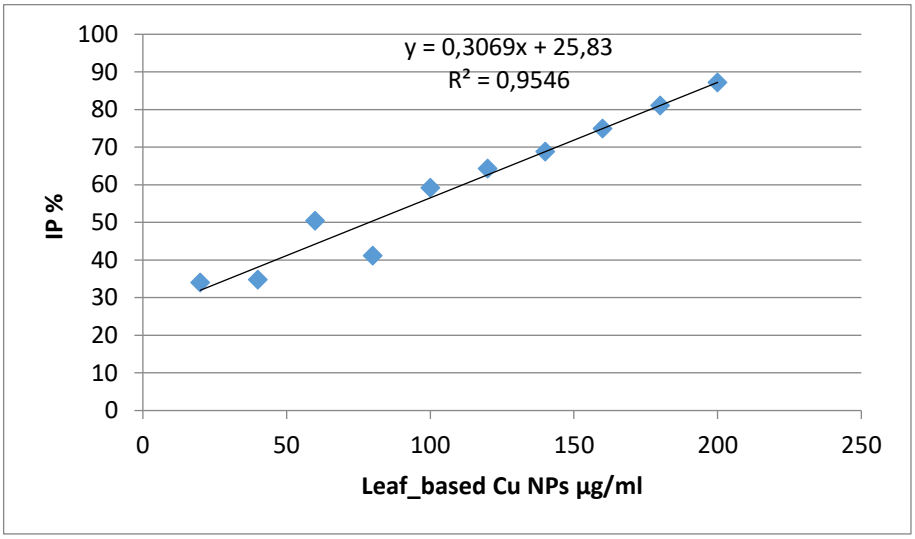

Annex 11: Inhibition percentage values of leaf-based Cu NPs (FRAP assay)

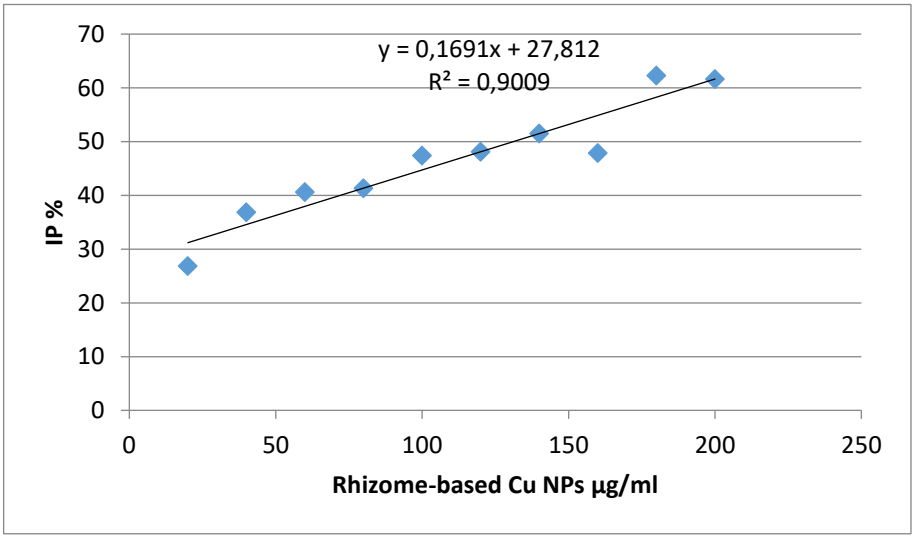

Annex 11: Inhibition percentage values of rhizome-based Cu NPs (FRAP assay)

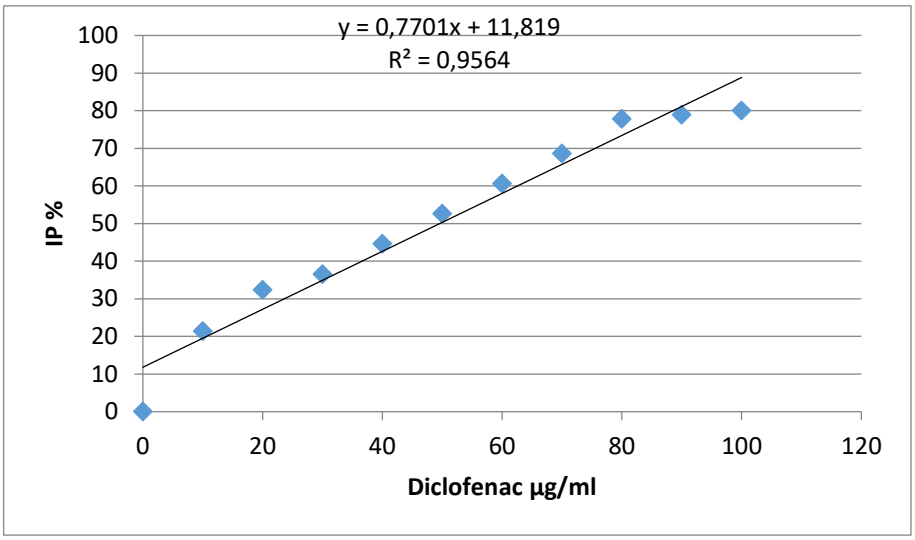

Annex 12: Inhibition percentage values of diclofenac (Protein assay)

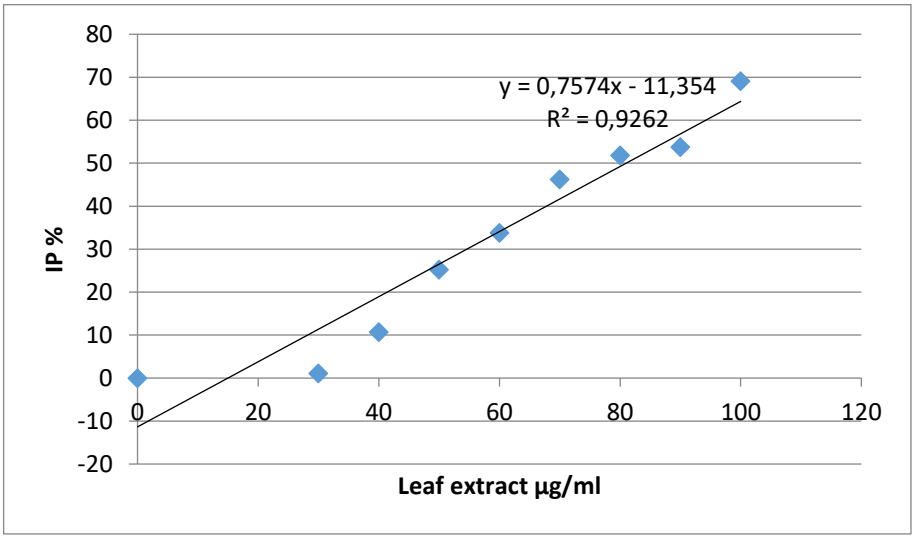

Annex 13: Inhibition percentage values of leaf extract (Protein assay)

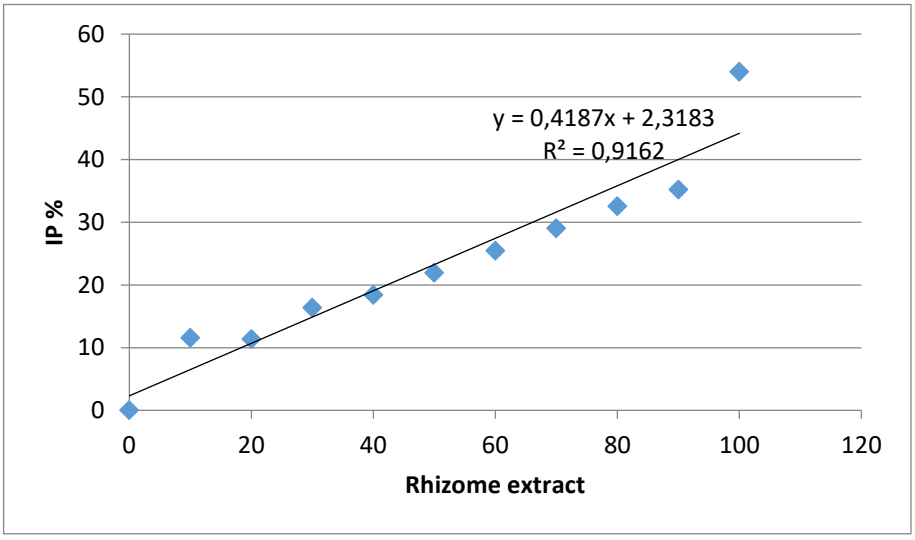

Annex 14: Inhibition percentage values of rhizome extract (Protein assay)

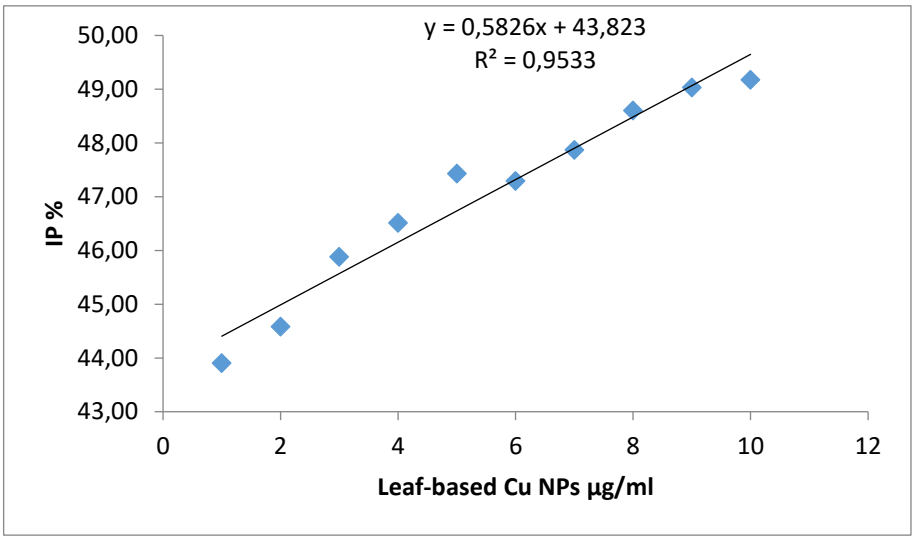

Annex 15: Inhibition percentage values of leaf-based Cu NPs (Protein assay)

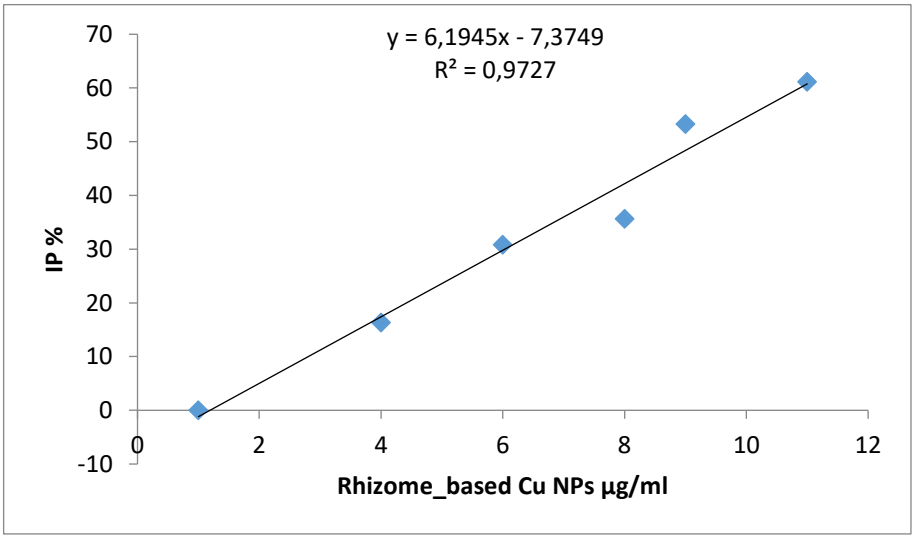

Annex 16: Inhibition percentage values of rhizome-based Cu NPs (Protein assay)

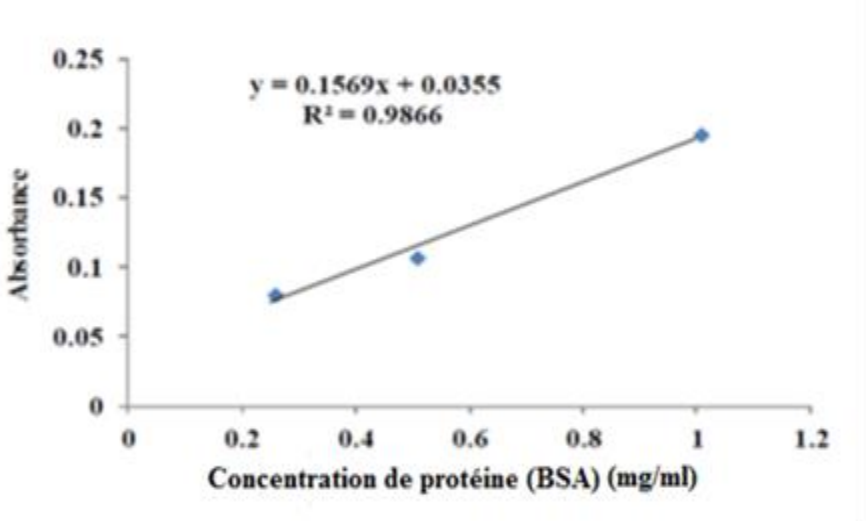

Annex 17: BSA calibration curve for protein assay

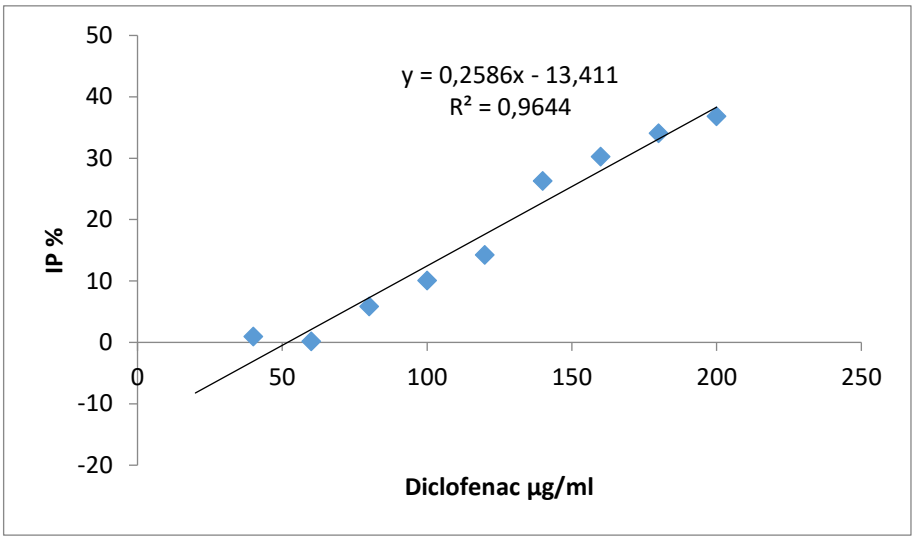

Annex 18: Inhibition percentage values of diclofenac (Hemolysis assay)

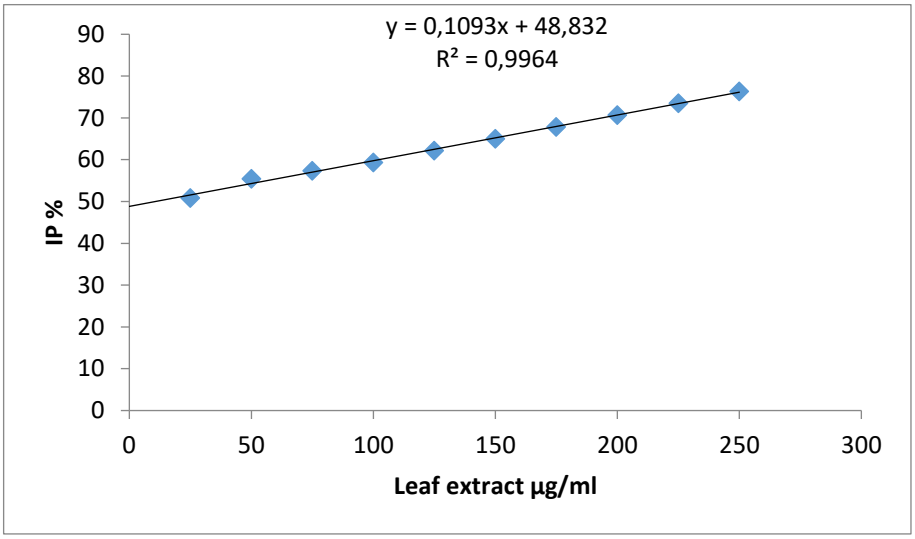

Annex 19: Inhibition percentage values of leaf extract (Hemolysis assay)

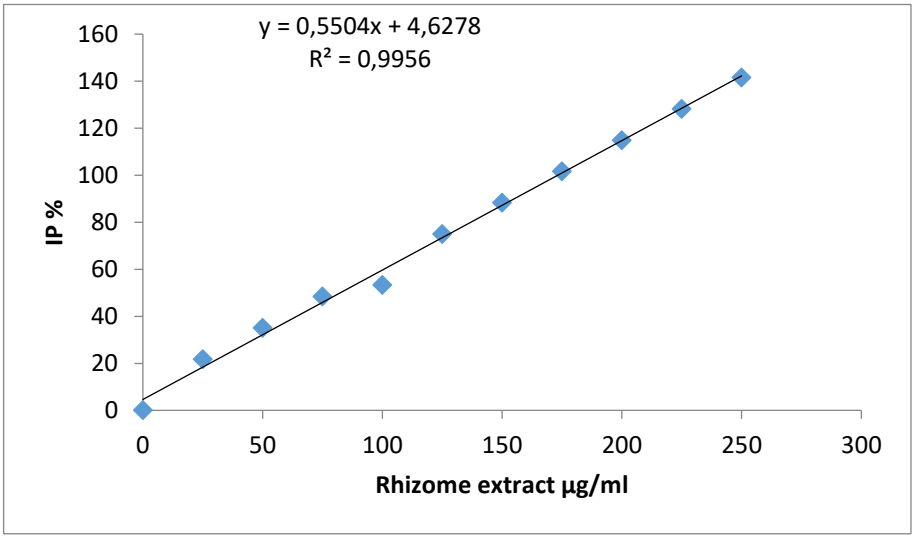

Annex 20: Inhibition percentage values of rhizome extract (Hemolysis assay)

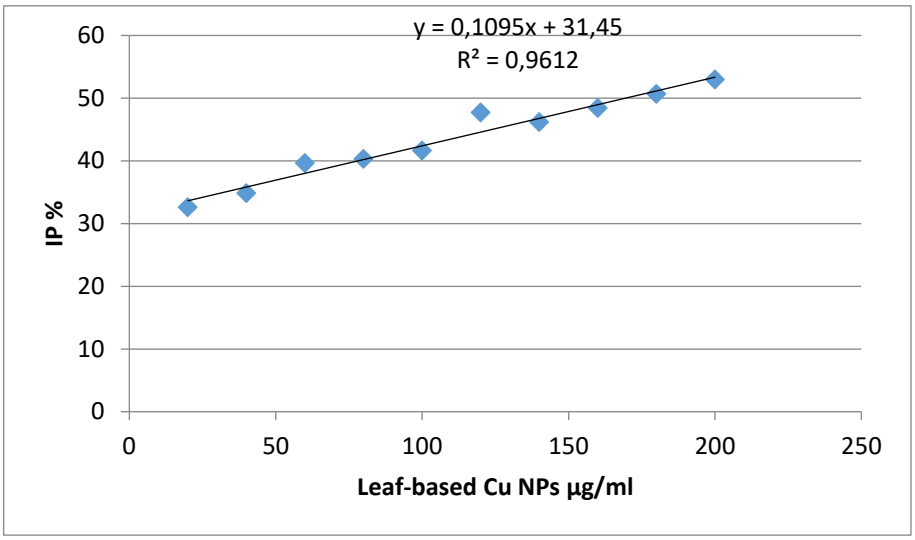

Annex 21: Inhibition percentage values of leaf-based Cu NPs (Hemolysis assay)

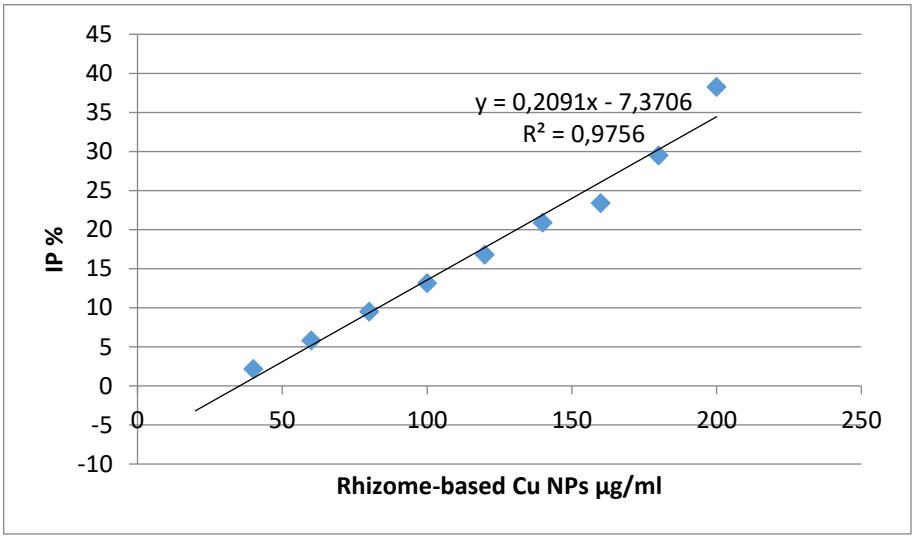

Annex 22: Inhibition percentage values of leaf-based Cu NPs (Hemolysis assay)